

Development of Eco-Driving Control System for Connected and Automated Hybrid Electric Vehicles

by

Siyang Wang

A thesis submitted to the
School of Graduate and Postdoctoral Studies in partial
fulfillment of the requirements for the degree of

Master of Applied Science in Automotive Engineering

Department of Automotive, Mechanical and Manufacturing Engineering
School of Graduate and Postdoctoral Studies
The Faculty of Engineering and Applied Science
University of Ontario Institute of Technology (Ontario Tech University)
Oshawa, Ontario, Canada

April 2020

© Siyang Wang, 2020

THESIS EXAMINATION INFORMATION

Submitted by: **Siyang Wang**

Master of Applied Science in Automotive Engineering

| |
|--|
| Thesis title: Development of Eco-Driving Control System for Connected and Automated Hybrid Electric Vehicles |
|--|

An oral defense of this thesis took place on April 9, 2020 in front of the following examining committee:

Examining Committee:

| | |
|------------------------------|------------------------|
| Chair of Examining Committee | Dr. Amirkianoosh Kiani |
| Research Supervisor | Dr. Xianke Lin |
| Examining Committee Member | Dr. Haoxiang Lang |
| External Examiner | Dr. Jing Ren |

The above committee determined that the thesis is acceptable in form and content and that a satisfactory knowledge of the field covered by the thesis was demonstrated by the candidate during an oral examination. A signed copy of the Certificate of Approval is available from the School of Graduate and Postdoctoral Studies.

ABSTRACT

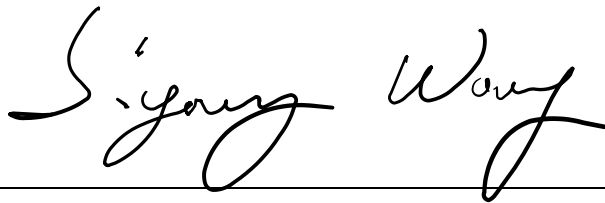
Hybrid electric vehicles (HEVs) were designed as a potential solution to the ever-increasing global problems of the energy crisis and global warming through flexibly utilizing both fuel and electrical energy. Besides, the emerging technologies of connected and automated vehicles (CAVs) have provided huge possibilities to push the boundaries of HEVs even further and thus have been extensively studied. In this study, a bi-level MPC-based eco-driving strategy for CAHEVs is proposed and designed to improve fuel economy, reduce exhaust emissions while ensuring driving safety under the most common driving scenarios. First, the HEV powertrain is modelled, and the real-time data sources in the intelligent transportation system (ITS) are introduced. Next, the multi-objective problem is formulated with three goals, namely, driving safety, fuel economy and emission reduction. The simulation is carried out on a map with realistic driving conditions. The results demonstrate the effectiveness and robustness of the proposed eco-driving strategy for CAHEVs.

Keywords: Eco-driving, energy management strategy (EMS), connected and automated hybrid vehicle (CAV), hybrid electric vehicle (HEV), intelligent transportation system (ITS)

AUTHOR'S DECLARATION

I hereby declare that this thesis consists of original work of which I have authored. This is a true copy of the thesis, including any required final revisions, as accepted by my examiners.

I authorize the University of Ontario Institute of Technology to lend this thesis to other institutions or individuals for the purpose of scholarly research. I further authorize University of Ontario Institute of Technology to reproduce this thesis by photocopying or by other means, in total or in part, at the request of other institutions or individuals for the purpose of scholarly research. I understand that my thesis will be made electronically available to the public.



Siyang Wang

STATEMENT OF CONTRIBUTIONS

Part of this thesis has been submitted for publication as:

S. Wang and X. Lin, “Eco-driving control of connected and automated hybrid vehicles in mixed driving scenarios”, *Applied Energy*, 2020. (Submitted)

The writing of the manuscript, vehicle modeling, platform setup, test simulation conducted in this work and the mentioned submission are completed by the author. Co-author reviewed and provided technical support when required.

ACKNOWLEDGEMENTS

I would like to thank my supervisor, Dr. Xianke Lin, for his consistent support and skillful guidance throughout this challenging thesis.

TABLE OF CONTENTS

| | |
|--|------------|
| ABSTRACT | iii |
| AUTHOR'S DECLARATION | iv |
| STATEMENT OF CONTRIBUTIONS | v |
| ACKNOWLEDGEMENTS | vi |
| TABLE OF CONTENTS | vii |
| LIST OF TABLES | x |
| LIST OF FIGURES | xii |
| LIST OF ABBREVIATIONS AND SYMBOLS | xvi |
| Chapter 1. Introduction | 1 |
| 1.1 <i>Background and motivation</i> | 1 |
| 1.2 <i>Objectives and assumptions</i> | 6 |
| 1.3 <i>Contributions</i> | 8 |
| 1.4 <i>Outline</i> | 9 |
| Chapter 2. Literature Review | 11 |
| 2.1 <i>Introduction</i> | 11 |
| 2.2 <i>Hybrid electric vehicles</i> | 11 |
| 2.2.1 <i>Series Hybrids</i> | 12 |
| 2.2.2 <i>Parallel Hybrids</i> | 13 |
| 2.2.3 <i>Series-Parallel Hybrids</i> | 15 |
| 2.2.4 <i>Driving Cycle</i> | 16 |
| 2.3 <i>Connected and automated vehicles (CAVs)</i> | 17 |

| | | |
|-------------------|--|-----------|
| 2.3.1 | Eco-Driving scenarios | 18 |
| 2.4 | <i>Literature review on control strategies for CAHEVs</i> | 20 |
| 2.4.1 | Energy management strategies (EMSs) for HEVs | 20 |
| 2.4.2 | Control strategies for CAHEVs | 31 |
| 2.4.3 | Existing research gaps in eco-driving for CAHEVs..... | 33 |
| 2.5 | <i>Summary</i> | 34 |
| Chapter 3. | Model Development | 35 |
| 3.1 | <i>Modelling of Hybrid Electric Vehicles (HEVs)</i> | 35 |
| 3.1.1 | HEV Configuration..... | 35 |
| 3.2 | <i>Intelligent transportation system (ITS)</i> | 43 |
| 3.2.1 | Vehicle-to-Vehicle (V2V) | 43 |
| 3.2.2 | Vehicle-to-Infrastructure (V2I)..... | 44 |
| 3.3 | <i>Summary</i> | 45 |
| Chapter 4. | Methodology | 46 |
| 4.1 | <i>Problem Formulation</i> | 46 |
| 4.2 | <i>Model predictive control-based eco-driving control strategy</i> | 47 |
| 4.2.1 | Optimization objectives | 48 |
| 4.2.2 | Model predictive control (MPC) | 57 |
| 4.3 | <i>Rule-based EACS</i> | 61 |
| 4.4 | <i>Summary</i> | 67 |
| Chapter 5. | Results and Discussion | 69 |
| 5.1 | <i>Experiment setup</i> | 69 |
| 5.1.1 | ADVISOR..... | 69 |

| | | |
|-------------------|--|------------|
| 5.1.2 | SUMO | 70 |
| 5.1.3 | Traffic simulation map | 73 |
| 5.2 | <i>Simulation results on a highway-urban trip</i> | 77 |
| 5.2.1 | Trip Setup | 77 |
| 5.2.2 | Driving Safety | 80 |
| 5.2.3 | Energy consumption and emission reduction | 88 |
| 5.3 | <i>Simulation results on a suburban-urban trip</i> | 90 |
| 5.3.1 | Trip Setup | 90 |
| 5.3.2 | Driving Safety | 93 |
| 5.3.3 | Energy consumption and emission reduction | 100 |
| 5.4 | <i>Summary</i> | 101 |
| Chapter 6. | Conclusion and Future Works | 103 |
| 6.1 | <i>Conclusion</i> | 103 |
| 6.2 | <i>Future Works</i> | 104 |
| Reference | | 106 |

LIST OF TABLES

CHAPTER 2

| | |
|--|----|
| Table. 2. 1 HEV working modes | 22 |
| Table. 2. 2 Summary on rule-based energy management strategies for HEV | 26 |
| Table. 2. 3 Summary on optimization-based energy management strategies for HEV | 30 |

CHAPTER 3

| | |
|--|----|
| Table. 3. 1 The studied HEV specifications | 37 |
| Table. 3. 2 V2V data for this study | 43 |
| Table. 3. 3 V2I data used for this study | 44 |
| Table. 3. 4 Listed traffic signal phases | 45 |

CHAPTER 4

| | |
|--|----|
| Table. 4. 1 Parameters concerning the driving safety | 49 |
| Table. 4. 2 Parameters for IDM | 62 |
| Table. 4. 3 Parameters for rule-based EACS | 65 |

CHAPTER 5

| | |
|--|----|
| Table. 5. 1 Background vehicle specifications | 75 |
| Table. 5. 2 Specifications of the simulation map | 75 |
| Table. 5. 3 Parameters for simulation | 76 |

| | |
|---|-----|
| Table. 5. 4 Specifications of the highway-urban trip..... | 78 |
| Table. 5. 5 Results from the proposed MPC-based eco-driving strategy and the EACS rule-based strategy (SOC corrected) on a highway-urban trip | 90 |
| Table. 5. 6 Specifications of the suburban-urban trip..... | 91 |
| Table. 5. 7 Results from the proposed MPC-based eco-driving strategy and the EACS rule-based strategy (SOC corrected) on a suburban trip..... | 101 |

LIST OF FIGURES

CHAPTER 1

| | |
|--|---|
| Fig. 1. 1 Energy consumption by the end-user sector [5] | 2 |
| Fig. 1. 2 Carbon dioxide emissions by the end-user sector [5]..... | 2 |
| Fig. 1. 3 V2V and V2I communications for CAVs in ITS | 6 |

CHAPTER 2

| | |
|--|----|
| Fig. 2. 1 The series hybrid powertrain | 13 |
| Fig. 2. 2 The parallel hybrid powertrain | 14 |
| Fig. 2. 3 The series-parallel hybrid powertrain..... | 16 |
| Fig. 2. 4 The Urban Dynamometer Driving Schedule (UDDS) | 17 |
| Fig. 2. 5 The classifications of control strategies for HEV..... | 21 |
| Fig. 2. 6 The vehicle working modes, (a) electric only, (b) hybrid / electric assist, (c) battery charging, (d) regenerative braking, (e) engine only..... | 23 |

CHAPTER 3

| | |
|---|----|
| Fig. 3. 1 Single-shaft pre-transmission HEV Powertrain | 36 |
| Fig. 3. 2 Operation points of Saturn 1.9L (63kW) SOHC SI Engine on fuel economy and engine-out emissions contour maps (a) Fuel economy (b) HC emission (c) CO emissions and (d) NOx emission..... | 39 |
| Fig. 3. 3 Equivalent circuit model for battery pack | 40 |
| Fig. 3. 4 Longitudinal vehicle dynamics..... | 42 |

CHAPTER 4

| | |
|--|----|
| Fig. 4. 1 Illustration for driving safety parameters | 50 |
| Fig. 4. 2 Driving scenario classifier (DSC) workflow | 51 |
| Fig. 4. 3 Sample cases at the TSCI without leading vehicles (a) brakes are applied due to the red signal, (b) brakes are applied because the green signal phase duration is not sufficient for passing (c) vehicle decides to drive across the intersection in 25s | 55 |
| Fig. 4. 4 The framework of the proposed MPC-based eco-driving strategy..... | 59 |
| Fig. 4. 5 Pseudo-code of the proposed algorithm | 60 |
| Fig. 4. 6 EACS rule-based illustrations | 64 |
| Fig. 4. 7 Pseudo code of rule-based EACS..... | 66 |
| Fig. 4. 8 Workflow of the EACS | 67 |

CHAPTER 5

| | |
|--|----|
| Fig. 5. 1 Sample ADVISOR interface for customizing vehicle parameters, a vehicle with a parallel hybrid powertrain is configured | 70 |
| Fig. 5. 2 Sample SUMO-GUI interface, zoomed-out view of the Cologne, Germany urban transportation network | 72 |
| Fig. 5. 3 A zoomed-in view of the Cologne, Germany urban transportation network [77] | 72 |
| Fig. 5. 4 Urban network map of Cologne, Germany [77]..... | 74 |
| Fig. 5. 5 The simulated highway-urban trip from point A to point B that passes point P [77]..... | 78 |
| Fig. 5. 6 Speed profile by MPC-based eco-driving strategy in on an highway-urban trip | 79 |
| Fig. 5. 7 Speed profile by the rule-based EACS strategy on an highway-urban trip.. | 79 |
| Fig. 5. 8 Speed profile by MPC-based eco-driving strategy with road speed limit throughout an highway-urban trip | 83 |

| | |
|--|----|
| Fig. 5. 9 Signal anticipation by MPC-based eco-driving strategy on an highway-urban trip..... | 83 |
| Fig. 5. 10 Car-following scenarios by MPC-based eco-driving strategy on an highway-urban trip..... | 84 |
| Fig. 5. 11 The MPC-based eco-driving strategy results including (a) Brake-specific fuel consumption (BSFC), (b) Efficiency of the electric motor (EM) and (c) SOC of the battery pack on an highway-urban trip | 85 |
| Fig. 5. 12 The EACS rule-based strategy results including (a) Brake-specific fuel consumption (BSFC), (b) Efficiency of the electric motor (EM) and (c) SOC of the battery pack on an highway-urban trip | 86 |
| Fig. 5. 13 The distribution of engine working points by the MPC-based eco-driving strategy and the EACS rule-based strategy on an highway-urban trip | 87 |
| Fig. 5. 14 The exhaust emissions of HC, CO, NO _x produced by the MPC-based eco-driving strategy and the EACS rule-based strategy on an highway-urban trip..... | 87 |
| Fig. 5. 15 The simulated suburban-urban trip from point A to point B [77] | 91 |
| Fig. 5. 16 Speed profile by MPC-based eco-driving strategy on a suburban-urban trip | 92 |
| Fig. 5. 17 Speed profile by the rule-based EACS strategy on a suburban-urban trip. | 92 |
| Fig. 5. 18 Speed profile by MPC-based eco-driving strategy with road speed limit throughout a suburban-urban trip..... | 95 |
| Fig. 5. 19 Signal anticipation by MPC-based eco-driving strategy on a suburban-urban trip..... | 95 |
| Fig. 5. 20 Car-following scenarios by MPC-based eco-driving strategy on a suburban-urban trip..... | 96 |
| Fig. 5. 21 The MPC-based eco-driving strategy results including (a) Brake-specific fuel consumption (BSFC), (b) Efficiency of the electric motor (EM) and (c) SOC of the battery pack on a suburban-urban trip | 97 |
| Fig. 5. 22 The EACS rule-based strategy results including (a) Brake-specific fuel consumption (BSFC), (b) Efficiency of the electric motor (EM) and (c) SOC of the battery pack on a suburban-urban trip | 98 |
| Fig. 5. 23 The distribution of engine working points by the MPC-based eco-driving strategy and the EACS rule-based strategy on a suburban-urban trip | 99 |

Fig. 5. 24 The exhaust emissions of HC, CO, and NO_x produced by the MPC-based eco-driving strategy and the EACS rule-based strategy on a suburban-urban trip..... 99

LIST OF ABBREVIATIONS AND SYMBOLS

| | |
|-----------------------|---|
| BSFC | Brake-Specific Fuel Consumption |
| CAV | Connected and Automated Vehicle |
| CAHEV | Connected and Automated Hybrid Electric Vehicle |
| CF | Car Following |
| CO | Carbon Monoxides |
| EACS | Electric-Assist Control Strategy |
| EM | Electric Motor |
| EMS | Energy Management Strategy |
| FD | Free Driving |
| HC | Hydrocarbons |
| HEV | Hybrid Electric Vehicle |
| ICE | Internal Combustion Engine |
| ITS | Intelligent Transportation System |
| MPC | Model Predictive Control |
| NO_x | Nitrogen Oxides |
| SA | Signal Anticipation |
| TSCI | Traffic Signal Controlled Intersection |
| V2I | Vehicle-to-Infrastructure |
| V2V | Vehicle-to-Vehicle |

Chapter 1. Introduction

1.1 Background and motivation

Since the birth of the first vehicle in the late 1880s, the automobile industry has been rapidly expanding globally, and yet automobiles are playing a crucial and indispensable role in modern civilization. According to the statistical report, more than 1 billion vehicles are running on the ground on a daily basis. The development of automobile technology has brought great convenience and economic benefits to human societies. Despite that, however, some serious problems also have come into existence and become urgent global concerns, such as air pollution caused by Greenhouse Gas (GHG) and depletion of nonrenewable energy sources, especially in fossil fuel [1–4].

According to the 2020 annual statistical report by U.S. Energy Information Administration (EIA), the total global energy consumption classified by end-use sector is illustrated in Fig. 1. 1, and the total global energy-related carbon dioxide emissions classified by end-use sector is illustrated in Fig. 1. 2 [5]. It is clearly shown that the transportation sector, which consumed approximately 28 Quadrillion Btu (8.21×10^{12} kWh), accounted for around 27% of total energy consumption in 2019 and is expected to keep a steady amount of use through 2050. On the other hand, the carbon dioxide emissions of approximately 1.9 Gt produced by the transportation sector accounted for around 37% of total carbon dioxide emissions in 2019 and is expected to stay as the top carbon dioxide producer through 2050. Meanwhile, the global trends of urbanization are significantly increasing the demand for more automobiles in big cities, which will inevitably deteriorate the problems of the energy crisis and exhaust emissions.

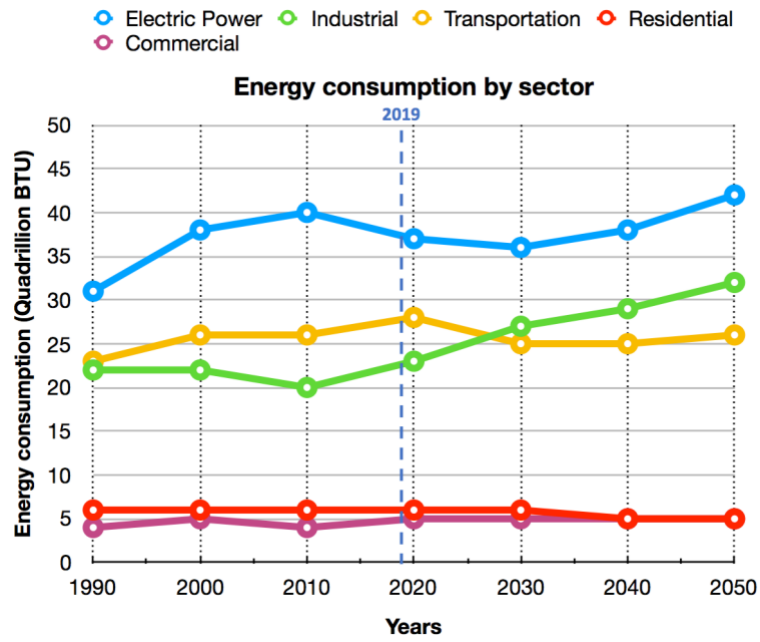


Fig. 1. 1 Energy consumption by the end-user sector [5]

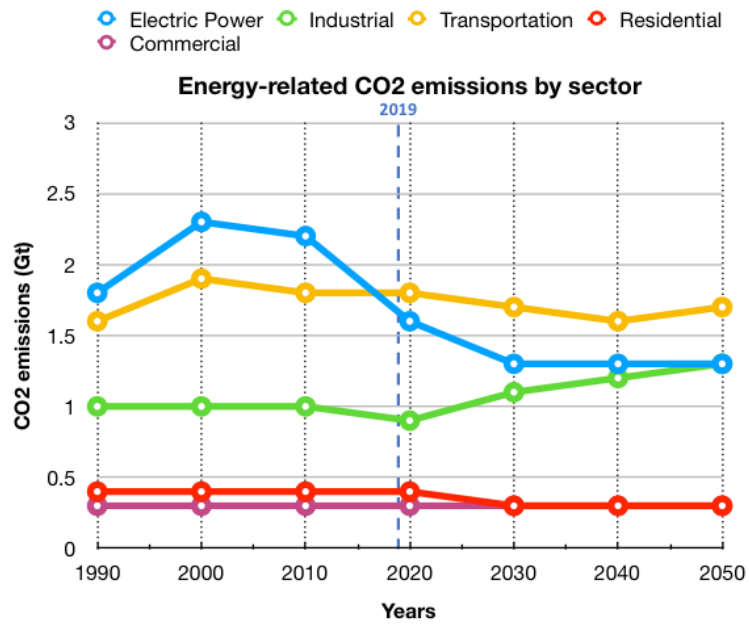


Fig. 1. 2 Carbon dioxide emissions by the end-user sector [5]

In response to those problems, many researchers in the past decades have proposed a variety of approaches, among which hybrid electric vehicles (HEVs) have shown tremendous potential to save energy and reduce pollutant emission [6, 7]. HEVs, as believed to be the transitional vehicles for automotive industry to migrate from conventional internal combustion engine vehicles to pure electric vehicles, stand out to address the problem by introducing a hybrid powertrain consisting of not only the conventional internal combustion engine but also the electric motor/generator supplied by the onboard battery pack [2, 8]. In addition, the regenerative braking technology utilized by HEVs enables the recycling of waste kinetic energy on the wheels. Such configuration design offers great flexibility in energy split control while ensuring the power demand from the wheels [2].

Since the commercialized production of HEV by Toyota and Honda, there is still an increasing effort to push for even better fuel economy and emission reduction from HEVs. This can be achieved through using a well-designed powertrain, light material to reduce aerodynamic resistance, optimal component sizing, and so on. Among those approaches, the most effective and cost-friendly one is through optimal control of power flows between the internal combustion engine and electric motor such that the powertrain can work in the most efficient state while meeting the driving demand. Therefore, adopt the right energy management strategies (EMSs) is crucial to the improvement of fuel economy and reduction in exhaust emissions [2].

For several years, great effort has been devoted to the study of energy management strategies (EMSs) for HEVs [3, 9, 10]. They can be divided into two main categories, optimization-based strategies and heuristic/rule-based strategies. In heuristic/rule-based strategies, a set of rules designed by human expertise, intuition and/or mathematical models are deployed in real-time to determine the control action for each time step [11]. Without taking into account the distinction in driving conditions, they can end up with results that have poor adaptability and accuracy. The optimization strategies, on the other hand, introduce numerical or analytical control strategies to derive the optimal actions [2]. They can be further categorized into global optimization methods and instantaneous optimization

methods. As a commonly used method of global optimization, dynamic programming (DP) can ensure the global optimality by being able to access the full information of the driving conditions *a priori* [12, 13]. Thus, it is often used as a benchmark method for many other EMSs. In real-world trips, however, it is impossible to obtain complete knowledge in advance. In addition, the complexity of DP usually leads to high computational cost, which is not suitable for the online control scenario. Pontryagin's minimum principle (PMP), as another popular global optimization method for HEVs, as compared to DP and the results showed that they were very close to the ones calculated by DP [14]. However, PMP is optimized concerning a certain driving cycle and hence cannot guarantee the optimality of other driving cycles [2, 15]. As two main instantaneous optimization methods, the equivalent consumption minimization strategy (ECMS) converts the electrical energy consumption to equivalent fuel consumption upon which the calculation for optimal control actions is based, and model predictive control (MPC), as explained by its name, makes explicit use of a model and predicted information to solve the optimal control problem over a given time horizon. Both strategies can be applied online due to relatively low computational cost and easy implementation. Unlike ECMS that determines the control for only one time instant, MPC obtains the optimal control action over a finite domain based on online rolling optimization, which ensures good control and strong robustness [15]. As a result, MPC has attracted much academic attention throughout the years, and it is widely exploited on HEV in combination with a variety of strategies, including the PMP [16], quadratic programming [17], nonlinear programming [18] or SDP [11, 19].

At the same time, the development of connected and automated vehicles (CAVs) in the intelligent transportation system (ITS) has provided a huge possibility in improving fuel economy and emission minimization as well as road safety. With the help of ITS and the upcoming ubiquitous 5G network, CAV is expected to obtain real-time data seamlessly from different sources including information via Vehicle-to-Infrastructure (V2I) communication, such as road speed limit, traffic flow data and accident location, and information via Vehicle-to-Vehicle (V2V) communication such as the position and velocity of other vehicles [20–24], as shown in Fig. 1. 3. In addition, in comparison to

human-driven vehicles, automated vehicles are designed to reliably and accurately execute real-time commands derived from control strategies [25]. Consequently, by combining the technologies of HEVs and CAVs, vehicles can achieve even better performance in road safety, energy management and emissions minimization. Current studies on connected and automated hybrid electric vehicles (CAHEVs) are limited to the applications to certain driving scenarios, such as regenerative braking scenario [26], car-following scenario [6] and traffic signal anticipation scenario [27]. However, since a common day-to-day driving trip can have complex driving conditions and consist of a combination of different driving scenarios, it is not optimal and implementable to apply the results from one scenario to some others.

Furthermore, the concept of eco-driving has been getting more and more attention because the fuel consumption and exhaust emissions are also highly correlated to the driving style of a vehicle [28]. Eco-driving, as the name explains, refers to an ecological and economical driving style that can reduce carbon emissions and improve fuel economy [29, 30]. The eco-driving method can involve techniques such as maintaining steady vehicle speed, reducing the frequency of brake pedal use, driving in a high transmission gear, shifting up in advance, and braking smoothly [31]. Conventionally, on an internal combustion engine (ICE) vehicle controlled by human drivers, eco-driving techniques are utilized through the application of Eco-Driving Assistance System (EDAS) or Eco-Driver Feedback System (EDFS) that are able to assist human drivers by providing fuel-saving information and eco indication and advice for achieving better driving behaviors [28, 31, 32]. Significant improvements have been observed by applying eco-driving techniques, according to a research [30] based on the eco-driving studies from 1985 to 2011, approximately 12% of fuel consumption was saved by implementing eco-driving systems in comparison to the results by conventional driving styles. However, with the future advancement of CAHEV technologies, the application of the eco-driving approach is expected to be more challenging yet effective on a fully automated vehicle in a connected traffic environment for the purpose of improving fuel economy and minimizing exhaust emissions.

The motivation of this research is to propose and design a novel eco-driving control strategy for connected and automated hybrid electric vehicles (CAHEVs) that is applicable to trips involving mixed driving scenarios. The objectives of the proposed strategy are improving energy management, reducing exhaust emissions and ensuring safe driving requirements. This research can also build the gap between the study of energy management strategy (EMS) applied to HEV and urban mobility regulation.

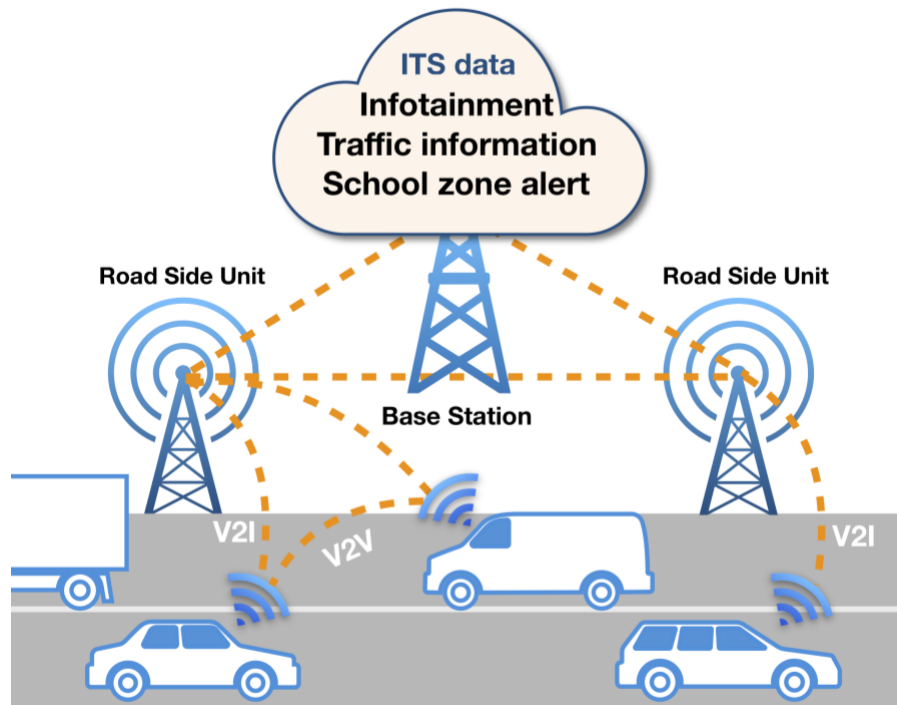


Fig. 1. 3 V2V and V2I communications for CAVs in ITS

1.2 Objectives and assumptions

The primary goal of this research is to design and develop an eco-driving strategy for CAHEVs such that safe driving can be accomplished with improved fuel economy and fewer exhaust emissions, under a combination of mixed eco-driving scenarios. The proposed control strategy outputs the real-time commands at two levels. At the upper level,

the vehicular longitudinal acceleration is determined based on the real-time data received from the communications of ITS. At the lower level, the split torque ratio between the internal combustion engine (ICE) and the electric motor (EM) is optimized. Although the lower level control strategy is designed specifically for HEVs, the vehicular longitudinal control strategy at the higher level can be easily extended to vehicles of various types, such as conventional internal combustion engine vehicles, plug-in hybrid electric vehicles, electric vehicles, etc.

The detailed objectives of this research include:

- (1) To model an HEV of the parallel hybrid configuration, which includes an internal combustion engine (ICE), an electric motor (EM) and a battery pack.
- (2) To build up the real-time data exchange based on Vehicle-to-Vehicle (V2V) and Vehicle-to-Infrastructure (V2I) communications in a realistic traffic simulation environment.
- (3) To design a model predictive control (MPC) based automated eco-driving strategy that optimizes three goals during driving 1) safe driving, 2) energy-saving, and 3) emission reduction.
- (4) To design a real-time classifier of driving scenarios for the studied vehicle in a realistic traffic simulation environment. The driving scenarios are classified into three cases 1) free driving scenario, 2) signal anticipation scenario and 3) car-following scenario.
- (5) To develop the cost function for the above three objectives. And to tune the weighting factors among the proposed multi-objective optimization to obtain reasonable and optimal results.

- (6) To make comparative studies between the proposed MPC-based strategy and the conventional rule-based strategy in a realistic traffic simulation environment

The following assumptions are made throughout the thesis

- (1) The communication time via Vehicle-to-Vehicle (V2V) and Vehicle-to-Infrastructure (V2I) is neglected.
- (2) All the roads in the network are assumed to be flat road, i.e. road grade is zero.
- (3) The distances covering the intersection regions are neglected in odometry
- (4) The background traffic simulation is accident-free and collision-free
- (5) Only the host vehicle is connected and automated vehicle (CAV), the background vehicles are assumed to be connected vehicles (CVs) only

1.3 Contributions

To the knowledge of the author, the main contributions of this research are listed below:

- (1) A bi-level MPC-based eco-driving for CAV is proposed to improve fuel economy, reduce emissions based on driving safety.
- (2) The proposed strategy can be adapted to trips with a combination of mixed driving scenarios, namely, the free driving, the signal anticipation at the traffic signal controlled intersections (TSCIs) and car-following scenarios.

- (3) The system makes use of real-time information via Vehicle-to-Vehicle (V2V) and Vehicle-to-Infrastructure (V2I) connections to exploit the potential of MPC in realizing the objectives.
- (4) The simulation results based on a realistic simulation map are presented and compared to the rule-based strategy.
- (5) The proposed strategy provides a promising opportunity to exploit the potential of CAHEVs under realistic trips with all-inclusive driving scenarios.

1.4 Outline

The thesis is organized as follows:

- **Chapter 1 Introduction** introduces the challenges in the research area and the latest technologies which the study is based on. Also, the motivation of this work is presented, as well as the unique contributions from this study.
- **Chapter 2 Literature Review** reviews the existing energy management strategies for HEVs, the eco-driving strategy for CAVs. A review of the blending of these two strategies is also given, and the research gaps are identified and explained.
- **Chapter 3 Model Development** introduces the studied HEV model, including the modelling of the internal combustion, electric motor, battery pack and the longitudinal dynamic model. Followed by the introduction of the Vehicle-to-Vehicle (V2V) and Vehicle-to-Infrastructure (V2I) in the intelligent transportation system (ITS)

- **Chapter 4 Methodology** describes the eco-driving problem to be solved, which is then formulated in the framework of the MPC-based algorithm regarding the objectives of driving safety, energy economy and emission. The benchmark eco-driving strategy that is made up of a rule-based energy management strategy and a realistic driver model is also introduced.
- **Chapter 5 Results and Discussion** provides the simulation details, and the results run by the proposed MPC-based eco-driving strategy and the rule-based strategy are shown and compared. Finally, the analysis based on the comparison results is given.
- **Chapter 6 Conclusion and Future Works** concludes the current work and suggest future works to be done.

Chapter 2. Literature Review

2.1 Introduction

So far, the control strategies for HEVs and CAVs have been extensively studied in the literature. This chapter aims to provide a comprehensive review of the existing literature, emphasizing mainly on the contributions to the control strategies for the connected and automated parallel hybrid vehicles (CAHEVs). In the end, the research gaps are also identified and explained.

The review will be initiated by the introduction to the research background, HEV configurations and CAV technologies. Then, the existing literature on control strategies for HEV and CAHEV will be reviewed and evaluated in depths, concerning their control principles, advantages, drawbacks, limitations as well the contributions towards the fulfillment of several optimization objectives, including the minimization in fuel consumption and exhaust emission, the ability to maintain the battery SOC and the driving safety-related issues, if applicable. Finally, the research gaps in the literature will be identified and explained to pave the way for developing the proposed strategy in the following chapters.

2.2 Hybrid electric vehicles

Hybrid electric vehicles refer to the type of vehicle that is equipped with a hybrid powertrain consisting of not only the conventional fuel supplier but also the additional electrical energy supplier from the onboard battery pack [2, 8]. For this reason, they are considered as the transitional technologies for the automotive industry to migrate from conventional internal combustion engine vehicles to pure electric vehicles. The hybrid

configuration design offers great flexibility in energy split control while ensuring the power demand from the wheels [2].

Compared with the operation of conventional vehicles, the internal combustion engine (ICE) on the HEVs can be assisted by the electric energy supplier when the engine efficiency is relatively poor, and it can be fully decoupled from the drivetrain when there is sufficient electric power to drive the vehicle. Besides, the regenerative braking can restore the kinetic braking energy from deceleration to charge the battery pack, which is otherwise wasted in the process of braking as for ICE vehicles [33]. As a result, a better fuel economy and fewer emissions from the engine can be achieved.

One of the widely used methods to classify HEVs is based on the configurations of the vehicle powertrain. They are classified as 1) Series Hybrid, 2) Parallel Hybrid, and 3) Series-Parallel Hybrid.

2.2.1 Series Hybrids

The series hybrid configuration generally involves an internal combustion engine (ICE), a generator, an electric motor (EM), an electrical energy storage system, as shown in Fig. 2. 1 [34]. It is often likened to the battery electric vehicle (BEV) configuration since there is no direct mechanical connection between the internal combustion engine (ICE) and the wheels, rather, the power provided from the ICE is converted to electrical power by the generator to charge both the battery pack and power the EM to drive the wheels [2] It's worth noting that the regenerative braking is taken to charge the battery pack when the vehicle is decelerating or driving downhill. During urban driving, the ICE is turned off, and the electrical energy stored in the battery is transmitted to the EM to propel the vehicle. During country driving, the ICE is turned on as there is a large amount of power required from the wheels at high speed [35]. The advantage of this design is that the ICE can always operate at its high-efficiency working region and reduce fuel consumption [10, 34]. This benefit, however, is outweighed by the fact that there is a high requirement for the onboard

battery pack to be expensive and powerful with high energy density [2]. Series hybrid configuration is often applied to heavy-duty commercial vehicles such as New Tesla Buses, TEMSA Avenue Hybrid Buses, Mercedes Citaro Buses, and so on [2, 35].

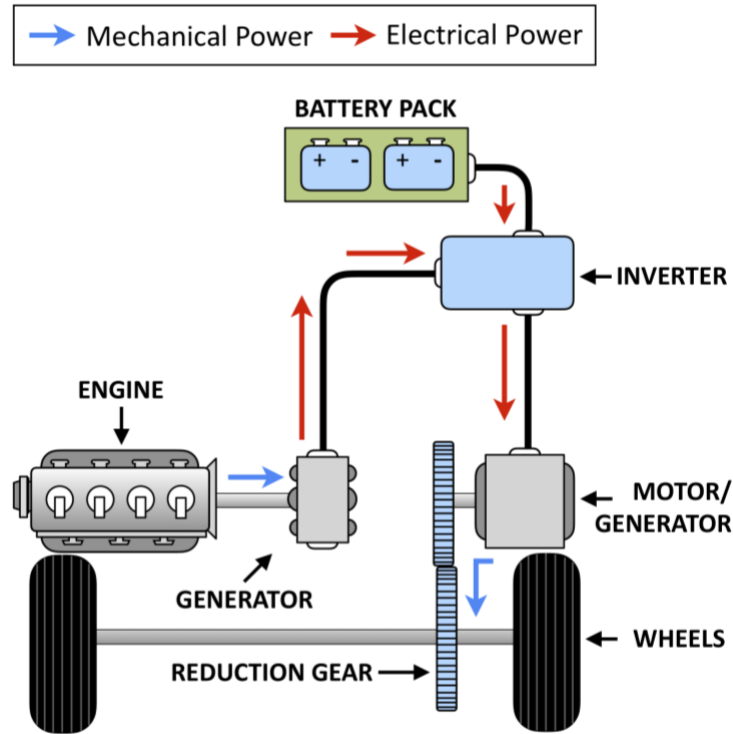


Fig. 2. 1 The series hybrid powertrain

2.2.2 Parallel Hybrids

In the parallel hybrid configuration, the powertrain consists of an internal combustion engine (ICE), an electric motor (EM), a battery pack as the electrical energy storage system, as shown in Fig. 2. 2. It is named parallel because both the ICE and EM can work independently or together to provide working torques to propel the vehicle [2, 34]. Different from the series hybrid configuration, the ICE of the parallel hybrid powertrain has a mechanical connection to the wheels via a gearbox. The EM can work as an assistant power supplier or the sole power supplier to the ICE depending on the power size of EM,

and it can work as a generator during the battery pack being charged by either the ICE or the kinetic power from regenerative braking [2]. When the battery state of charge (SOC) is high, the vehicle can be driven by the EM alone or by both ICE and EM together. When the battery state of charge (SOC) is low, the redundant power output from the ICE can be used to charge the battery pack. The advantage of this design is the flexibility of choosing between the ICE and EM to propel the vehicle, which decouples the ICE from the powertrain and enables it to work in the high-efficiency mode. However, with dual driving machines, it often leads to a more complex control strategy and high computational cost [35]. In addition, the working modes of parallel hybrid vehicles do not perform well in the frequent stop-and-go condition as in urban driving. Examples of vehicles with hybrid electric configurations include Honda Insight, Ford Escape Hybrid SUV and Lexus Hybrid SUV [35].

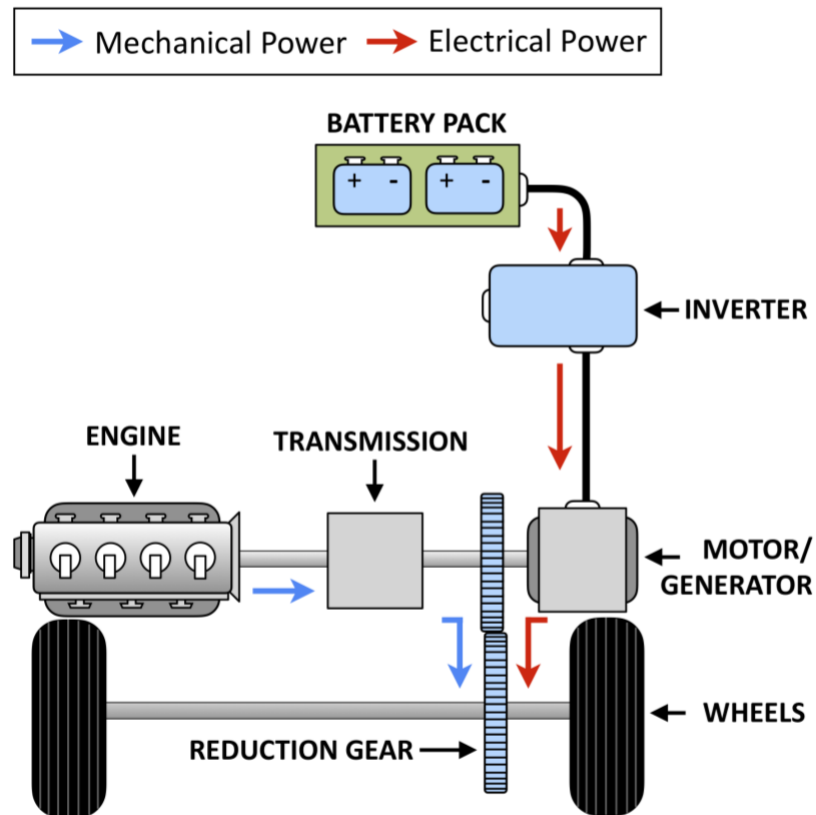


Fig. 2. 2 The parallel hybrid powertrain

2.2.3 Series-Parallel Hybrids

The series-parallel hybrid configuration consists of an internal combustion engine (ICE), motor/generator (M/G1), motor/generator (M/G2), inverter, battery pack, and power-split device, as shown in Fig. 2. 3. As the name explains, the series-parallel hybrid combines the advantages of both series hybrid design and parallel hybrid design while getting rid of their disadvantages by integrating both the series and parallel energy path, as shown in Fig. 2. 3 [10, 36]. As a result, the powertrain component sizing problem can be solved by running the parallel hybrid mode. On the other hand, the frequent stop-and-go condition, which is unsuitable for parallel hybrid design, is overcome by the ability to have the battery charged when the vehicle remains stopped [10]. However, in comparison to the aforementioned configuration, the additional flexibility offered by the series-parallel hybrid configuration adds more complexity in the powertrain structure and the control strategy that can take the full use of its potential. Applications of the series-parallel hybrid configuration on commercial vehicles include Toyota Prius, Lexus LS 600h and Nissan Tino [37].

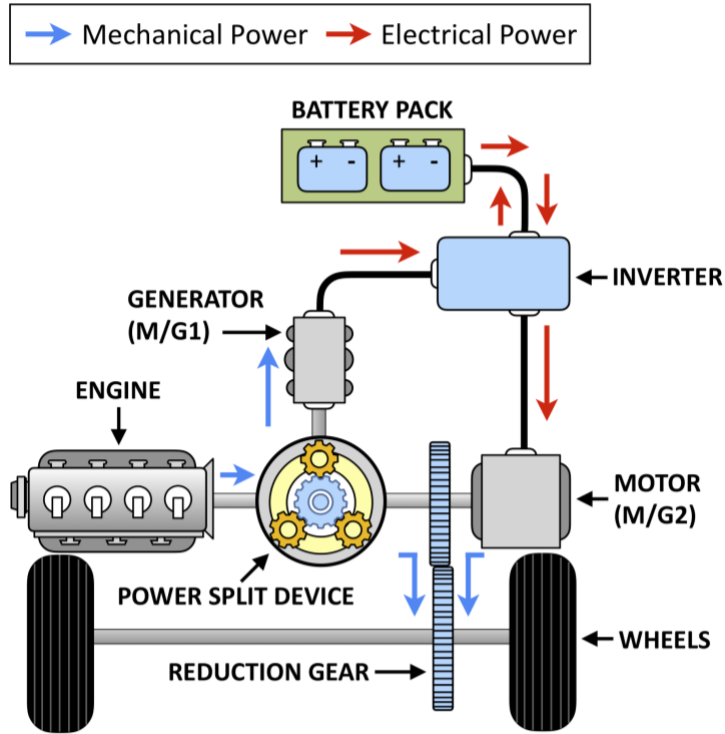


Fig. 2. 3 The series-parallel hybrid powertrain

2.2.4 Driving Cycle

A driving cycle is a sequence of data points representing vehicle speed versus time [38, 39]. Besides, it can also include many other driving parameters concerning the resultant vehicle performances, such as vehicle powertrain conditions, dynamometer settings, transmission shift points, cold start conditions, and so on [40]. As a result, driving cycles are often used as a way to evaluate and compare vehicle performances, *e.g.* fuel/energy management and exhaust emissions, in a reproducible way [40].

Since the 1970s, great effort has been contributed to developing standard driving cycles in many countries [41]. Among the well-established driving cycles, the widely used ones include the New European Driving Cycle (NEDC) of Europe, Urban Dynamometer

Driving Schedule (UDDS) and EPA Federal Test Procedure (FTP-75) of USA and Japan Cycle 08 (JC08) of Japan. Fig. 2. 4 illustrates the UDDS driving cycle.

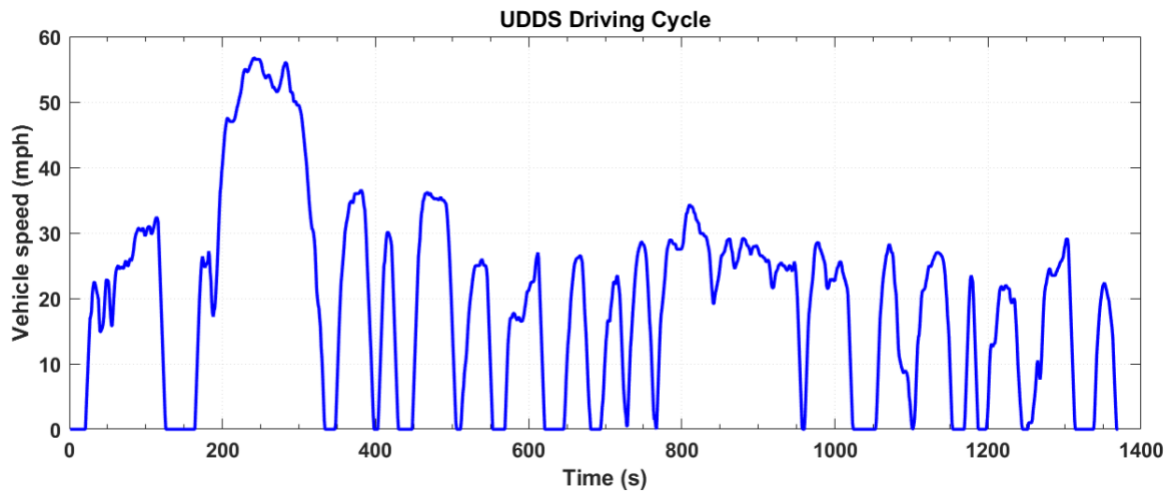


Fig. 2. 4 The Urban Dynamometer Driving Schedule (UDDS)

2.3 Connected and automated vehicles (CAVs)

Connected and automated vehicles (CAV), as the name explains, is the combination of connected vehicle (CV) and the automated vehicle (AV). In the technology of CV, road vehicles are able to get real-time access to information from different resources via wireless connections. With access to the information in the network, the driving performance can thus be improved such as accident avoidance, road safety, time-saving, energy-saving and emission reduction. The connections are classified into two main types, Vehicle-to-Infrastructure (V2I) communication and Vehicle-to-Vehicle (V2V) communication. Via Vehicle-to-Infrastructure (V2I) communication, a vehicle is able to access information through the roadside infrastructures about the speed limit, weather forecast, school zone and collision alert, traffic congestion location, and so on. With the help of Vehicle-to-Vehicle (V2V) communication, vehicles in the same region mutually share vehicular data, including vehicle type, position, speed, acceleration, intended action, route, and so on. As

a result, the comprehensive knowledge of the network gained in real-time can assist the vehicle in a better decision-making process.

On the other hand, the automated vehicle (AV), which is fully controlled by vehicular control systems, was designed to compensate for the inaccuracy and inconsistency in human driving. For example, even with the knowledge of the road speed limit, the human driver may exceed the limit by occasionally over pushing the pedal position. Also, limited by the human attention span, a driver could make some fatal mistakes after an excessive and continuous long driving. Therefore, the automated vehicle system is able to consistently execute real-time driving commands accurately to the vehicle that ensures on-road driving safety.

CAVs also offers great potential in improving the fuel economy and reduce the pollutant emissions, as will be reviewed in Chapter 2.3.

2.3.1 Eco-Driving scenarios

Eco-driving stands for the type of control policy that the driver, either human or smart vehicle, execute to minimize the fuel consumption and exhaust emissions. In this study, the eco-driving is narrowed to the set of control commands by the automated vehicle system to drive the connected and automated hybrid electric vehicles (CAHEVs) for reducing the fuel consumption and pollutant emissions. Many factors are involved that affect the eco-driving performance, including vehicle speed, acceleration and deceleration, idling state, and so on. On the other hand, the optimal route choice belongs to the category of eco-routing. Therefore, it is out of the scope of this study.

Some of the most common eco-driving scenarios can be presented in a non-exhaustive list, which includes [25]:

1. Accelerating to a cruise speed: the vehicle begins with a given speed v_i , and continuously accelerates to a target speed v_f ($v_f > v_i$)
2. Cruising: the vehicle keeps the speed v_i constant to a target speed $v_f = v_i$
3. Decelerating to a final speed: the vehicle continuously decelerates its speed v_i to a lower target speed v_f ($v_f < v_i$)
4. Driving between stops: the vehicle begins with $v_i = 0$ and ends the trip with $v_f = 0$
5. TSCI approaching: the vehicle approaches a TSCI from a speed v_i to a speed v_f either $v_f = 0$ when the traffic signal does not permit vehicle passing, or $v_f > 0$ when the traffic light allows vehicle passing
6. Urban trip: the vehicle drives in urban condition with frequent stop-and-go which can involve 1~5
7. Highway trip: the vehicle drives in highway condition in a relatively high driving speed with few to none stop, which can involve 1~4
8. Car following: the vehicle speed v_i is constrained by the preceding vehicle speed v_f since a safe inter-vehicle distance is meant to be kept

For the sake of designing an eco-driving system for all the above scenarios, the listed ones are therefore classified into three main categories, as (I) free driving scenario: includes case 1~4, (II) signal anticipation scenario: includes case 5, and (III) car-following scenario: includes case 8. Case 6 and 7 are compounded cases that can be achieved by realizing their component cases. In the rest of the study, the control strategies for connected and automated hybrid electric vehicles (CAHEVs) will be proposed and designed in accordance with each of the above-mentioned categories.

2.4 Literature review on control strategies for CAHEVs

2.4.1 Energy management strategies (EMSs) for HEVs

The main challenge in the powertrain operation of HEV comes from the optimal control of power flow between the ICE and the EM to meet the driving demand while improving the energy economy and reduce the exhaust emissions at the same time [10]. Regardless of the type of HEVs, adopting the right energy management strategies (EMSs) are crucial to the realization of these goals [2].

The topic of EMS has been extensively studied with the development of HEV during the past decades, and a great many strategies have been proposed. For the EMS, the inputs usually include vehicle power demand, vehicle speed and acceleration, battery state of charge (SOC) and sometimes the future traffic condition obtained from GPS or intelligent transportation system, if applicable [2]. The output commands of control strategies decide in what mode the vehicle should operate, for example, regenerative braking mode, ICE-only mode, and so on [2]. Until now, the existing EMS can be classified into two main categories: 1) rule-based control and 2) optimization-based control, as shown in Fig. 2. 5. Prior to the introduction to different types of EMSs, the HEV operation modes will be described.

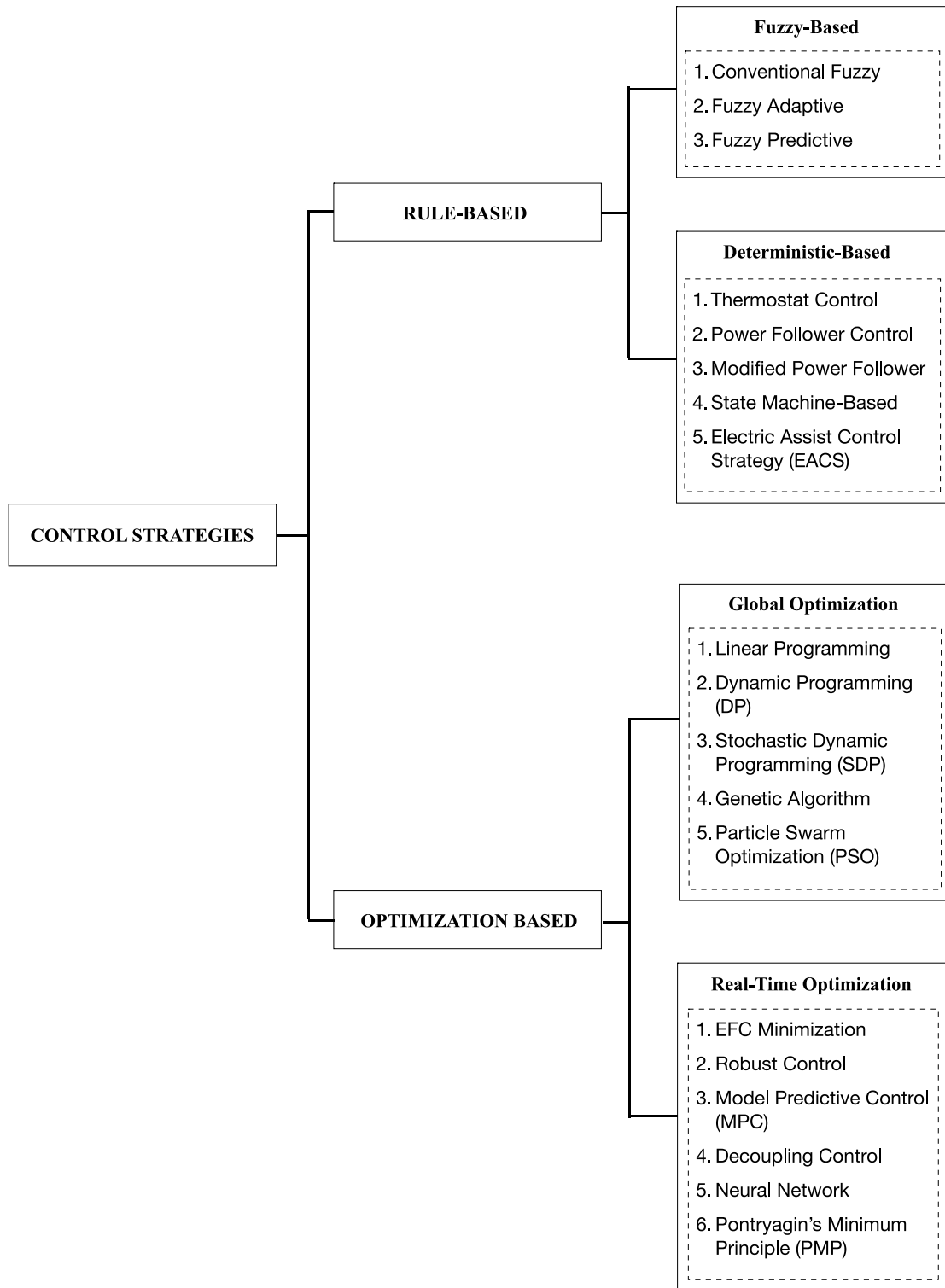


Fig. 2. 5 The classifications of control strategies for HEV

2.4.1.1 HEV working modes

The control action in a parallel hybrid electric powertrain mainly concerns how to determine the best split ratio between the mechanical power provided by the ICE and the electrical power provided by EM in a way that minimizes the optimization goals. The power paths, along with the vehicle modes, are shown in Fig. 2. 6 and Table. 2. 1, and the split ratio to be determined is defined as the ratio of the electrical power $P_{EM}(t)$ to the total required power $P_{req}(t)$ as,

$$u(t) = \frac{P_{EM}(t)}{P_{req}(t)} \quad (1. 1)$$

Table. 2. 1 HEV working modes

| Operation mode | $u(t)$ | Clutch |
|--------------------------|----------------|---------------|
| Engine only | 0 | Open |
| Electric only | 1 | Closed |
| Hybrid / Electric assist | (0,1) | Open |
| Battery charging | $(-\infty, 0)$ | Open |
| Regenerative Braking | $(-\infty, 0)$ | Closed |

Among the above working modes, the engine only mode is when the sole vehicle power depends on the output power of ICE that helps ICE to remain in its high-efficiency region. The electric-only mode refers to the mode when the vehicle is propelled by the electrical energy supplied by the EM. It is on when the ICE operates in low efficiencies, such as at low vehicle speed. The hybrid / electric assist is on either when the required power from the wheels is higher than the power provided by the ICE, or to make the ICE work at high torque region. When the battery SOC is lower than the preset limit, the vehicle switches to battery charging mode to charge the battery using excessive engine power. When the

vehicle is decelerating, the EM is able to work as a generator to absorb the braking kinetics to charge the battery.

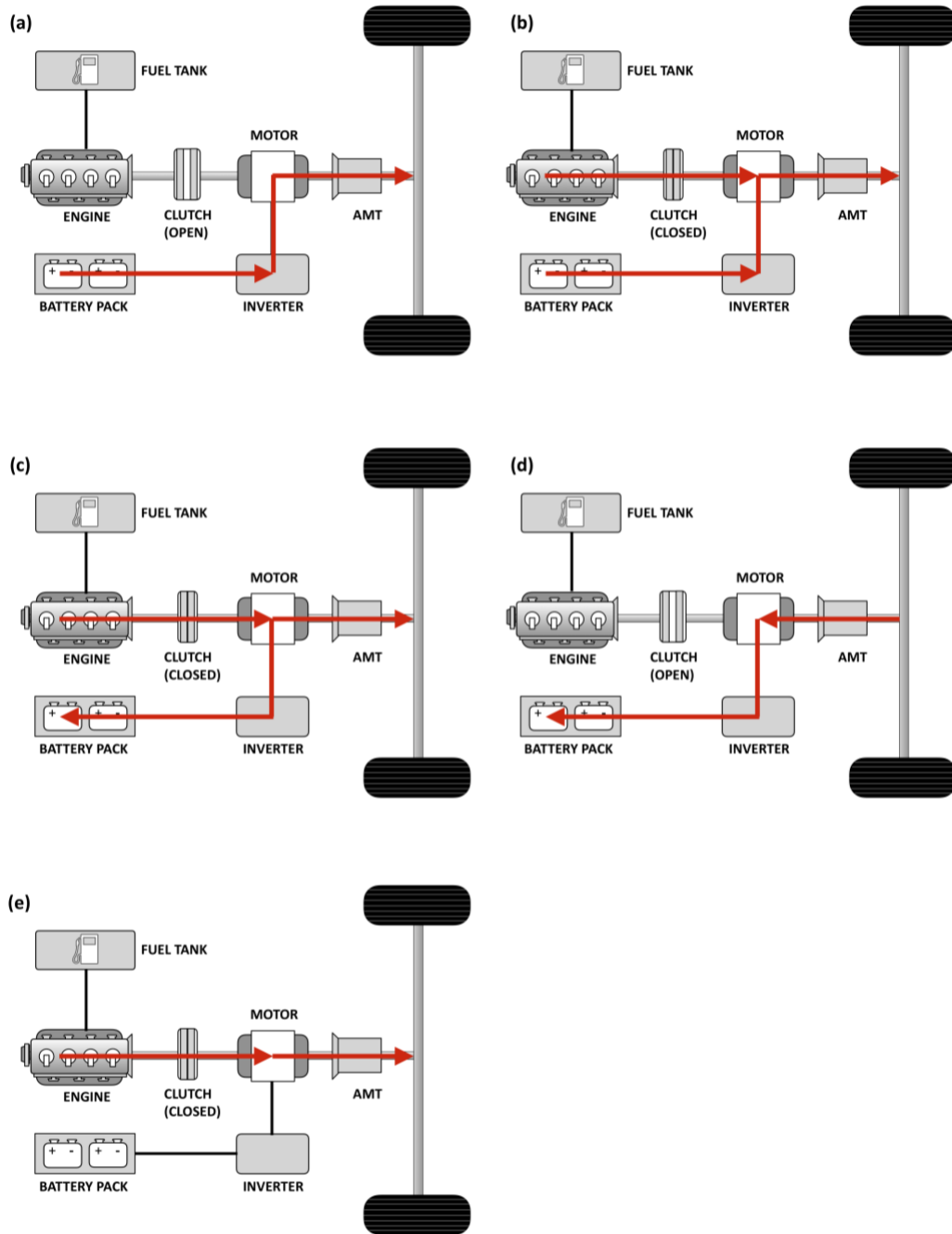


Fig. 2. 6 The vehicle working modes, (a) electric only, (b) hybrid / electric assist, (c) battery charging, (d) regenerative braking, (e) engine only

2.4.1.2 *HEV rule-based control strategies*

The rule-based control strategies, as the name indicates, make use of simple rules derived from human expertise (engineering knowledge), mathematical models, intuition with the *a priori* information of a driving cycle, to control the power flow in the hybrid powertrain [35, 37]. They are the most widely used strategy to implement in real-time for an HEV [2]. The advantage of rule-based control strategies is their low computational cost and simplicity in real-time execution [10]. The drawbacks, however, are that the set of pre-defined rules is only optimized for a certain driving cycle or driving condition. Therefore it produces results that are non-optimal or sometimes far from optimal unless the knowledge of real-time driving cycle is fully apprehended [10]. The rule-based strategies can be further categorized as deterministic-based strategies and fuzzy-based strategies.

In deterministic-based strategies, a pre-defined lookup table that has a set of fixed rules is used to deliver real-time control to the vehicle [37]. For example, Kim *et al.* [42] proposed a deterministic rule-based strategy for HEV with the continuously variable transmission (CVT) that derived the hybrid optimal operation line (HOOL) based on a set of principles for converting battery power to equivalent fuel consumption. As a result, optimal control variables such as gear ratio, engine torque and motor torque can be obtained online, and fuel consumption can be reduced. Similarly, in order to make a parallel HEV work properly according to the power demand and battery SOC, the power follower (baseline) control strategy [43] controls the engine on/off state based on a set of pre-defined rules. Also, Jalil *et al.* [44] designed a thermostat control strategy for a series HEV that applied a simple rule to maintain the battery SOC in the upper and lower bounds by turning the engine on/off. The results were compared to another rule-based strategy to show the improvement in fuel economy. Electric-assist control strategy (EACS) [45] probably is the most successfully applied and widely used deterministic rule-based strategy for HEV in which the engine works as the main power source while the motor serves to assist the engine when the required demand is higher than the engine can provide, or when the engine works in low-efficiency region [2]. The maintenance of the SOC level is also considered

in the rules. However, a large number of parameters in EACS increase the sensitivity to driving patterns and result in less robustness.

Though the above mentioned deterministic rule-based strategies show good results in certain driving condition and profile, however, a huge amount of time will be needed to tune and calibrate the strategies to work for other driving conditions, thus are less adaptive and robust to complex driving conditions such as real-world traffic scenario. In response to the above disadvantages of deterministic rule-based strategies, fuzzy rule-based strategies were designed to tackle those issues.

Basically, fuzzy-based control strategies are derived from conventional deterministic rule-based strategies. However, unlike the deterministic rules as in previous methods, in a fuzzy rule-based controller, the linguistic commands are converted into multivalued logical rules using fuzzy set theory. Consequently, they are more robust and tolerant of imprecise measurements and system variations and more adaptive to various driving conditions [46]. For example, in [47], a fuzzy rule-based strategy was proposed for a parallel HEV. A dynamo test was performed to set up the fuzzy relationship between the inputs of acceleration pedal stroke and motor speed, and the output motor torque command. The results show the robustness to disturbances and a 20% reduction in NO_x emissions with balanced battery level. Moreover, as the objectives of minimizing fuel consumption and emissions are often conflicting, for instance, a decrease in fuel consumption would lead to an increase in exhaust emissions, an adaptive fuzzy rule-based strategy [48] as designed to make a trade-off between the objectives of fuel and emissions by using the weighted sum approach. With the relative weights assigned, a significant reduction was found in emissions at the expense of a negligible increase in fuel consumption. In addition, unlike the above fuzzy rule-based strategies that aim to achieve local best solutions, a global best solution can be obtained by obtaining the knowledge of the trip in advance. Therefore, Ichikawa *et al.* [49] proposed a predictive fuzzy rule-based strategy that is able to predict the future driving pattern from the historical data. Based on the predicted driving pattern, a set of fuzzy rules were set up to execute better engine commands for an HEV.

Typically, the rule-based strategies are easy to implement, hence widely used in real-time control. Due to the fact that they are derived from heuristic rules and human expertise rather than an optimization approach based on numerical models, they often produce near-optimal results. The summary of rule-based strategies is listed in Table. 2. 2.

Table. 2. 2 Summary on rule-based energy management strategies for HEV

| Strategy | Category | Online/Offline | Descriptions |
|-------------------------|--------------------------|-----------------------|---|
| HOOL-based [42] | Deterministic rule-based | Online | <ul style="list-style-type: none"> ▪ The hybrid optimal operation line (HOOL) derived from a set of pre-defined rules ▪ Tuned for specific driving conditions |
| Power follower [43] | Deterministic rule-based | Online | <ul style="list-style-type: none"> ▪ Engine power state controlled by a set of rules ▪ Tuned for specific driving conditions |
| Thermostat [44] | Deterministic rule-based | Online | <ul style="list-style-type: none"> ▪ Engine controlled by a set of rules for balancing battery SOC ▪ Tuned for specific driving conditions |
| EACS [45] | Deterministic rule-based | Online | <ul style="list-style-type: none"> ▪ Most widely used deterministic rule-based strategy for HEV ▪ Motor assisting engine based on a set of rules with battery SOC considered ▪ Tuned for specific driving conditions |
| Conventional fuzzy [47] | Fuzzy rule-based | Online | <ul style="list-style-type: none"> ▪ Motor operation determined by a set of fuzzy rules from dynamo test ▪ More adaptive and robust than deterministic rules |
| Adaptive fuzzy [48] | Fuzzy rule-based | Online | <ul style="list-style-type: none"> ▪ Weighted-sum optimization based on adaptive fuzzy rules ▪ More adaptive and robust than deterministic rules |
| Predictive fuzzy [49] | Fuzzy rule-based | Online | <ul style="list-style-type: none"> ▪ A set of fuzzy rules for predicting future driving patterns based on historical data ▪ More adaptive and robust than deterministic rules |

2.4.1.3 *HEV optimization-based control strategies*

In optimization-based strategies, the control system adopts an analytical or numerical approach to minimize a cost function that can have either single or multiple objectives [37]. They can ensure a higher degree of optimality than rule-based strategies. However, the calculation usually imposes a heavy burden on the computer. They can be further divided into global optimization and real-time optimization.

In global optimization, the entire knowledge of driving conditions is required *a priori* to derive the global optimal control policies for HEV. For example, dynamic programming (DP), which is derived from Bellman optimality equations, is often used as a benchmark method for other strategies because it can guarantee global optimal results once the knowledge of driving pattern is given. In the study [50], dynamic programming (DP) was applied on a hybrid electric truck to find the global optimal control policies, including the gear shifts and power split between the engine and motor while keeping the battery in a balanced SOC. The optimal results show a considerable amount of emissions were reduced in the sacrifice of a small amount of fuel increase. However, the results calculated by the dynamic programming are only optimized for a specific driving cycle, that is to say, the results are not guaranteed to be global optimal when the results are applied in other driving conditions. As a remedy, stochastic dynamic programming (SDP) was utilized by Lin *et al.* [51] on a parallel HEV to obtain optimal instantaneous engine output power. In this SDP, on the basis of a few pre-defined typical driving cycles, the vehicle power demand is modelled as a random Markov process in which the current state variables can be derived by a state transition probability solely from the previous state instead of from the historical states. As a result, the optimized control policy is in the form of stationary full-state feedback over a set of preset random driving cycles in an average sense [2] and can be applied to different driving cycles. Though more adaptive than DP, the optimality of SDP is highly concerned with the similarity between the pre-defined driving cycle and the tested driving conditions, including the type of roads, the impact of weather, mixed traffic congestion, and so on. Moreover, DP and SDP suffer from high computational cost due to

the intrinsic complexity of Bellman equations. Genetic algorithm (GA) is another approach to achieve global optimality, which is inspired by Darwin's theory of evolution. GA begins with a group of chromosomes representing the preliminary solutions. The chromosomes can perform mutation and crossover in order to produce the offspring candidate for the optimal solution, and this process repeats itself until the terminal condition is reached [2]. It is useful for solving constrained nonlinear optimization problems [46]. For example, GA was adopted in [52] for a series HEV. In this study, the problem of fuel economy and emission reduction is formulated as a multi-objective optimization and is solved by GA. The results demonstrate the effectiveness of GA in solving constrained multi-objective optimization. Nevertheless, due to the time-consuming computation spent on mutation, crossover and selection, GA is not readily implementable in real-time. Another approach originated from natural phenomenon is particle swarm optimization (PSO). It was inspired by the social behaviour of bird-flocking in which the particles that are the representation of birds are searching around a solution space for improving better solutions over the steps [2]. In [53], for example, Huang *et al.* adopted PSO on the multilevel hierarchical control to minimize the fuel consumption for a parallel HEV. The results showed an improved fuel economy was achieved in comparison to a built-in control strategy in the PNGV system analysis toolkit (PSAT). Like previously mentioned global optimization strategies, PSO also suffers from high computational cost and is not suited to be used online.

On the other hand, the real-time optimization strategies intend to minimize the instantaneous cost function in a short domain. This is accomplished by breaking down the global optimization into a sequence of local optimization. Consequently, the total time cost can be greatly shortened [2]. Despite producing sub-optimal results when compared with global optimization approaches, real-time optimization strategies have received great attention from researchers in the field of HEV control [2]. For instance, Pontryagin's minimum principle (PMP) is among the most popular real-time optimization strategies for HEV power management. PMP can be used under the assumption that the optimal solution can be found through the instantaneous minimization of a Hamiltonian function over a given driving cycle [2, 54]. For example, in the study of [55], PMP was employed to derive

the control law for a plug-in HEV. The results demonstrate that by an acceptable approximation of the co-state from the past driving patterns, the produced results can be near-optimal in comparison to the global optimal solutions produced by DP. The drawback of PMP lies in that the co-state as the only variable is highly related to the selected driving patterns. As a result, the optimally tuned PMP that works for a family of driving patterns can be suboptimal in other driving patterns. While in equivalent consumption minimization strategy (ECMS), the solving Hamiltonian function is simplified to the calibration of the equivalent factor λ that balances the use between fuel and electrical energy. It is proposed by Paganelli *et al.* [56] as a way to achieve an optimal solution by minimizing the instantaneous weighted sum cost function consisting of the actual fuel consumption, and the equivalent fuel consumption from the electrical energy [11]. In the study by Sciarretta *et al.* [57], the cost function that adds up the instantaneous fuel consumption and the equivalent fuel consumption based on the electrical energy is minimized at each time step, and a fuel reduction up to 50% was found when compared with other conventional algorithms. The problem with ECMS is that the calibration of the equivalent factor λ requires full knowledge of the driving cycle or future driving prediction in the optimization [58]. Whereas the actual driving pattern often differs from the pre-defined one in ECMS, the results will be compromised and thus is not optimal. Model predictive control (MPC) is another type of strategy that can be implemented in real-time. In MPC, the optimal control problem in the finite control horizon is solved at each time instant, and the optimal set of control actions is obtained as the first element of the optimal control policy in the control horizon. To solve optimization problems, MPC can be matched to a variety of strategies including the PMP [16], quadratic programming [17], nonlinear programming [18], or SDP [11, 19]. In recent years, different types of MPC have been widely used in HEVs due to its rapid computation, capability in dealing with constrained multivariable problems and potential for solving optimization problems as a receding horizon control strategy [11]. For example, Sun *et al.* [59] developed a bi-level MPC-based energy management strategy for plug-in HEV that utilizes the real-time traffic data to control the battery SOC and reduce fuel consumption simultaneously. The results showed a 94%~96% fuel optimality was achieved in comparison to the results by DP. Similarly, in the study

[27], a bi-level MPC was applied to an HEV to achieve eco-driving in an urban driving condition. In this control strategy, the optimal vehicle velocity is determined at the upper level, while the torque split ratio and gear shift are optimized at the lower level. The results show an improvement in fuel economy. The summary of optimization-based strategies is listed in Table. 2. 3.

Table. 2. 3 Summary on optimization-based energy management strategies for HEV

| Strategy | Category | Online/Offline | Descriptions |
|--------------|------------------------|----------------|---|
| DP [50] | Global optimization | Offline | <ul style="list-style-type: none"> ▪ Often used as a benchmark strategy ▪ Required knowledge of driving conditions ▪ Optimized for the specific driving cycle(s) ▪ High computational cost |
| SDP [51] | Global optimization | Offline | <ul style="list-style-type: none"> ▪ Based on a state transition probability obtained by driving cycles ▪ More adaptive than DP ▪ High computational cost |
| GA [52] | Global optimization | Offline | <ul style="list-style-type: none"> ▪ Inspired by Darwin’s theory of evolution ▪ Complexity growing with solution spaces ▪ High computational cost |
| PSO [53] | Global optimization | Offline | <ul style="list-style-type: none"> ▪ Inspired by natural phenomenon ▪ High computational cost |
| PMP [55] | Real-time optimization | Online | <ul style="list-style-type: none"> ▪ Among the most popular strategies ▪ Tuned for specific driving cycles ▪ For real-time implementation |
| ECMS [57] | Real-time optimization | Online | <ul style="list-style-type: none"> ▪ Simplified version of PMP ▪ Tuned for specific driving cycles ▪ For real-time implementation |
| MPC [27, 59] | Real-time optimization | Online | <ul style="list-style-type: none"> ▪ Widely used strategy on HEVs ▪ Capable of dealing with constrained multivariable problems ▪ A receding horizon control strategy ▪ For real-time implementation |

2.4.2 Control strategies for CAHEVs

In addition to the potentials of improving the powertrain working efficiency enabled by various EMSs of HEVs, the recent emergence of connected and autonomous vehicles (CAVs) in the context of Intelligent Transportation Systems (ITS) have offered an unprecedented opportunity for energy saving and emission reduction in automobiles. So far, some studies have been done concerning the control strategies for connected and automated hybrid electric vehicles (CAHEVs). The following reviews will be done for each of the categories listed in Chapter 2.3.1.

For the scenario of free driving, for example, in [60], the integration of V2I data into the MPC-based EMS enables the system to obtain an optimal driving profile, and reduced vehicle emissions for a hybrid electric bus over a fixed route with knowledge obtained *a priori*. Also, in the study [61], based on a reference driving cycle, the vehicle speed trajectory was generated offline by dynamic programming (DP) to realize the goal of fuel economy, and the results indicate the effectiveness of applying eco-driving to vehicles with HEV configuration. Similarly, in [62], given a series of target speed points, the torques and speeds of ICE and EM are determined by an MPC-based strategy to control the vehicle speed to improve the driving performance. In [26], Wu *et al.* designed a hierarchical control strategy with the consideration of the battery ageing problem for HEV in the case of regenerative braking. During the braking process, an upper-level controller is able to control the decelerating speed, which is sent to the lower level to optimize the power path in the vehicle powertrain system. The simulation was carried out on a hybrid electric bus, and the results were superior to the one computed by a logic-based strategy.

Considering the scenario that involves a traffic signal system, for example, in [27], Guo *et al.* proposed a bi-level MPC-based strategy. At the upper level, the optimal speed profile is achieved based on the traffic signal information. At the lower level, the MPC strategy is utilized for energy management problem in HEV. In the study [63], the author proposed an MPC-based eco-driving strategy for HEV that is capable of optimizing the speed profile in the scenario of TSCI and sloped roads. The results were compared to the case of the

human driver. It was demonstrated that by equipping this speed control strategy, the speed profile along with the fuel economy was improved greatly.

In order to achieve eco-driving during the car-following scenario, for example, in the study [6], a two-level strategy is devised for a multi-objective problem. The upper level of the system aims at keeping the host vehicle within a safe distance while following the preceding vehicle. The lower level applies the cost derived from ECMS on the powertrain to help the engine work in high efficiency and keep a balance between the fuel energy and electrical energy use. Similarly, Shieh *et al.* [64] designed an online eco-driving strategy for HEV to achieve the objectives of fuel-saving and driving performance. This strategy particularly deals with the pulse and glide (PnG) operation in the car-following scenarios.

As to the eco-driving in a combination of different scenarios, for example, in [65], based on the real-time data obtained from ITS communications, Zhao *et al.* proposed an integrated eco-driving control strategy for intelligent hybrid vehicles (IHV) for two scenarios 1) adaptive cruise control (ACC) during car-following case and 2) regenerative braking control (RBC) during vehicle deceleration. There are three key components in this strategy, namely, the ACC to keep the safe distance with the preceding vehicle, the RBC to determine the optimal powertrain torque distribution, and the coordinated control strategy for both ACC and RBC. The simulation was performed on a straight single-lane with no traffic lights, and the result demonstrates that 5.9% in the energy cycling efficiency can be achieved by this algorithm when compared with a rule-based strategy. In work [66], in order to achieve optimal fuel economy, maintain SOC level and execute safe driving, the author developed a multi-level eco-driving algorithm for HEV that includes two stages. At the first stage, a global optimal speed profile is generated offline based on the historical data on a chosen route with traffic conditions indicated by the distance between the host and the preceding vehicle. At the second stage, the host vehicle adapts its speed to the simulated traffic on a short horizon. Though the combination of these two stages produces an effective eco-driving method for HEV, however, throughout the trip, the host vehicle only interacts with the single preceding vehicle, and the measurement in traffic congestion

level is embodied in the distance between those two vehicles which makes it oversimplified and impractical in real driving situations.

2.4.3 Existing research gaps in eco-driving for CAHEVs

As reviewed thus far, most of the research efforts have addressed the eco-driving problem of CAHEVs in limited driving scenarios, for example, regenerative braking control as studied in [6], car-following control as studied in [6, 65], speed regulation based on traffic signals as studied in [45]. However, to address the eco-driving problem on an actual day-to-day trip in ITS, a vehicle can encounter mixed driving scenarios [67]. For instance, a vehicle may accelerate from a complete stop until its speed reaches the road speed limit, then the vehicle anticipates the upcoming traffic signal when it is approaching an intersection, or a vehicle may follow a preceding vehicle until a right turn comes that leads it to another vehicle to follow [67]. As a result, regarding the application of CAHEVs in ITS, an eco-driving strategy that deals with a certain driving scenario may be far from optimality or adaptability when it is applied to another driving scenario. Therefore, it is desirable to design an eco-driving algorithm for CAHEVs to apply in ITS that can deal with a combination of the most common driving scenarios. In this study, an actual day-to-day driving can be broken down into three basic scenarios depending on most common driving scenarios in Chapter 2.3.1, as 1) free driving: when the vehicle can drive with no obstacle ahead to reach the road speed limit; 2) signal anticipation: when the vehicle makes safe decisions in approaching a traffic signal-controlled intersection; 3) car-following: when the vehicle follows a preceding vehicle in the same lane [67].

In addition, as two of the main goals in eco-driving problem, the optimization of fuel economy and the reduction of engine-out pollutant emissions are usually achieved separately in current studies as they are often conflicting, e.g. when the fuel is decreased, the exhaust emissions may go up and vice versa [45, 67]. However, with the approach of weighted-sum optimization, they can be achieved simultaneously by making a tradeoff in

the eco-driving problem [45]. So far, no work has been done regarding the application of CAHEVs to simultaneously improve energy economy and exhaust emissions reduction with driving safety ensured on a day-to-day ITS trip that involves mixed driving scenarios.

To explore the eco-driving potential of CAHEVs and address the limitations of the aforementioned literature, an online eco-driving control strategy for CAHEV is proposed and designed in this study. The objectives to consider are fuel economy, exhaust emission reduction and driving safety. To achieve the above goals, a bi-level MPC-based approach is taken to solve the multi-objective optimization problem. At the lower level, the control strategy aims to determine the optimal power distribution between ICE and EM, while at the upper level, the vehicle speed profile is fully controlled and optimized by the intelligent system.

2.5 Summary

In this chapter, the background of HEV and CAV technologies were introduced first, and then, a literature review was done on the energy management strategies (EMS) for HEV. A variety of EMSs were analyzed concerning their principles, advantages and limitations, and contributions. Next, a number of control strategies that are applied to CAHEV were assessed. The existing research gap was pointed out at the end.

Chapter 3. Model Development

3.1 Modelling of Hybrid Electric Vehicles (HEVs)

In this chapter, the host vehicle configuration is modelled first, followed by the modelling of the intelligent transportation system (ITS) that provides real-time Vehicle-to-Vehicle (V2V) and Vehicle-to-Infrastructure (V2I) data to help the host vehicle derive optimal strategy for eco-driving scenarios.

3.1.1 HEV Configuration

This study considers a single-shaft hybrid electric vehicle (HEV) for the host vehicle, which is equipped with a 63kW/1.9L internal combustion engine (ICE), a 49 kW electric motor (EM), an automated mechanical transmission (AMT) and a battery pack, as shown in Fig. 3. 1. The parallel power flow paths include the mechanical power path that transfers the power supplied by the fuel tank to the ICE, then goes through the EM and drives the wheels and the electrical power path that brings the electrical power from the battery pack to the EM to propel the vehicle. The configuration of the host HEV is illustrated as follows.

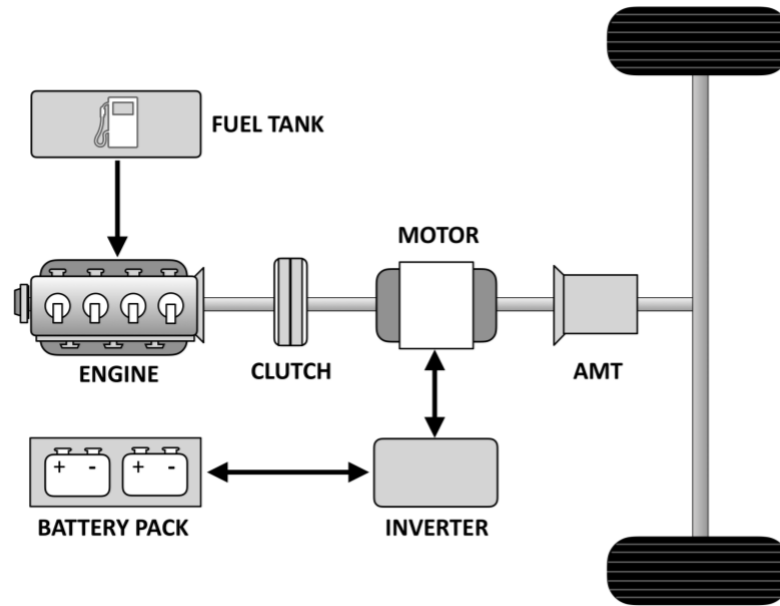


Fig. 3. 1 Single-shaft pre-transmission HEV Powertrain

The powertrain is equipped with an internal combustion engine (ICE), a clutch, a battery pack, an electric motor (EM), an inverter and an AMT transmission box. The parallel power flow paths include the mechanical power path that transfers the power supplied by the fuel tank to the ICE, then goes through the EM and drives the wheels and the electrical power path which brings the electrical power from the battery pack to the EM to propel the vehicle. The component specifications are listed in Table. 3. 1, which is acquired from ADVISOR.

Table. 3. 1 The studied HEV specifications [68]

| Components | Specification |
|---|--|
| Architecture | Parallel hybrid electric |
| Vehicle Length | 4.3 m |
| Vehicle Mass (m) | 1751 kg |
| Frontal Area (A) | 2.66 m ² |
| Engine | Saturn 1.9L (63kW) SOHC SI Engine |
| Motor | Honda 49kW Permanent Magnet Motor |
| Battery | 13Ah, 120 cells, ESS_NIMH6 |
| Transmission | AMT, Gear ratio: [3.79, 2.17, 1.41, 1, 0.86] |
| Final Drive | 4.55 |
| Friction Coefficient (μ) | 0.0150 |
| Aerodynamic Coefficient (C_d) | 0.30 |
| Air Density (ρ_{air}) | 1.20 kg/m ³ |

The clutch works as an ON-OFF switch of the ICE, and it can either be engaged or disengaged, denoted as $S_{ICE} = [0,1]$ [58]. When the clutch is engaged, $S_{ICE} = 1$, the ICE is connected to the powertrain thus can provide mechanical power. When the clutch is disengaged, $S_{ICE} = 0$, the ICE is decoupled from the powertrain while the electric motor is the only machine that drives the vehicle.

The inverter can convert between the direct current (DC) power, which is the electricity stored in the battery pack, and the alternating current (AC) power, which is generated by the electric motor [69].

3.1.1.1 Internal combustion engine (ICE) model

ICE is the main mechanical power supplier of an HEV. In propelling the vehicle, the ICE outputs the mechanical power at the sacrifice of the fuel supplied by the fuel tank, at the same time, the exhaust emissions (HC, CO, NO_x) are emitted into the air. The fuel

consumption rate of the ICE can be modelled as a function of the instantaneous engine torque T_{ICE} and angular speed ω_{ICE} , as follows [6],

$$BSFC = f_{ICE}(T_{ICE}, \omega_{ICE}) \quad (3.1)$$

where $BSFC$ stands for Brake Specific Fuel Consumption, and it is often in the unit of g/kWh . The BSFC map of the studied Saturn 1.9L (63kW) SOHC SI Engine is illustrated in Fig. 3.2 (a).

The instantaneous fuel consumption per second of the ICE can be derived, as follows [6],

$$\dot{m}_{fuel} = \frac{T_{ICE} \cdot \omega_{ICE} \cdot BSFC}{3.6 \times 10^6} \quad (3.2)$$

and it is in the unit of g/s . It is worth mentioning that the ICE can not operate below the idle speed.

Similarly, the instantaneous ICE exhaust emissions (HC, CO, NO_x) can be modelled concerning the instantaneous engine torque T_{ICE} and angular speed ω_{ICE} , as follows [6],

$$\begin{cases} \dot{m}_{hc} = \frac{T_{ICE} \cdot \omega_{ICE} \cdot f_{hc}(T_{ICE}, \omega_{ICE})}{3.6 \times 10^6} \\ \dot{m}_{co} = \frac{T_{ICE} \cdot \omega_{ICE} \cdot f_{co}(T_{ICE}, \omega_{ICE})}{3.6 \times 10^6} \\ \dot{m}_{nox} = \frac{T_{ICE} \cdot \omega_{ICE} \cdot f_{nox}(T_{ICE}, \omega_{ICE})}{3.6 \times 10^6} \end{cases} \quad (3.3)$$

where \dot{m}_{hc} , \dot{m}_{co} and \dot{m}_{nox} are the instantaneous emissions of HC, CO, NO_x in the unit of g/s . The studied Saturn 1.9L (63kW) SOHC SI engine-out emission efficiency maps for HC, CO, NO_x are displayed in Fig. 3.2 (b), (c), (d), respectively.

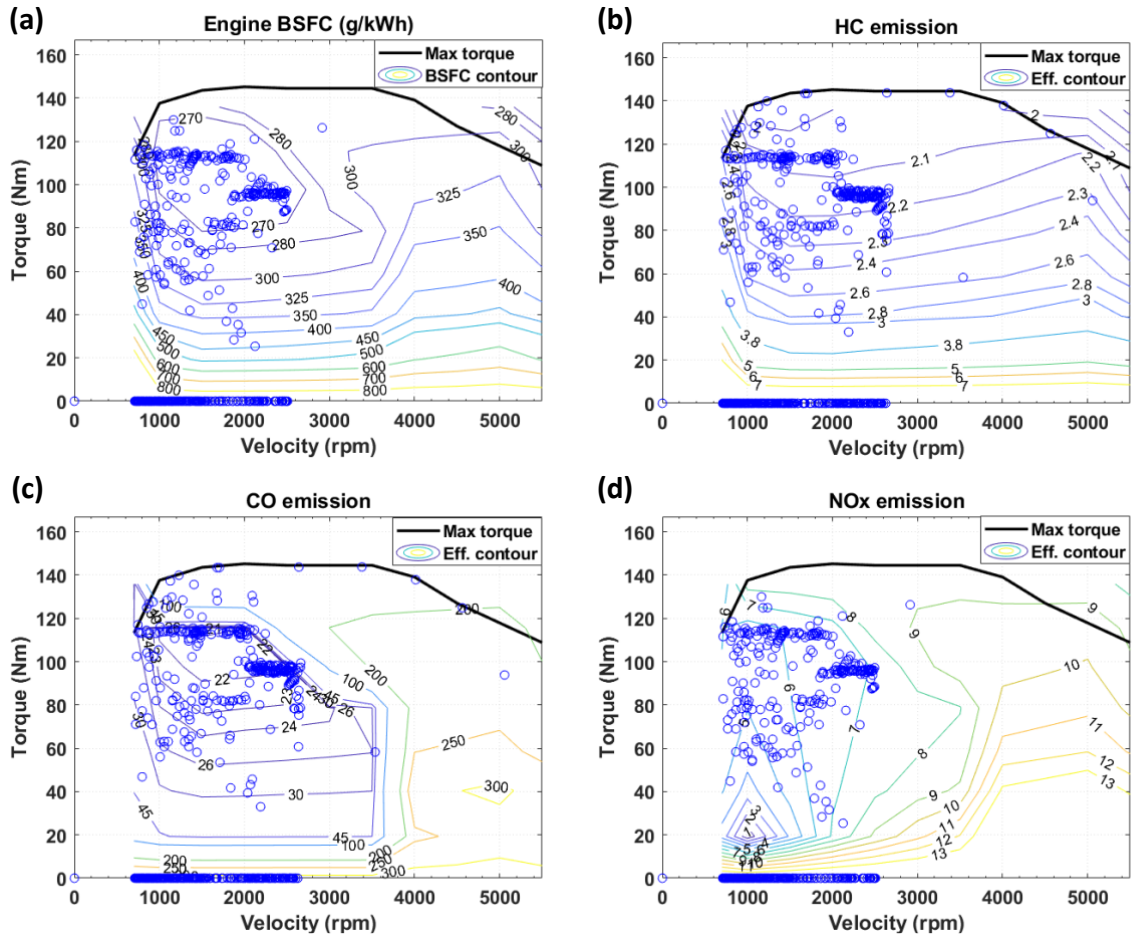


Fig. 3. 2 Operation points of Saturn 1.9L (63kW) SOHC SI Engine on fuel economy and engine-out emissions contour maps (a) Fuel economy (b) HC emission (c) CO emissions and (d) NOx emission

3.1.1.2 Electric motor (EM) model

The EM is the electrical power supplier of the studied vehicle. Working as an electric motor, it takes power from the battery pack and output to drive the vehicle. Working as a generator, on the other hand, it absorbs the power sent from the ICE either from redundant engine power or regenerative braking power, to charge the battery. The motor efficiency can be

modelled as a function of the instantaneous EM torque T_{EM} and angular speed ω_{EM} , as follows [6],

$$\eta_{EM} = f_{EM}(T_{EM}, \omega_{EM}) \quad (3.4)$$

The power of the EM can then be written as follows [6],

$$P_{EM} = T_{EM} \cdot \omega_{EM} \cdot \eta_{EM}^{\alpha} \quad (3.5)$$

where α equals to 1 when the EM works as a generator, and it equals to -1 when the EM works as an electric motor.

3.1.1.3 Battery pack model

The battery pack is modelled using the equivalent circuit model with an open circuit voltage equipped with an internal resistance [70], as shown in Fig. 3. 3. The battery power that supplies the EM can be written as follows [59],

$$P_{batt} = V_{oc}I_{batt} - I_{batt}^2R_{batt} \quad (3.6)$$

where V_{oc} , I_{batt} , R_{batt} are the open-circuit voltage, current in the circuit, and internal resistance, respectively.

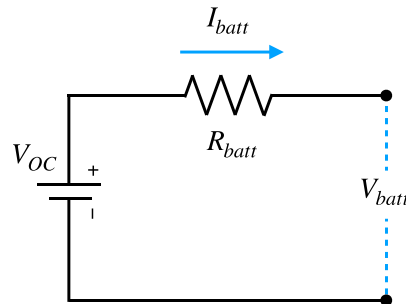


Fig. 3. 3 Equivalent circuit model for battery pack

The rate of the state of charge (SOC) that shows the remaining battery energy is modelled as follows,

$$\dot{SOC} = -\frac{I_{batt}}{Q_{batt}} \quad (3.7)$$

where Q_{batt} is the maximum battery capacity.

Combining Eq. (3.6) and Eq. (3.7) results in the following equation,

$$\dot{SOC} = -\frac{V_{oc} - \sqrt{V_{oc}^2 - 4P_{batt}R_{batt}}}{2Q_{batt}R_{batt}} \quad (3.8)$$

The power exchange between the battery pack and the EM is represented as follows,

$$P_{batt} = T_{EM} \cdot \omega_{EM} \quad (3.9)$$

where T_{EM} and ω_{EM} are the EM torque and its rotational speed. When T_{EM} is positive, the battery power P_{batt} is positive, the battery pack is discharging. When T_{EM} is negative, the battery power P_{batt} is negative, the battery pack is charging.

3.1.1.4 Vehicle Dynamics

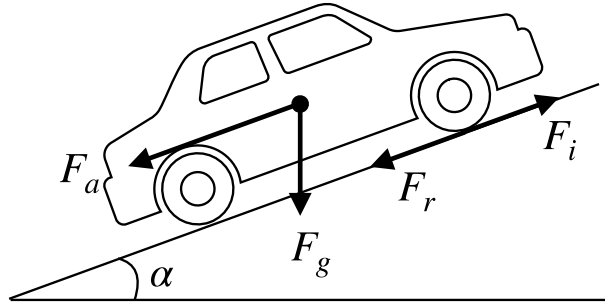


Fig. 3. 4 Longitudinal vehicle dynamics

The required power for the vehicle is depicted in Fig. 3. 4 and given by the following equation [71, 72],

$$\left\{ \begin{array}{l} P_{req} = (F_r + F_g + F_a + F_i) \cdot v \\ F_r = mgf_r \cos \alpha \\ F_g = mg \sin \alpha \\ F_a = 0.5\rho AC_d v^2 \\ F_i = m_e \dot{v} \\ m_e = 1.08m \end{array} \right. \quad (3.10)$$

where the F_r , F_g , F_a , F_i are the rolling resistance, gradient resistance, aerodynamic drag force and acceleration resistance, respectively. m , v , and α are the vehicle mass, vehicle velocity and road slope angle, respectively. The road slope α is set to zero. m_e is the effective mass including the vehicle gravimetric mass and rotational inertias of components [73]. It is estimated to be 1.08 times the vehicle gravimetric mass [72, 73].

3.2 Intelligent transportation system (ITS)

In order to optimize the control strategy for the host CAHEV in ITS, real-time traffic data is obtained via Vehicle-to-Vehicle (V2V) communication and Vehicle-to-Infrastructure (V2I) communications. As the ITS communication technology is not the main concern in this study, the delay in data transmission is omitted in both V2V and V2I.

3.2.1 Vehicle-to-Vehicle (V2V)

With V2V connectivity, a vehicle can get the real-time information of the neighbouring vehicles to make better control decisions, for example, in the car-following scenario, the real-time data of the preceding vehicle enables the host vehicle to keep the safe distance without the potential of collision. The V2V data used in this study includes the distance to the preceding vehicle in the same lane, Δs , and the speed of the preceding vehicle, v_{lead} , as listed in the following table.

Table. 3. 2 V2V data for this study

| Data | Variable Definition | Sample Value |
|------------------|---|--------------|
| Δs (m) | The distance to the closet vehicle ahead in the same lane towards the destination | 25.2m |
| v_{lead} (m/s) | The speed of the ahead vehicle in the same lane | 13.8m/s |

3.2.2 Vehicle-to-Infrastructure (V2I)

In the urban network, the traffic situation is crucial in deriving an effective and safe vehicle control strategy, and this is made possible via V2I communication. In the V2I communication, the V2I data is sent from the roadside units to the host vehicle about the requested real-time environment and traffic information such as the maximum lane speed, the traffic light, the distance to the intersection, and so on. In this study, the V2I data used includes the distance to the next intersection, Δd , the traffic signal of the upcoming TSCI, S_{ryg} , the remaining time for the current traffic signal phase, Δt_{TL} , the speed limit for the lane where the host vehicle is running on, v_{lane} , as listed in the following table.

Table. 3. 3 V2I data used for this study

| Data | Variable Definition | Sample Value |
|---------------------|---|--------------|
| Δd (m) | The distance to the upcoming TSCI | 121.5m |
| S_{ryg} | The traffic signal of the upcoming TSCI | 'g' |
| Δt_{TS} (s) | The remaining time for the current traffic signal phase | 23s |
| v_{lane} (m/s) | The speed limit for the lane where the host vehicle is running on | 27.8m/s |

The traffic signal phases are defined as follows,

Table. 3. 4 Listed traffic signal phases

| Phase | Meaning |
|--------------|--|
| g | Green light signal, vehicles are allowed to pass |
| y | Yellow light signal, vehicles must decelerate |
| r | Red light signal, vehicles must stop |

3.3 Summary

In this chapter, the studied HEV powertrain has been modelled consisting of the internal combustion engine (ICE), the electric motor (EM) and the battery pack. Next, the vehicle dynamics have been built up to compute the required vehicle power demand at the wheels. Finally, the intelligent transportation system (ITS) concerning the data communications via Vehicle-to-Vehicle (V2V) and Vehicle-to-Infrastructure (V2I) have been introduced, which lays the foundation for the design of the proposed eco-driving strategy in the following chapters.

Chapter 4. Methodology

4.1 Problem Formulation

The control objective is to synthesize static function mapping the bi-level state variables to the inputs such that with the driving safety along the route ensured, both the energy consumption cost (i.e. fuel and electrical energy) and vehicle exhaust emissions (HC, CO, NO_x) are minimized. The state variables include the ones from the upper (external) level, i.e. the accumulated driving distance of the host vehicle, s , and the ones from the lower (internal) level, i.e. the instantaneous host vehicle velocity, v , and battery pack state of charge (SOC). The control inputs are the instantaneous host vehicle acceleration a , and the split ratio between the ICE torque and the EM torque, γ . The problem is thus formulated into a multi-objective optimization problem, as follows,

$$\min: \quad J_{opt} = \sum_{k=1}^{\infty} c(x_k, u_k) \quad (4.1)$$

$$\begin{aligned} \text{subject to:} \quad & x_{k+1} = f(x_k, u_k) \\ & x \in X, u \in U(x) \end{aligned} \quad (4.2)$$

where J_{opt} is the total cost to be optimized and $c(x_k, u_k)$ is a function that maps the state and control variables to an instantaneous cost at one timestep. Although the problem is formulated into an infinite-horizon problem, it is meant to be finite since the system terminates once the host vehicle arrives at the pre-defined destination. Thus, J_{opt} is guaranteed to be a finite value.

The split ratio as one of the state variables is defined as,

$$\gamma = T_{EM}/T_{req} \quad (4.3)$$

where T_{EM} is the torque of the EM, and T_{req} is the demanding torque transmitted to the ICE and EM by the gearbox.

As mentioned before, the optimization problem involves three objectives, namely, 1) the objective of driving safety, 2) the objective of energy management and 3) the objective of emission reduction. Therefore the cost function $c(x_k, u_k)$ can be written as,

$$c(x_k, u_k) = J_{SF}(x_k, u_k) + \alpha \cdot J_{EN}(x_k, u_k) + \beta \cdot J_{EX}(x_k, u_k) \quad (4.4)$$

where $J_{SF}(x_k, u_k)$, $J_{EN}(x_k, u_k)$ and $J_{EX}(x_k, u_k)$ are the instantaneous cost of driving safety, the instantaneous cost of energy consumption and the instantaneous cost of exhaust emission, respectively. α and β serve as the weighting factors to make a trade-off between different costs.

4.2 Model predictive control-based eco-driving control strategy

In this section, the model predictive control (MPC) based eco-driving strategy for a connected and automated vehicle (CAV) with hybrid electric configuration, as described in Chapter 2, is proposed. Prior to solve the problem in the context of model predictive control (MPC) framework, the control objectives with corresponding cost functions are introduced first, with regard to (1) the objective of driving safety that can realize the safe driving by complying with traffic rules and keeping a safe distance with preceding vehicles (2) the objective of energy management that aims to reduce the fuel consumption with a balanced battery SOC level (3) the objective of emission reduction that serves to reduce the exhaust emissions HC , CO and NO_x . Then, the objective functions are fit in the MPC framework to derive the optimal control strategy for the vehicle.

4.2.1 Optimization objectives

4.2.1.1 *The objective of driving safety*

The goal of safe driving can be exemplified by the scenarios when the host vehicle aims to keep a collision-free distance with other vehicles, make decisions at a TSCI, and comply with the speed limit set by each road. In order to achieve this goal, cost penalties need to be applied to prevent unsafe driving actions. The driving scenarios are therefore classified into different situations to make the strategy adaptive. They are a). free driving scenario, b). signal anticipation scenario and c). car-following scenario. The instantaneous cost of driving safety $J_{SF}(x_k, u_k)$, as in the previous equation, is then represented as follows,

$$J_{SF}(x_k, u_k) = \lambda_1 \cdot w_1 \cdot J_{FD} + \lambda_2 \cdot w_2 \cdot J_{SA} + \lambda_3 \cdot w_3 \cdot J_{CF} \quad (4.5)$$

where J_{FD} , J_{SA} and J_{CF} correspond to the instantaneous cost during the free driving scenario, signal anticipation scenario, and car-following scenario, respectively. λ_1 , λ_2 and λ_3 are the Boolean factors ($[0,1]$) that turn ON/OFF for each cost. It is worth noting that at each time step, only one out of three scenarios is triggered, hence the corresponding cost is applied for safe driving. w_1 , w_2 and w_3 are the weighting factors to make an appropriate trade-off between different costs.

From the V2I and V2V connections, the real-time driving data that ensure the driving safety are Δd , Δs , S_{ryg} , Δt_{TS} , v_{lead} and v_{lane} , as listed in the following table. The illustration is shown in Fig. 4. 1.

Table. 4. 1 Parameters concerning the driving safety

| Data | Variable Definition | Sample Value |
|---------------------|---|--------------|
| Δd (m) | The distance to the upcoming TSCI | 121.5 m |
| Δs (m) | The distance to the closet vehicle ahead in the same lane towards the destination | 13.8m |
| S_{ryg} | The traffic signal of the upcoming TSCI | g |
| Δt_{TS} (s) | The remaining time for the current traffic signal phase | 23s |
| v_{lead} (m/s) | The speed of the ahead vehicle in the same lane, if applies | 13.8m/s |
| v_{lane} (m/s) | The speed limit for the lane where the host vehicle is running on | 27.8m/s |

To model the driving scenario classifier (DSC) of the studied vehicle, the general vehicle braking distance equation is given as follows [6],

$$S_{brk} = S_{min} + v(k) \cdot t_{brk} + \frac{v(k)^2}{2 \cdot a_{brk}} \quad (4. 6)$$

where S_{brk} denotes the braking distance in the unit of m, S_{min} is the minimum distance to keep in the unit of m, $v(k)$ is the host vehicle speed at time instant k in the unit of m/s, t_{brk} is the reaction time before braking in s, a_{brk} is the braking deceleration in m/s^2 .

Δd_L and Δs_L are the thresholds for the TSCI distance, Δd , and inter-vehicle distance, Δs , respectively, in the unit of m. Their equation is modelled as the maximum braking distance based on Eq. (4. 6), with parameters taken from the study [6], as follows,

$$\Delta d_L = \Delta s_L = 10 + v(k) + 0.0825 \times v(k)^2 \quad (4. 7)$$

when the actual distance of the host vehicle to the upcoming TSCI, Δd , is smaller than the threshold distance, Δd_L , the signal anticipation scenario can be triggered by the control system. The reactions of the host vehicle in approaching the TSCI will be anticipated.

Similarly, when the actual car-following distance, Δs , is smaller than the inter-vehicle distance threshold Δs_L , the car-following scenario is triggered by the control system.

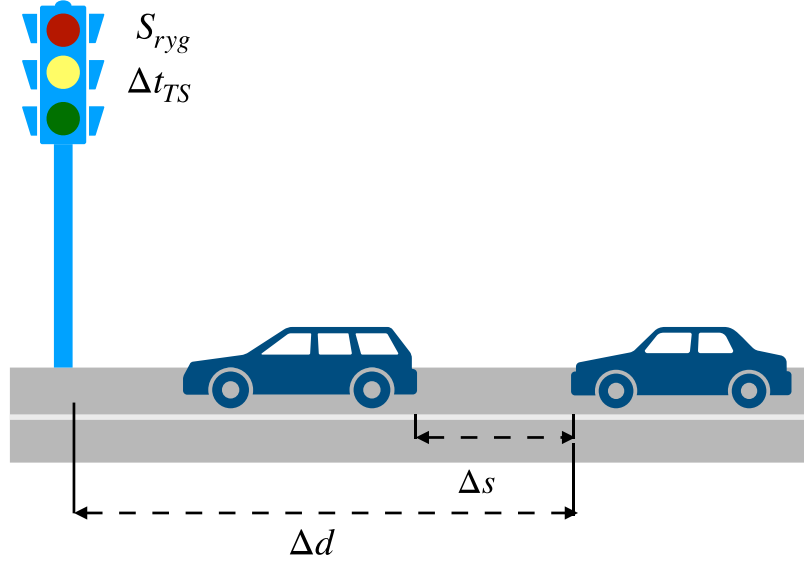


Fig. 4. 1 Illustration for driving safety parameters

The threshold used when determining if the host vehicle should pass the intersection is determined by the following estimated passing time Δt_r , as follows,

$$\Delta t_r = \begin{cases} \frac{\Delta d}{a_{max}}, & v(k) = 0 \\ \frac{\Delta d}{v(k)}, & v(k) > 0 \end{cases} \quad (4.8)$$

where a_{max} is the maximum allowed speed for the vehicle.

The driving scenarios are thus classified based on the above parameters in real time, illustrated as follows, where FD, SA, and CF stand for free driving, signal anticipation and car-following mode, respectively.

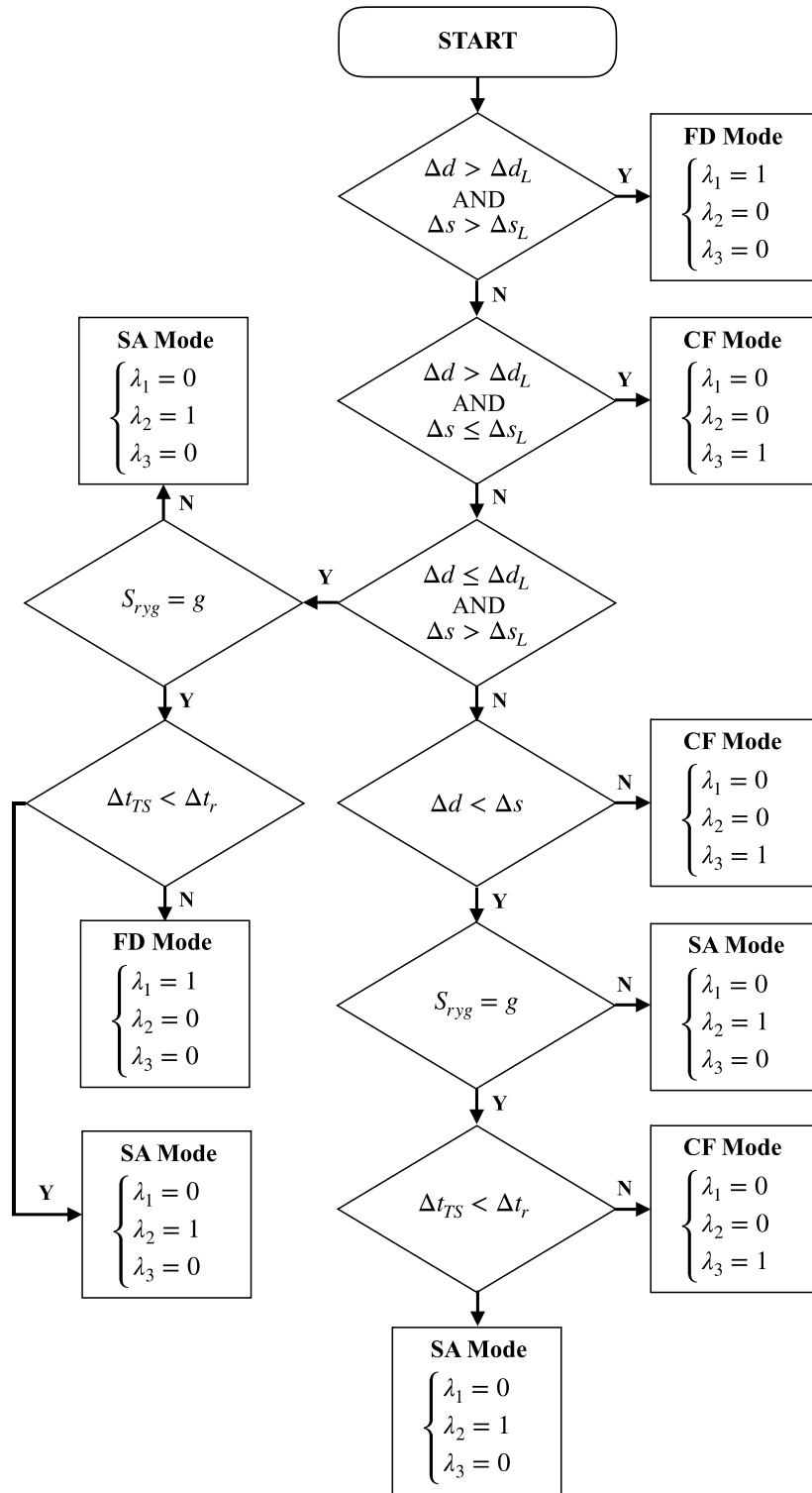


Fig. 4. 2 Driving scenario classifier (DSC) workflow

(I) *Free driving*

In the free driving scenario, the host vehicle is driving with speed no higher than either the maximum speed limit imposed by the current lane or the maximum constraint speed of the vehicle. When the vehicle accelerates to the maximum allowed speed, it then enters into the steady speed control until the traffic conditions start to change.

The cost associated with the free driving scenario is defined as a quadratic function,

$$J_{FD} = (v_{lim}(k) - v(k))^2 \quad (4.9)$$

where $v_{lim}(k)$ is the maximum allowed speed for the host vehicle at time step k , and it is defined as,

$$v_{lim}(k) = \min(v_{lane}, v_{max}) \quad (4.10)$$

which refers to the smaller one of the two, the speed limit on the lane at time step k , v_{lane} , and the maximum allowed speed of the host vehicle, v_{max} .

(II) *Signal anticipation*

When the host vehicle is in the signal anticipation scenario where there is a need to decelerate depending on the conditions defined in DSC, the cost function J_{SA} is triggered to control the subsequent reactions of the vehicle to safely reach a complete stop at the intersection. Sample cases at the TSCI are illustrated in Fig. 4. 3,

In the cost function of the signal anticipation scenario, the minimum safe distance to stop at the intersection, based on the braking distance modelled in Eq. (4. 6), is defined with static minimum distance s_{min} equaling 2 m, reaction time t_{brk} equaling 0.5 s, and emergency deceleration equaling 8 m/s² [6],

$$\Delta d_{min} = 2 + 0.5 \cdot v(k) + 0.0625 \times v(k)^2 \quad (4.11)$$

Therefore, the cost is applied according to the distance of the vehicle to the intersection, modelled as follows [68],

$$J_{SA} = \begin{cases} \tan\left(\frac{\pi}{2}\right), & \Delta d < \Delta d_{min} \\ q \cdot \tan\left(\frac{\Delta d - \Delta d_L}{\Delta d_{min} - \Delta d_L} \cdot \frac{\pi}{2}\right), & \Delta d_{min} \leq \Delta d \leq \Delta d_L \end{cases} \quad (4.12)$$

where Δd is the actual distance of the host vehicle to the upcoming intersection and q is the weighting factor in the cost function. In approaching the intersection, as the Δd gets smaller, the penalty gets larger to help reduce the vehicle speed. If the distance of Δd becomes less than the minimum allowed distance Δd_{min} , an infinite cost is applied to the system.

(III) Car following

When the host vehicle enters the car-following scenario, triggered by the conditions defined in DSC, the cost function is applied according to the inter-vehicle distance so that a safe following distance can be achieved and any potential collision can be prevented.

The minimum and maximum following distance are derived from the Eq. (4. 7) and Eq. (4. 11), which are relevant to the instantaneous host vehicle speed, as follows [6],

$$\Delta s_{min} = 2 + 0.5 \cdot v(k) + 0.0625 \times v(k)^2 \quad (4.13)$$

$$\Delta s_{max} = 10 + v(k) + 0.0825 \times v(k)^2 \quad (4.14)$$

Within the boundaries of the minimum and maximum following distances, the optimal following distances, which are bounded by the lower optimal limit Δs_{opt}^{inf} and upper optimal limit Δs_{opt}^{sup} , are constructed based on the minimum and maximum following distances, the parameters are taken from the study [68],

$$\Delta S_{opt}^{inf} = 0.6 \cdot \Delta S_{max} + 0.4 \cdot \Delta S_{min} \quad (4.15)$$

$$\Delta S_{opt}^{sup} = 0.4 \cdot \Delta S_{max} + 0.6 \cdot \Delta S_{min} \quad (4.16)$$

Therefore, the cost function for the car-following scenario is derived based on the study [6],

$$J_{CF} = \begin{cases} +\infty, & \Delta S < \Delta S_{min} \\ f_1 \cdot \tan\left(\frac{\Delta S - \Delta S_{opt}^{inf}}{\Delta S_{min} - \Delta S_{opt}^{inf}} \cdot \frac{\pi}{2}\right), & \Delta S_{min} \leq \Delta S < \Delta S_{opt}^{inf} \\ \left| \Delta S - \frac{\Delta S_{opt}^{inf} + \Delta S_{opt}^{sup}}{2} \right|, & \Delta S_{opt}^{inf} \leq \Delta S \leq \Delta S_{opt}^{sup} \\ f_2 \cdot (\Delta S - \Delta S_{opt}^{sup})^2, & \Delta S_{opt}^{sup} < \Delta S \leq \Delta S_{max} \\ 0, & \Delta S > \Delta S_{max} \end{cases} \quad (4.17)$$

where f_1 and f_2 are the weighting factors in the function. As the vehicle enters the car-following scenario, the penalty is applied to favor the car-following distance that falls within the range defined by the lower optimal limit ΔS_{opt}^{inf} and upper optimal limit ΔS_{opt}^{sup} . When the inter-vehicle distance gets less than the minimum allowed distance ΔS_{min} , an infinite penalty will be applied.

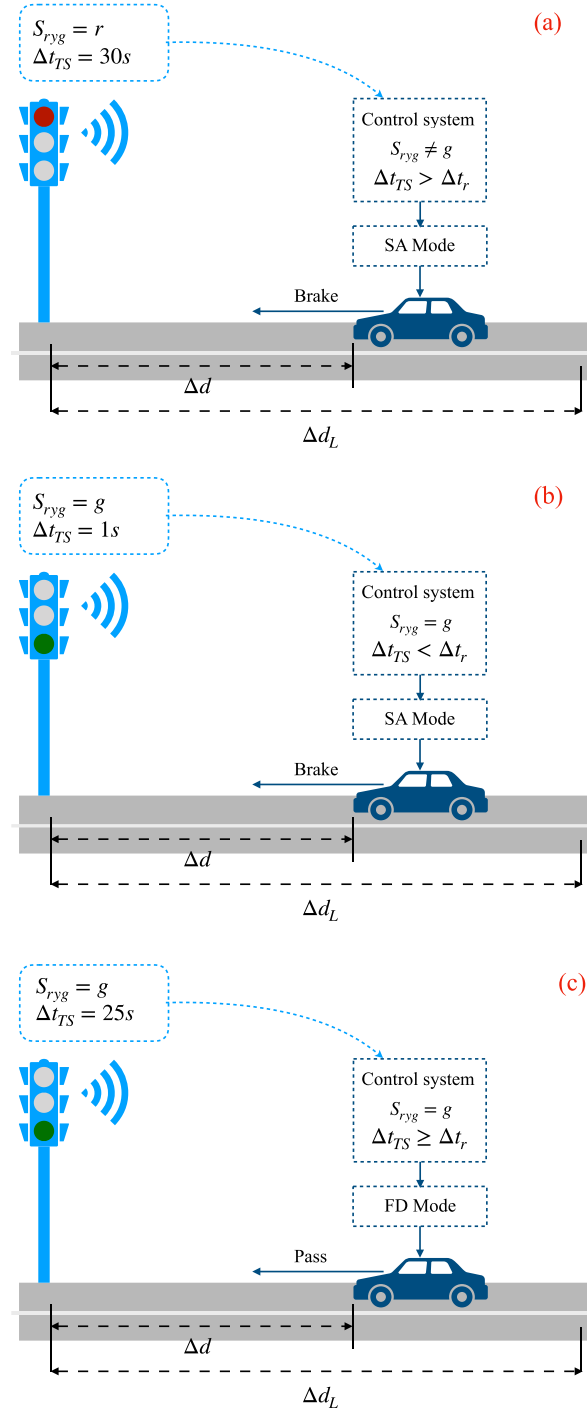


Fig. 4. 3 Sample cases at the TSCI without leading vehicles (a) brakes are applied due to the red signal, (b) brakes are applied because the green signal phase duration is not sufficient for passing (c) vehicle decides to drive across the intersection in 25s

4.2.1.2 *The objective of energy management*

The cost function of the energy management objective is applied across the driving schedule for all the driving scenarios to minimize the energy cost, i.e. the fuel energy and the electrical energy.

The equation to calculate the instantaneous fuel cost \dot{m}_{fuel} can be referred to as Chapter 3.1.1.

As to the electrical energy, since the overuse of the battery will inevitably impose intractable damage to the battery health, equivalent consumption minimization strategy (ECMS) is adopted as an approach to bound the battery state of charge (SOC) within the range from 0.5 to 0.75. As a result, a balance can be achieved between fuel consumption and electrical energy consumption. The equivalent factor s_e is defined as [6],

$$s_e = \begin{cases} 0.001, & SOC \geq 0.75 \\ -6 \cdot SOC + 5 & 0.5 < SOC < 0.75 \\ Inf & SOC \leq 0.5 \end{cases} \quad (4.18)$$

The instantaneous equivalent fuel consumption of the EM is given as [6],

$$\dot{m}_{em} = \frac{\overline{Q}_f \cdot P_{batt}}{3.6 \times 10^6 \cdot \bar{\eta}_{EM}} \quad (4.19)$$

where \overline{Q}_f is the average fuel consumption rate, which is set to 240 g/kWh, $\bar{\eta}_{EM}$ is the average efficiency of the EM and it is assumed to be 0.88.

Therefore, the energy cost that has both the fuel consumption and the electrical energy consumption is derived as,

$$J_{EN} = \dot{m}_{fuel} + s_e \cdot \dot{m}_{em} \quad (4.20)$$

4.2.1.3 *The objective of emission reduction*

During driving, the vehicle engine mainly produces three types of exhaust pollutants (HC, CO, NO_x) into the air that are toxic to human health [74]. They are to be reduced by manipulating the engine speed and torque. The cost of exhaust emissions, therefore, include the cost of HC, CO and NO_x , as follows,

$$J_{EX} = \dot{m}_{hc} + \dot{m}_{co} + \dot{m}_{nox} \quad (4.21)$$

The equation for the emission cost \dot{m}_{hc} , \dot{m}_{co} and \dot{m}_{nox} can be referred to as Chapter 3.1.1. And they are in the unit of g/s .

4.2.2 Model predictive control (MPC)

Due to the simplicity and fast computation, the problem presented in Chapter 34.1 is solved online using the bi-level nonlinear model predictive control (BL-NLMPC) strategy. Based on the state variables at each time step, the BL-NLMPC computes a future control sequence in the prediction horizon that minimizes the total cost in the horizon, and apply the first element of the control sequence to the HEV model [18]. The process is repeated at each time step with the prediction horizon moving one step forward until the system reaches the terminal state [18]. In the control sequence, at the upper level, the controller finds the optimal acceleration for the HEV that minimizes the total cost in the prediction horizon. Similarly, at the lower level, the controller derives the optimal split ration between the ICE torque and EM torque in the powertrain that minimizes the prediction horizon cost. Thus, the optimization problem can be rewritten as follows,

$$J_{opt} = \min_{u_t} \left(\sum_{t=k}^{k+N_p-1} (J_{SF}(x_t, u_t) + \alpha \cdot J_{EN}(x_t, u_t) + \beta \cdot J_{EX}(x_t, u_t)) \cdot T_s \right), \quad (4.22)$$

$$k = 0, 1, 2, \dots$$

$$\text{state variables: } x_k = [s, v, \text{SOC}] \quad (4.23)$$

$$\text{control variables: } u_k = [a, \gamma] \quad (4.24)$$

$$\text{subject to: } s > 0$$

$$0 < v < v_{max}$$

$$\text{SOC}_{min} < \text{SOC} < \text{SOC}_{max} \quad (4.25)$$

$$a_{min} < a < a_{max}$$

$$\gamma_{min} < \gamma < \gamma_{max}$$

where T_s is the sampling time, N_p denotes the receding prediction horizon. The state variables include the upper-level states, accumulated driving distance of the ego host vehicle, s and the instantaneous ego host vehicle velocity, and the lower-level state v , battery pack state of charge (SOC). The control variables are the vehicle acceleration, a , at the upper level, and the torque split ratio between ICE and EM, γ , at the lower level. To obtain a quick control response, the control horizon N_c is set to be 1, which means one set of derived control inputs is applied across the prediction horizon. It is worth noting that the control variables are assumed to be constant in the prediction horizon. The illustration and workflow are described and obtained as the pseudo-code in Fig. 4. 4 and Fig. 4. 5.

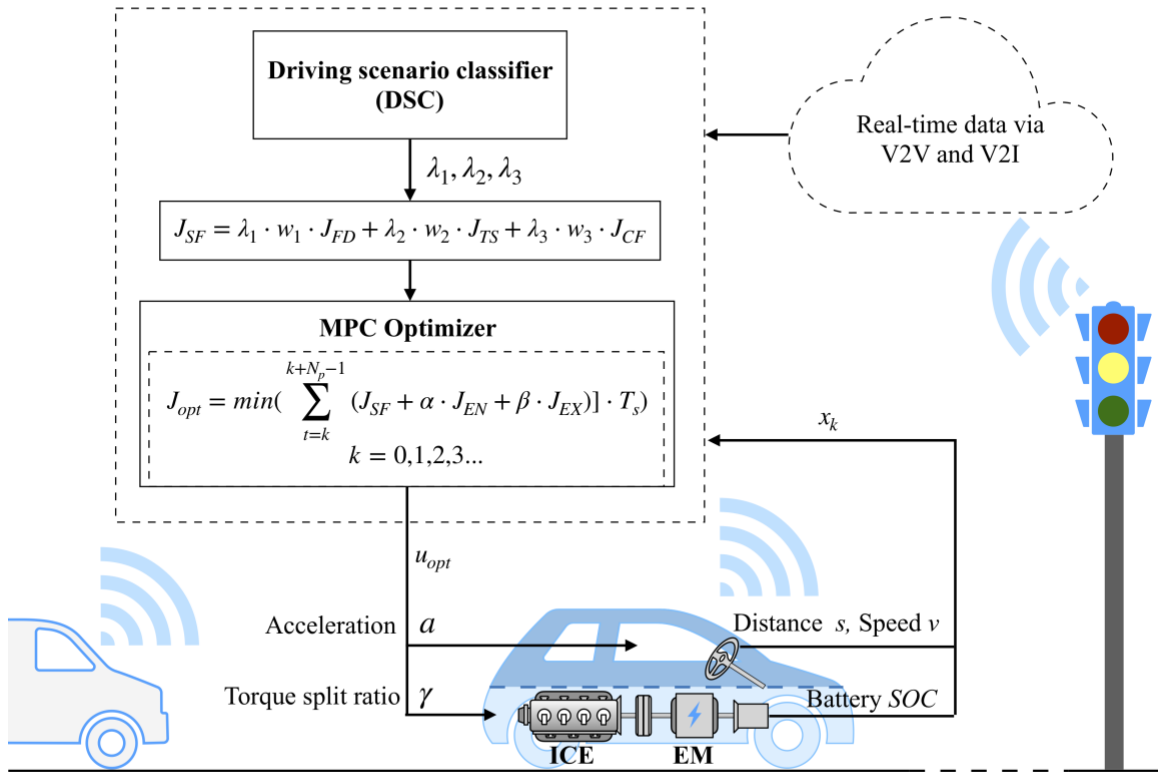


Fig. 4. 4 The framework of the proposed MPC-based eco-driving strategy

Algorithm: MPC-based Eco-driving for CAHEV

```
1 function ECO_DRIVING ( $s, SOC, v, \Delta d, S_{ryg}, \Delta t_{TS}, \Delta s, v_{lead}, loc_t$ );
   Input: Driving distance  $s$ , instantaneous vehicle speed  $v$ , battery
          $SOC$ , distance to the upcoming TSCI  $\Delta d$ , traffic signal of the
         upcoming TSCI  $S_{ryg}$ , remaining duration of the upcoming
         TSCI signal  $\Delta t_{TS}$ , distance to the leading vehicle  $\Delta s$ , speed of
         the leading vehicle  $v_{lead}$ , current location  $loc_t$ 
   Output: Acceleration  $\alpha$  and split ratio  $\gamma$ 
2 Initialization();
   /* Check if vehicle has arrived at the destination */
3 while  $loc_t \neq destination\ location$  do
4   Simulation_step();
5    $[\lambda_1, \lambda_2, \lambda_3] = Driving\_Scenario\_Classifier()$ ;
   /* Switch to the corresponding mode */
6   switch  $[\lambda_1, \lambda_2, \lambda_3]$  do
   /* Free Driving Scenario */
7   case  $[1, 0, 0]$  do
8     for every solution in the solution space do
9       /* enumerate a pair of acceleration  $a$  and split ratio  $\gamma$  */
10       $[a, \gamma] = Enumerator()$ ;
11      /* update the costs of the optimization objectives */
12       $J_{SF}(x_t, u_t) = w_1 \cdot J_{FD}(x_t, u_t)$ ;  $J_{EN}(x_t, u_t)$ ;  $J_{EX}(x_t, u_t)$ ;
13       $J_{opt} = \min_{u_t} (\sum_{t=k}^{k+N_p-1} J_{SF}(x_t, u_t) + \alpha \cdot J_{EN}(x_t, u_t) + \beta \cdot$ 
14       $J_{EX}(x_t, u_t)) \cdot T_s$ 
15      if  $J_{opt} < J_{min}$  then
16         $J_{min} = J_{opt}$ ;
17        /* get optimal acceleration  $a$  and split ratio  $\gamma$  */
18        return  $u_{opt} = [a, \gamma]$ ;
   /* Signal Anticipation Scenario */
19   case  $[0, 1, 0]$  do
20     for every solution in the solution space do
21       /* enumerate a pair of acceleration  $a$  and split ratio  $\gamma$  */
22       $[a, \gamma] = Enumerator()$ ;
23      /* update the costs of the optimization objectives */
24       $J_{SF}(x_t, u_t) = w_2 \cdot J_{SA}(x_t, u_t)$ ;  $J_{EN}(x_t, u_t)$ ;  $J_{EX}(x_t, u_t)$ ;
25       $J_{opt} = \min_{u_t} (\sum_{t=k}^{k+N_p-1} J_{SF}(x_t, u_t) + \alpha \cdot J_{EN}(x_t, u_t) + \beta \cdot$ 
26       $J_{EX}(x_t, u_t)) \cdot T_s$ 
27      if  $J_{opt} < J_{min}$  then
28         $J_{min} = J_{opt}$ ;
29        /* get optimal acceleration  $a$  and split ratio  $\gamma$  */
30        return  $u_{opt} = [a, \gamma]$ ;
   /* Car Following Scenario */
31   case  $[0, 0, 1]$  do
32     for every solution in the solution space do
33       /* enumerate a pair of acceleration  $a$  and split ratio  $\gamma$  */
34       $[a, \gamma] = Enumerator()$ ;
35      /* update the costs of the optimization objectives */
36       $J_{SF}(x_t, u_t) = w_3 \cdot J_{CF}(x_t, u_t)$ ;  $J_{EN}(x_t, u_t)$ ;  $J_{EX}(x_t, u_t)$ ;
37       $J_{opt} = \min_{u_t} (\sum_{t=k}^{k+N_p-1} J_{SF}(x_t, u_t) + \alpha \cdot J_{EN}(x_t, u_t) + \beta \cdot$ 
38       $J_{EX}(x_t, u_t)) \cdot T_s$ 
39      if  $J_{opt} < J_{min}$  then
40         $J_{min} = J_{opt}$ ;
41        /* get optimal acceleration  $a$  and split ratio  $\gamma$  */
42        return  $u_{opt} = [a, \gamma]$ ;

```

Fig. 4. 5 Pseudo-code of the proposed algorithm

4.3 Rule-based EACS

To evaluate the performance of the proposed strategy, a bi-level benchmark eco-driving control strategy for CAHEV is designed. At the upper level, the instantaneous vehicle speed is constructed using the intelligent driver model (IDM). At the lower level, the rule-based electric-assist control strategy (EACS) aims to control the energy split ratio in the electric hybrid powertrain.

4.3.1 Intelligent driver model (IDM)

As one of the most simple, comprehensive and collision-free driver models that produce realistic profiles, the intelligent driver model (IDM) calculates the real-time acceleration based on a set of driving conditions [75]. The acceleration is defined as follows [75],

$$\dot{v} = a \left[1 - \left(\frac{v}{v_0} \right)^\delta - \left(\frac{s^*(v, \Delta v)}{s} \right)^2 \right] \quad (4.26)$$

$$\Delta v = v - v_1 \quad (4.27)$$

$$s^*(v, \Delta v) = s_0 + \max \left(0, vT + \frac{v\Delta v}{2\sqrt{ab}} \right) \quad (4.28)$$

where v is the current vehicle speed and v_0 is the target speed. a and b denote the acceleration ability and deceleration capacity of the vehicle, respectively. s is the current distance to the obstacle, either the preceding vehicle or the TSCI. $s^*(v, \Delta v)$ is the desired distance which is defined in Eq. (4.28). T is the time gap that is set to 1.0 s. Δv is defined as the speed difference between the host vehicle current speed v and the obstacle speed v_1 . If the obstacle ahead is a preceding vehicle, $v_1 > 0$, or $v_1 = 0$ for the TSCI. s_0 is the minimum allowed gap between the host vehicle and the obstacle. The parameters are selected according to [75] in combination with an estimation of real-world vehicles, which are listed in the following table.

Table. 4. 2 Parameters for IDM

| Intelligent Driver Model | | |
|--------------------------------------|----------------|---------------|
| Parameters | Symbols | Values |
| Time gap (s) | T | 1.0 |
| Minimum gap (m) | s_0 | 2 |
| Acceleration exponent (-) | δ | 4 |
| Acceleration (m/s^2) | a | 2 |
| Comfortable deceleration (m/s^2) | b | 2 |

4.3.2 Electric-assist control strategy (EACS)

The electric-assist control strategy (EACS) is one of the most commonly used and practical rule-based strategies for a parallel HEV [76], in which the ICE is used as the main power source while the battery provides assistant power. The EM runs either when the torque demand is too high, or when the ICE is operating inefficiently. As a result, the total fuel economy can be improved over the trip. A visualization of the rules in EACS is shown in Fig. 4. 6.

The control strategy determines the power split between ICE and EM in the powertrain, with the driving conditions taken into consideration. The application of EACS can help achieve a better fuel economy and fewer exhaust emissions [76]. The variables that determine the rule-based policies are defined in Table. 4. 3 [45]. The basic rules in EACS can be described as follows,

1. If SOC is higher than the upper bound SOC_H , then ICE turns off, EM turns on
2. If SOC is lower than the upper bound SOC_H and higher than the lower bound SOC_L ,

- (1) If the vehicle speed is lower than the vehicle low-speed threshold V_L or if the demand torque T_{req} is lower than the ICE off torque curve, then ICE turns off, EM turns on
- (2) Otherwise, if the demand torque T_{req} is lower than the maximum ICE torque T_{ICE}^{max} , then ICE turns on, EM turns off
- (3) Otherwise, if the demand torque T_{req} is higher than the maximum ICE torque T_{ICE}^{max} , then ICE turns on, also EM turns on to assist ICE in supplying the power by $T_{EM} = T_{req} - t_{dis} \cdot T_{ICE}^{max}$ where t_{dis} is the discharge factor

3. If SOC is lower than the lower bound SOC_L

- (1) If the demand torque T_{req} is lower than the ICE minimum torque curve, then ICE turns to drive the vehicle while charging the battery by redundant torque defined as $t_{min} \cdot T_{ICE}^{max} - T_{req}$ where t_{min} denotes the ICE minimum torque threshold factor, EM turns on to switch to generator mode
- (2) If the demand torque T_{req} is higher than the ICE minimum torque curve, then ICE turns to drive the vehicle while charging the battery by redundant torque defined as $t_{ch} \cdot T_{ICE}^{max}$ where t_{ch} denotes the ICE charging factor, EM turns on to switch to generator mode
- (3) If the demand torque T_{req} is higher than the maximum ICE torque T_{ICE}^{max} , there is not enough power to drive the vehicle

4. If the vehicle is completely stopped, then ICE turns off, EM turns on

- If the vehicle is braking, then ICE turns off, EM turns on to switch to generator mode to charge the battery

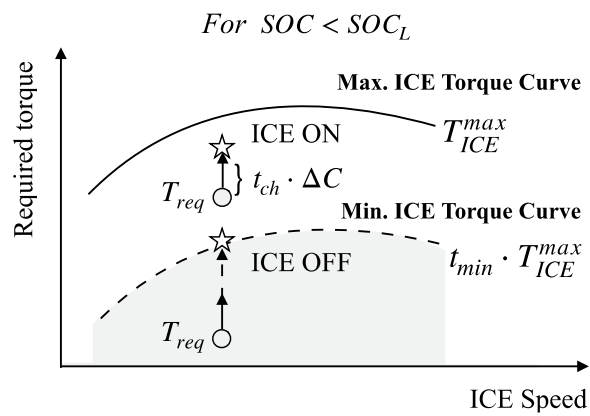
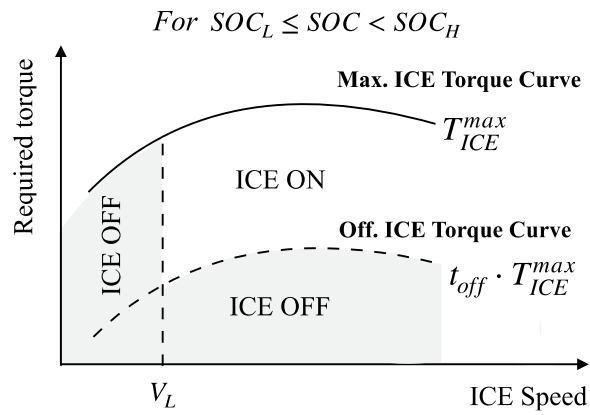


Fig. 4. 6 EACS rule-based illustrations

Table. 4. 3 Parameters for rule-based EACS

| Parameter | Description |
|------------------|--|
| SOC_L | The lowest SOC allowed |
| SOC_H | The highest SOC allowed |
| t_{off} | The threshold factor for the ICE to shut off during $SOC_L < SOC < SOC_H$ |
| t_{min} | The threshold factor for the ICE to charge the EM during $SOC < SOC_L$ |
| t_{ch} | The charging factor for the ICE during $SOC_L < SOC < SOC_H$ |
| t_{dis} | The discharging factor for ICE during $SOC_L < SOC < SOC$ |
| V_L | The lowest vehicle speed threshold |

The algorithm is described in the following pseudo-code,

Algorithm: EACS for HEV

```

1 function EACS ( $T_{req}, SOC, V$ );
   Input : Torque demand  $T_{req}$ , battery  $SOC$  and instantaneous vehicle
           speed  $V$ 
   Output:  $T_{ICE}, T_{EM}$ 
2 if  $SOC \geq SOC_H$  then
3   EV Mode;
4    $T_{ICE} = 0$ ;
5    $T_{EM} = T_{req}$ ;
6   return  $T_{ICE}, T_{EM}$ ;
7 else
8   if  $SOC \geq SOC_L$  then
9     if  $V > V_L$  then
10      if  $T_{req} > t_{off} \cdot T_{ICE}^{max}$  then
11        if  $T_{req} > T_{ICE}^{max}$  then
12          Hybrid Mode;
13           $T_{ICE} = T_{req} - t_{dis} \cdot T_{ICE}^{max}$ ;
14           $T_{EM} = T_{req} - T_{ICE}$ ;
15          return  $T_{ICE}, T_{EM}$ ;
16        else
17          ICE Mode;
18           $T_{ICE} = T_{req}$ ;
19           $T_{EM} = 0$ ;
20          return  $T_{ICE}, T_{EM}$ ;
21        end
22      else
23        EV Mode;
24         $T_{ICE} = 0$ ;
25         $T_{EM} = T_{req}$ ;
26        return  $T_{ICE}, T_{EM}$ ;
27      end
28    else
29      EV Mode;
30       $T_{ICE} = 0$ ;
31       $T_{EM} = T_{req}$ ;
32      return  $T_{ICE}, T_{EM}$ ;
33    end
34  else
35    if  $T_{req} > t_{min} \cdot T_{ICE}^{max}$  then
36      Charge Mode;
37       $T_{ICE} = T_{req} + t_{ch} \cdot \Delta C$ ;
38       $T_{EM} = T_{req} - T_{ICE}$ ;
39       $\Delta C = \frac{SOC_H + SOC_L}{2} - SOC$ ;
40      return  $T_{ICE}, T_{EM}$ ;
41    else
42      Charge Mode;
43       $T_{ICE} = t_{ch} \cdot T_{ICE}^{max}$ ;
44       $T_{EM} = T_{req} - T_{ICE}$ ;
45      return  $T_{ICE}, T_{EM}$ ;
46    end
47  end
48 end

```

Fig. 4. 7 Pseudo code of rule-based EACS

The policy is illustrated in Fig. 4. 8.

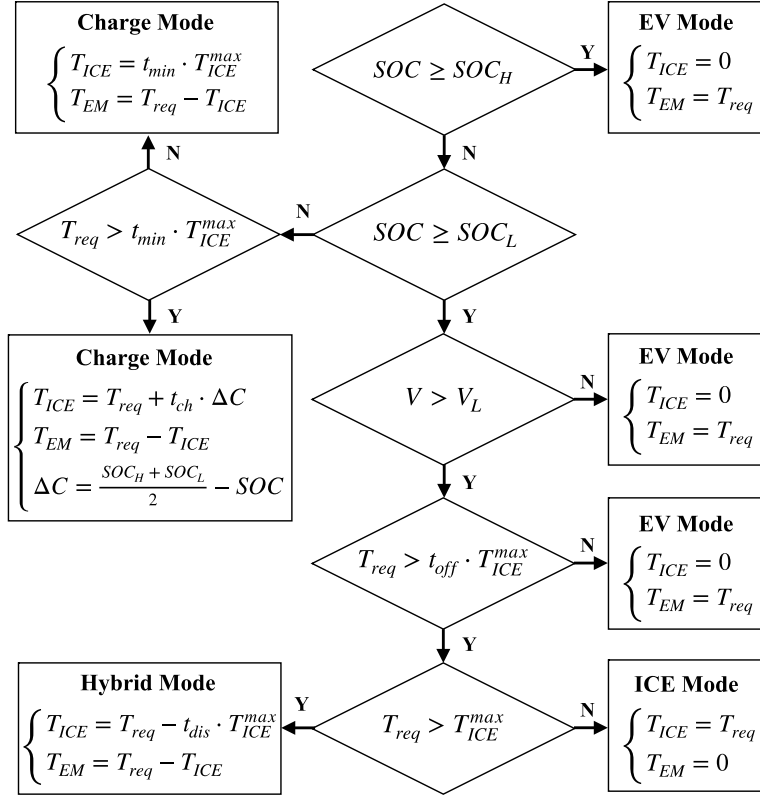


Fig. 4. 8 Workflow of the EACS

4.4 Summary

In this chapter, the eco-driving problem has been formulated first. The goal is to achieve a fuel-efficient and low-emission trip on the basis of driving safety.

To achieve this goal, a bi-level model predictive control (MPC) based control strategy is designed for a connected and automated hybrid electric vehicle (CAHEV). In this framework, the problem is first modelled as multi-objective optimization problem with

regard to (1) the objective of driving safety that can realize the safe driving by complying with traffic rules and keeping a safe distance with preceding vehicles (2) the objective of energy management that aims to reduce the fuel consumption with a balanced battery SOC level (3) the objective of emission reduction that serves to reduce the exhaust emissions HC , CO and NO_x . Next, a cost function is assigned to each objective. At the upper level of the control strategy, based on the driving variables via V2I and V2V communications, a driving scenario classifier is built up to recognize the instantaneous driving case so as to assign the corresponding cost in the optimization function. Then, the optimal vehicle acceleration that determines the velocity at the next time step is computed. At the lower level, given the torque demand on the wheels, the control system derives the optimal torque split ratio between ICE and EM to enable the powertrain working in a high-efficiency state. As a result, the overall fuel consumption and the engine-out emissions can be minimized, with the driving safety always ensured over the trip.

In order to evaluate the performance of the proposed eco-driving control strategy, the rule-based electric-assist control strategy (EACS), as one of the widely applied approaches for HEV energy management, in combination with the intelligent driver model (IDM) is synthesized as a comparison. In this benchmark strategy, The IDM model decides the realistic driving velocity at each time instant over the trip while the rule-based EACS computes the real-time torque split ratio in the powertrain based on the torque demand.

Chapter 5. Results and Discussion

5.1 Experiment setup

The simulation is running in MATLAB and SUMO, with the vehicle parameters obtained from ADVISOR. The background map for the studied vehicle with realistic traffic demand is from the TAPAS-Cologne project [77].

5.1.1 ADVISOR

ADVISOR is the short term for “Advanced Vehicle Simulator.” It is a vehicle powertrain simulator designed by National Renewable Energy Laboratory (NREL) in 1994 [78]. ADVISOR is based on empirical drivetrain components to evaluate vehicle performance under given driving cycles, such as fuel economy and exhaust emissions [78]. The drivetrain types in ADVISOR ranges from the ones for conventional internal combustion engine vehicles, hybrid electric vehicles, plug-in hybrid electric vehicles to pure electric vehicles. In this research, the studied parallel hybrid electric vehicle data is obtained from ADVISOR, including the data of internal combustion engine, electric motor, battery pack, transmission shift ratio, and vehicle physical parameters. The sample ADVISOR user interface is presented in Fig. 5. 1,

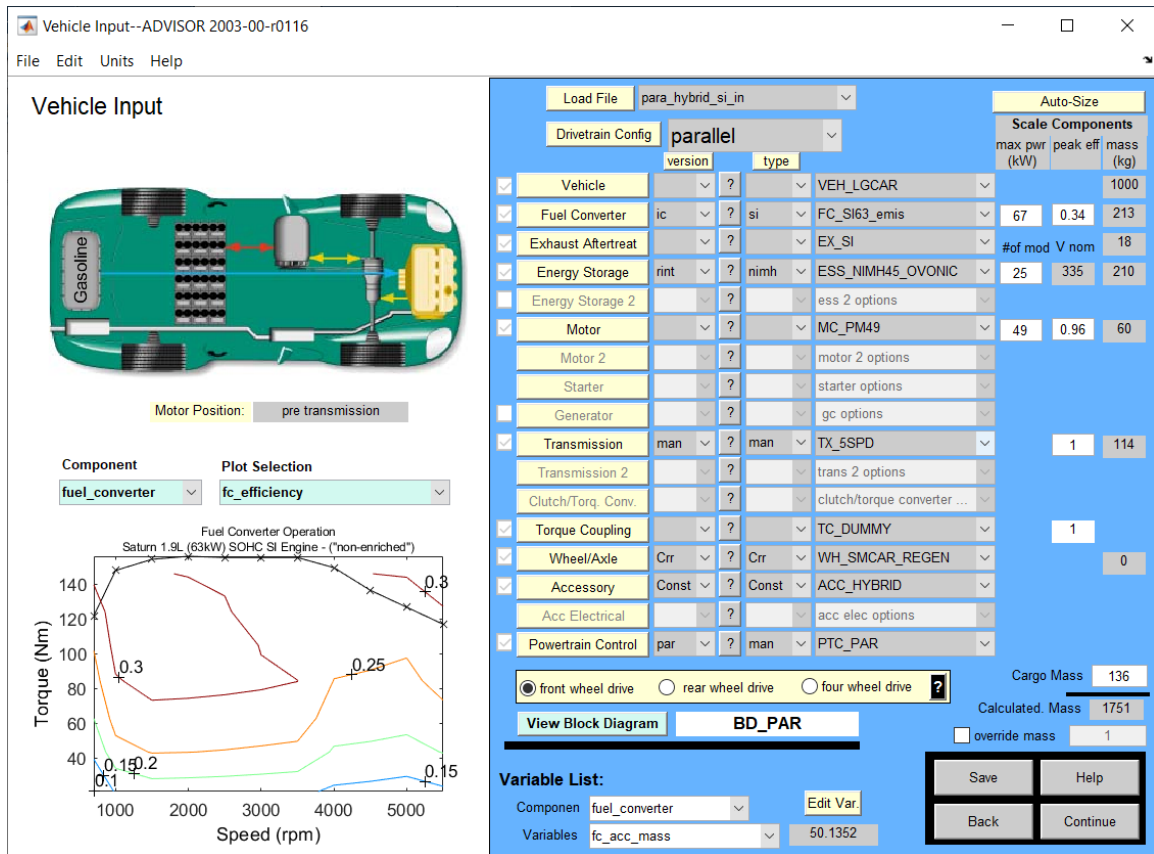


Fig. 5. 1 Sample ADVISOR interface for customizing vehicle parameters, a vehicle with a parallel hybrid powertrain is configured

5.1.2 SUMO

SUMO stands for “Simulation of Urban MObility,” and it is an open-source platform that is able to simulate realistic microscopic and macroscopic urban traffic flow mobility [79]. In this environment, an individual vehicle is considered as an agent that is running in the simulated map. The attributes of the agent can be customized to mimic the real-world vehicle, such as the vehicle type, the vehicle length, the speed limit, the acceleration limit, the frontal surface area and the like. On the other hand, the urban simulation map that can be either modelled using the built-in tool, or imported from the real world map involves

most realistic traffic elements, from the highway and urban roads, bus stops, induction loop to the road speed limit, customizable traffic lights program, and right-of-way rules, etc.

SUMO was first initiated in 2001 by a group of researchers associated with the German Aerospace Center (DLR) and some universities. Within the past ten years' development, SUMO has become a comprehensive suite for traffic simulation. Some of the main tools from SUMO are listed:

- (1) NETEDIT: a tool that is capable of reading and importing the real-world maps from different sources into SUMO
- (2) OD2TRIPS: that can map the traffic demand via the format of Origin/Destination (O/D) Matrices into individual vehicle trips on the map.
- (3) TraCI: short term for "Traffic Control Interface", which allows the online TCP-based communication with the simulated objects, such as running vehicles, traffic lights, and the online manipulation via commands
- (4) SUMO-GUI: the graphical user interface to display the online traffic simulation (Fig. 5. 2 shows a sample simulation on SUMO-GUI)

In this research, SUMO is used as the main platform to simulate and verify the bi-level eco-driving strategy for a connected and automated hybrid electric vehicle.

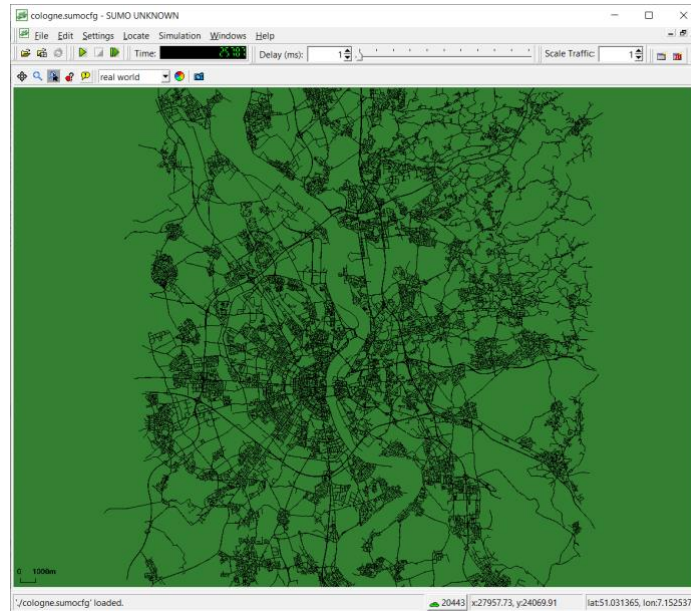


Fig. 5. 2 Sample SUMO-GUI interface, zoomed-out view of the Cologne, Germany urban transportation network

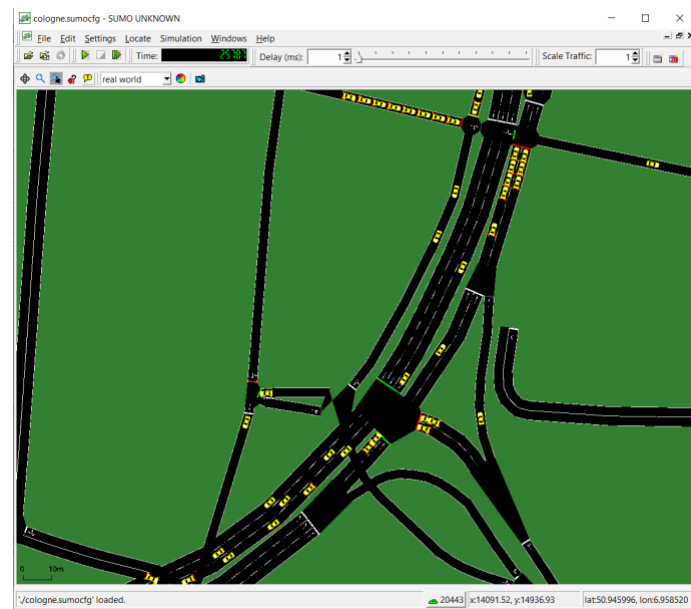


Fig. 5. 3 A zoomed-in view of the Cologne, Germany urban transportation network

[77]

5.1.3 Traffic simulation map

The simulation is running in MATLAB and SUMO on a PC with a 1.8 GHz Intel Core i5-8250U CPU and 16 GB of internal memory. The host connected and automated vehicle (CAV) is modelled as an HEV with a single-shaft pre-transmission hybrid electric powertrain, as depicted in Fig. 3. 1. The vehicle specifications are obtained from ADVISOR. Unlike the host CAV, the background vehicles in traffic are assumed to be of the same type - conventional passenger vehicles that are driven by a human. Their dynamic actions, including the instantaneous speed and acceleration, are determined by the car-changing model. The specifications are given in Table. 5. 1.

The simulation uses an urban map of Cologne, a typical medium-sized city in Germany, with a realistic traffic demand dataset from the TAPAS-Cologne project by the Institute of Transportation Systems at the German Aerospace Center (ITS-DLR) [77]. The road network covers the area of Cologne approximately 400 km^2 formed by 71,368 road segments. The realistic 24-hour traffic dataset, comprising of more than 700,000 individual trips, faithfully models the daily traffic activities of the drivers from Cologne [80]. Table. 5. 2 lists the attributes of the map. Fig. 5. 4 presents the city map of Cologne.

The host CAV starts from a complete stop (i.e. speed begins with 0 m/s and acceleration begins with 0 m/s^2) with battery state of charge at the level of 60%. As a result, the initial state variables can be represented as $[0,0,0.6]$. At each time instant, the longitudinal speed and acceleration of the host CAV are controlled by the proposed MPC-based strategy. The lateral dynamics is controlled by a simple lane-changing model, which triggers a lane-changing signal to the lane that leads the vehicle to the next road on the trip every time the vehicle enters a new road, and then keeps the vehicle stay in the lane until the next intersection. To evaluate the energy performance of the proposed eco-driving strategy, the host CAV is also controlled by the IDM strategy on the same trip, and the EACS rule-based strategy is applied on the vehicle powertrain to determine the instantaneous split ratio between the mechanical power and electrical power at each time instant.

The parameters for the constraint optimization problem, the proposed strategy, and the rule-based strategy are listed in Table. 5. 3

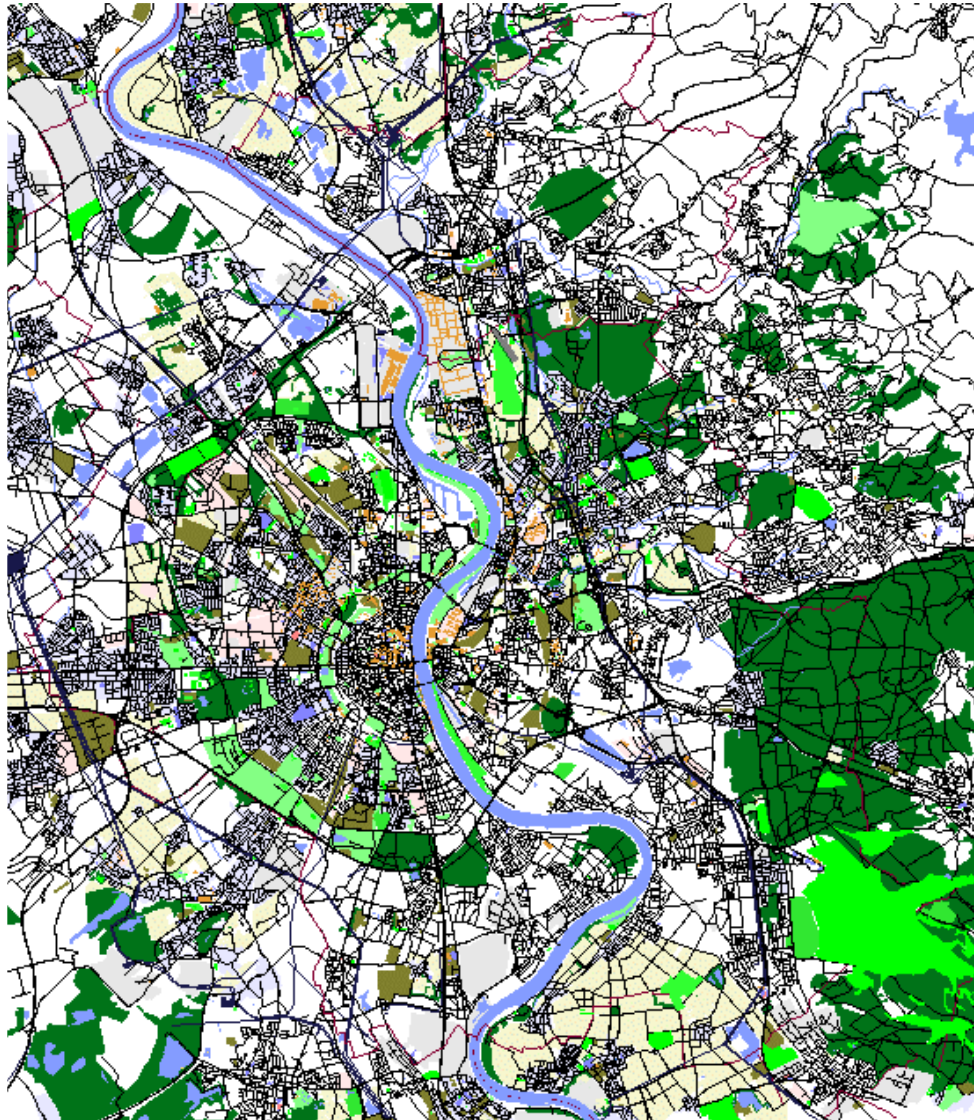


Fig. 5. 4 Urban network map of Cologne, Germany [77]

Table. 5. 1 Background vehicle specifications

| Components | Specification |
|--|----------------------------|
| Architecture | Conventional passenger car |
| Vehicle Length | 4.3 m |
| Acceleration ability (m/s^2) | 2.6 m/s^2 |
| Deceleration ability (m/s^2) | -4.5 m/s^2 |
| Lane-changing Model | LC2013 [81] |
| Car-following Model | Krauss [82] |

Table. 5. 2 Specifications of the simulation map

| | |
|---------------------------------|--|
| City | The metropolitan area of Cologne, Germany |
| Area (km^2) | approx. 400 km^2 |
| No. of Roads | 71,368 |
| No. of Intersections | 10,153 |
| No. of individual Trips | Over 700,000 |
| Duration | 24 <i>hours</i> |

Table. 5. 3 Parameters for simulation

| HEV constraints | | |
|--|----------------|---------------|
| Parameters | Symbols | Values |
| Maximum speed (km/h) | v_{max} | 162 |
| Deceleration ability (m/s ²) | a_{min} | -5 |
| Acceleration ability (m/s ²) | a_{max} | 5 |
| Minimum SOC (%) | SOC_{min} | 0 |
| Maximum SOC (%) | SOC_{max} | 100 |
| Split ratio lower bound (-) | γ_{min} | -10 |
| Split ratio upper bound (-) | γ_{max} | 10 |
| MPC-Based Eco-Driving Strategy | | |
| Parameters | Symbols | Values |
| Sampling time (s) | T_s | 1 |
| Prediction horizon (s) | N_p | 5 |
| Control horizon (s) | N_c | 1 |
| The weighting factor for energy cost (-) | α | 2.5 |
| The weighting factor for emission cost (-) | β | 8 |
| The driving safety weight factor I (-) | w_1 | 1 |
| The driving safety weight factor II (-) | w_2 | 1 |
| The driving safety weight factor III (-) | w_3 | 1 |
| The driving safety weight factor IV (-) | q | 0.01 |
| The driving safety weight factor V (-) | f_1 | 0.2 |
| The driving safety weight factor VI (-) | f_2 | 2 |
| EACS Rule-Based Strategy | | |
| Parameters | Symbols | Values |
| The lowest SOC allowed (-) | SOC_L | 0.5 |
| The highest SOC allowed (-) | SOC_H | 0.7 |
| The threshold for ICE shut off (-) | t_{off} | 0.2 |
| The charging threshold for low SOC (-) | t_{min} | 0.5 |
| The charging torque for normal SOC (-) | t_{ch} | 50 |
| The discharging factor (-) | t_{dis} | 0.2 |
| The threshold for vehicle speed (m/s) | V_L | 4 |

5.2 Simulation results on a highway-urban trip

5.2.1 Trip Setup

A 10 km-trip is chosen to perform the simulation, as shown in Fig. 5. 5. The trip begins from a start point located at the suburban area (Point A in Fig. 5. 5) to the destination in the urban area (Point B in Fig. 5. 5) in Cologne, Germany around 7:30 in the morning, which mimics a daily home-work commute. The roads that constitute the route are chosen based on the shortest distance between the start and the endpoint. Point P that lies in the middle of the trip is the border point between the suburban routes which are mainly made up of highspeed highway roads (between Point A to Point P), and the urban routes which are mainly made up of urban roads (between Point P to Point A). Details of the trip are provided in the following table.

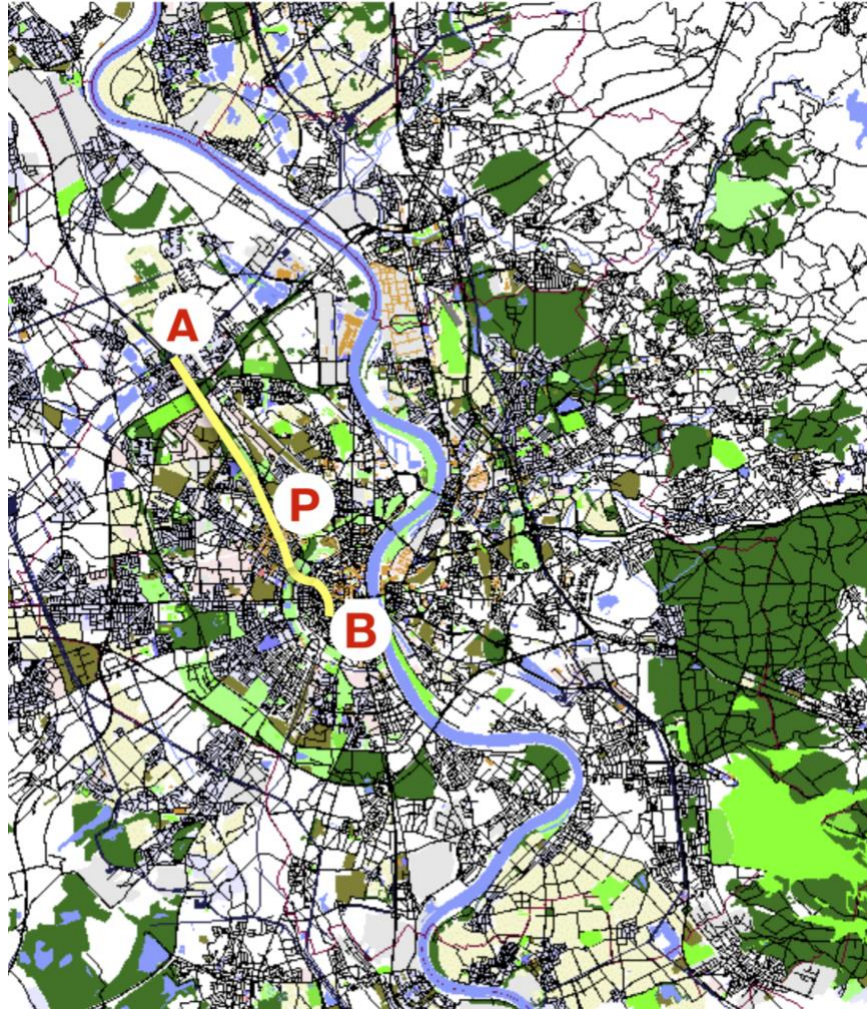


Fig. 5. 5 The simulated highway-urban trip from point A to point B that passes point P [77]

Table. 5. 4 Specifications of the highway-urban trip

| | Highway-Urban Trip |
|-----------------------------|---------------------------|
| Total Length (km) | 10.407 km |
| No. of Roads | 49 |
| Highway / A – P (km) | 6.862 km |
| Urban / B – P (km) | 3.545 km |

The speed profiles produced by the proposed eco-driving strategy and the IDM + EACS are presented in Fig. 5. 6 and Fig. 5. 7, respectively.

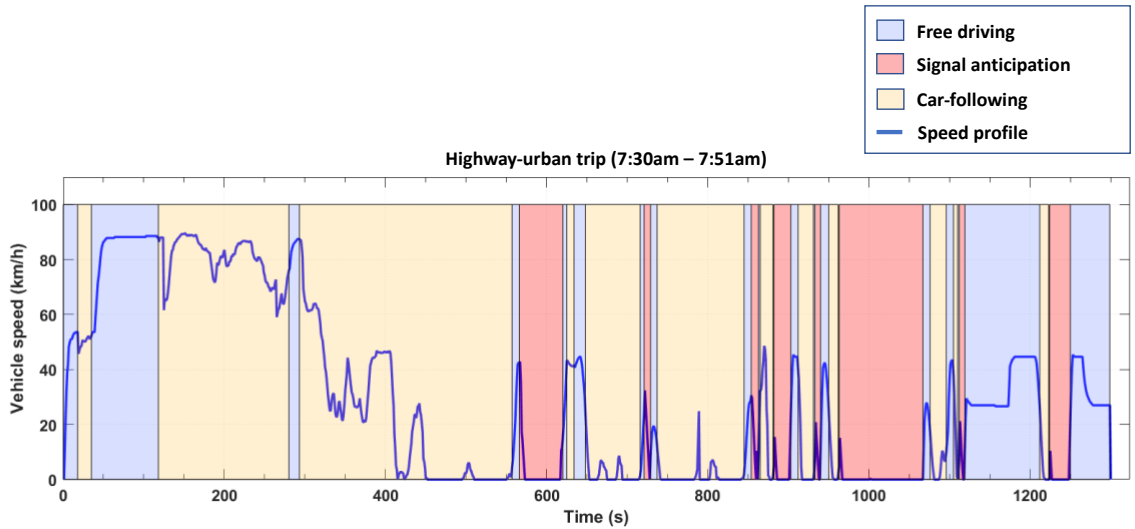


Fig. 5. 6 Speed profile by MPC-based eco-driving strategy in on an highway-urban trip

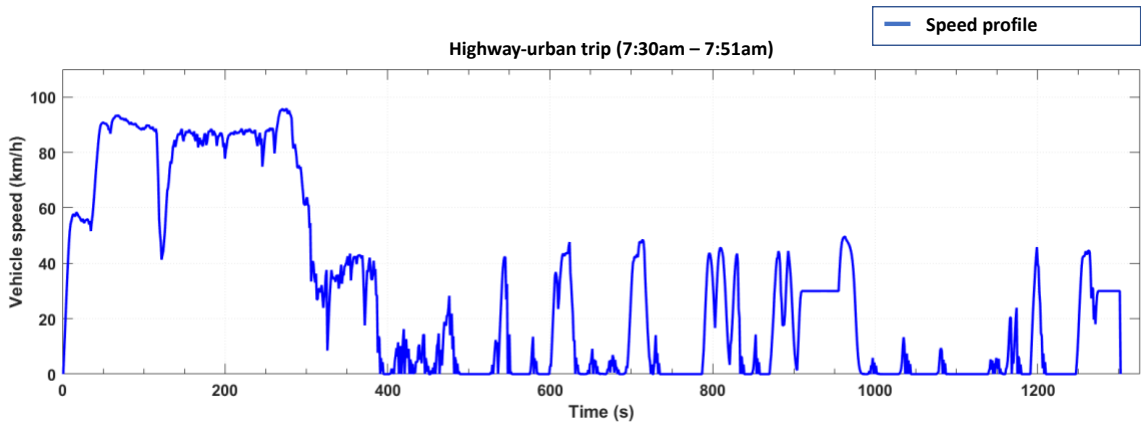


Fig. 5. 7 Speed profile by the rule-based EACS strategy on an highway-urban trip

In Fig. 5. 8, it is clearly shown that the highway driving (from point A to point P over the trip in Fig. 5. 5) corresponds to the speed profile from 0 s to around 300th s, and the rest of the speed profile mainly consists of urban driving with congested traffic conditions. According to the driving scenario classifier, the complete trip can be broken down into three scenarios triggered by the real-time driving parameters listed in Table. 4. 1, they are 1) free driving scenario 2) Signal anticipation scenario and 3) car-following scenario, illustrated in Fig. 5. 6. The speed profile by running IDM for EACS, as shown in Fig. 5. 7, on the other hand, results in a collision-free safe driving along the same trip.

5.2.2 Driving Safety

5.2.2.1 *Free driving*

With the cost for free driving described in Chapter 4.2.1.1 applied, the resultant vehicle driving in Fig. 5. 8 demonstrates that, first, before reaching the maximum speed limit, the control system is able to make vehicle speed gradually converge to the target speed when there is no vehicle, secondly, by adding extra penalties on the maximum allowed speed, the control system can always ensure that the instantaneous vehicle speed strictly complies with the maximum allowed speed set by each road where the vehicle is running on.

Moreover, in the zoomed-in region in Fig. 5. 8, *J*, *K*, and *L* represent three connecting roads on the trip with the maximum allowed speed as 50 km/h, 30 km/h and 50 km/h, respectively. Combined with Fig. 5. 6, it can be observed that the speed fluctuation on the road *J* was caused by the car-following actions. On entering the road *K*, the vehicle is switched to the free driving mode by the driving scenario classifier, and its speed gradually reaches the speed limit and keeps constant until, at the end of this road, it enters the next road *L* with a higher speed limit. Then the vehicle accelerates to gradually adapt its speed to the road speed limit of 50 km/h on the road *L* and stays constant in the free driving mode.

The above proves the proposed control strategy can execute an adaptive and safe control of the vehicle speed throughout the entire driving trip.

5.2.2.2 *Signal anticipation*

Over the entire trip, the vehicle has driven through seven TSCIs in total, as illustrated in the red shaded regions in Fig. 5. 9. The control strategy for signal anticipation is designed so as to stop the vehicle at the yellow and red lights, or the green lights with insufficient remaining phase duration to pass, and let the vehicle pass the green signal intersection given enough remaining phase time, as modelled in Chapter 4.2.1.1.

The zoomed-in region of Fig. 5. 9 shows the vehicle speed profile at a TSCI where the signal has gone through the phases from green, yellow, red and green for the next round. It can be clearly observed that the signal is green before the driving scenario classifier turns on the signal anticipation mode for the vehicle. At the moment when the vehicle starts to react to the traffic lights, though it is still green which permits the passing, the control system sends the braking command based on the result that the estimated passing time Δt_r (in Eq. (4. 8)) for the vehicle to pass the intersection turns out to be more than the remaining green signal duration; in other words, the signal will turn red before the vehicle is able to drive through the TSCI. As a result, the vehicle braking command causes the deceleration in green phase #1 and yellow signal phase #2 in the figure. Then the vehicle remains completely stopped during the red signal phase #3. When the signal turns to green again, as denoted as phase #4, the control signal compares the estimated passing time Δt_r and the remaining phase time, and sends out the pass command, which triggers the vehicle start-up until the vehicle leaves the intersection. In this way, safe automated driving that conforms to the traffic rules are guaranteed, especially, the use of estimated passing time helps to anticipate the travel time and avoid the unnecessary emergency braking at the intersection when the remaining signal phase time is insufficient for the vehicle to pass.

5.2.2.3 *Car-following*

The control strategy for the car-following scenario, as described in Eq. (4. 17), works toward keeping the following distance between the host and preceding vehicle at a safe range bounded by the minimum and maximum allowed following distances, which are changing with instantaneous vehicle speed over time, as described in Eq. (4. 13) and Eq. (4. 14). Fig. 5. 10 depicts the car-following distances with shaded regions representing different driving scenarios over the trip. The car-following distances thereby are only displayed in the yellow shaded regions as car-following scenarios. It's worth noting that each yellow shaded segment denotes a complete car-following action with a single preceding vehicle. Due to the dynamic and mixed traffic conditions in the realistic simulation map (as can be seen in Fig. 5. 6), the car-following scenario of the host vehicle can be interrupted by different real-time cases, such as the preceding vehicle left the lane or the road, or the host vehicle turns to another road. The host vehicle driving mode is then switched accordingly until another preceding vehicle is detected in the range threshold Δs_L which triggers a next car-following mode.

It can be clearly seen from Fig. 5. 10 that the following distance of the host vehicle never violates the upper and lower bounds. As a result, the safe car-following requirement is satisfied. In the zoomed-in region, the region P , Q and R are the car-following scenarios, the free-driving scenario, and the car-following scenario, respectively. In the car-following scenario P , the vehicle keeps a safe distance with the preceding vehicle, then completes the following action as the preceding vehicle changes to another lane. As no preceding vehicle is found in the detection range threshold Δs_L , the vehicle is switched to the free driving mode in scenario Q . Soon, as a new preceding vehicle is found in scenario R . The host vehicle starts to keep a safe distance with the preceding vehicle in R . The upper and lower bound distance bounds vary as the host vehicle speed changes throughout the trip.

With the car-following control strategy applied, the host vehicle is able to keep a safe distance from the preceding vehicle and initiates adaptive car-following actions across the whole trip.

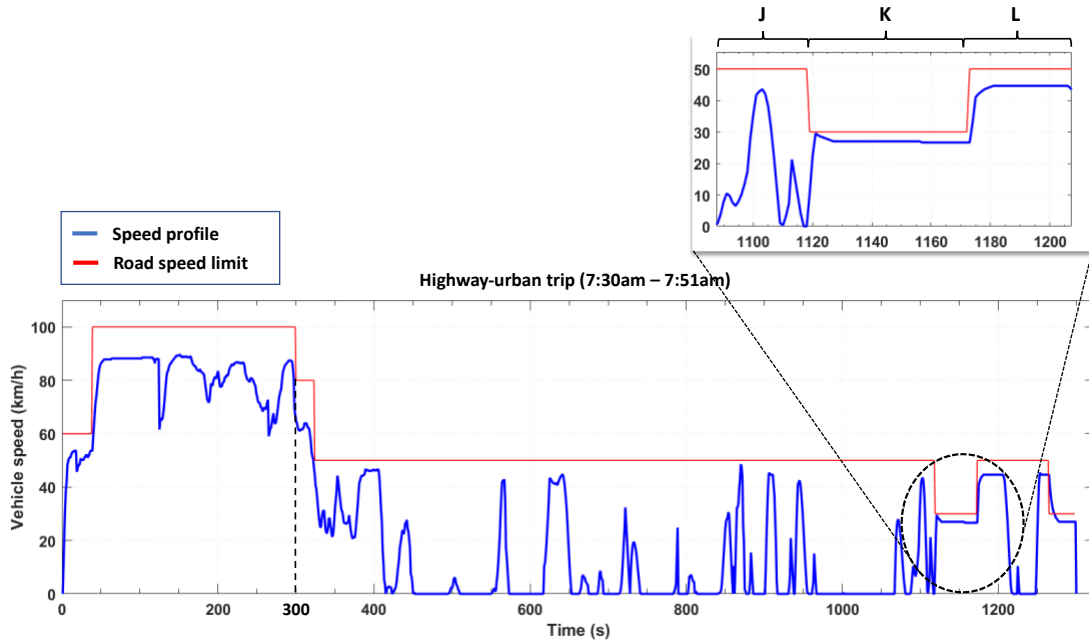


Fig. 5. 8 Speed profile by MPC-based eco-driving strategy with road speed limit throughout an highway-urban trip

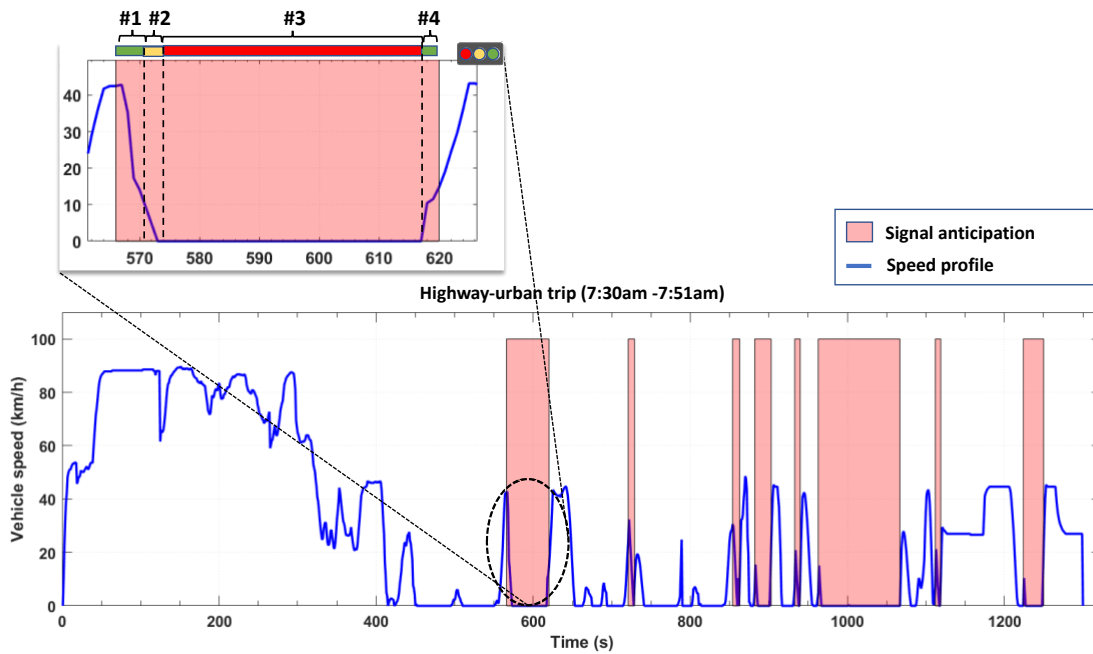


Fig. 5. 9 Signal anticipation by MPC-based eco-driving strategy on an highway-urban trip

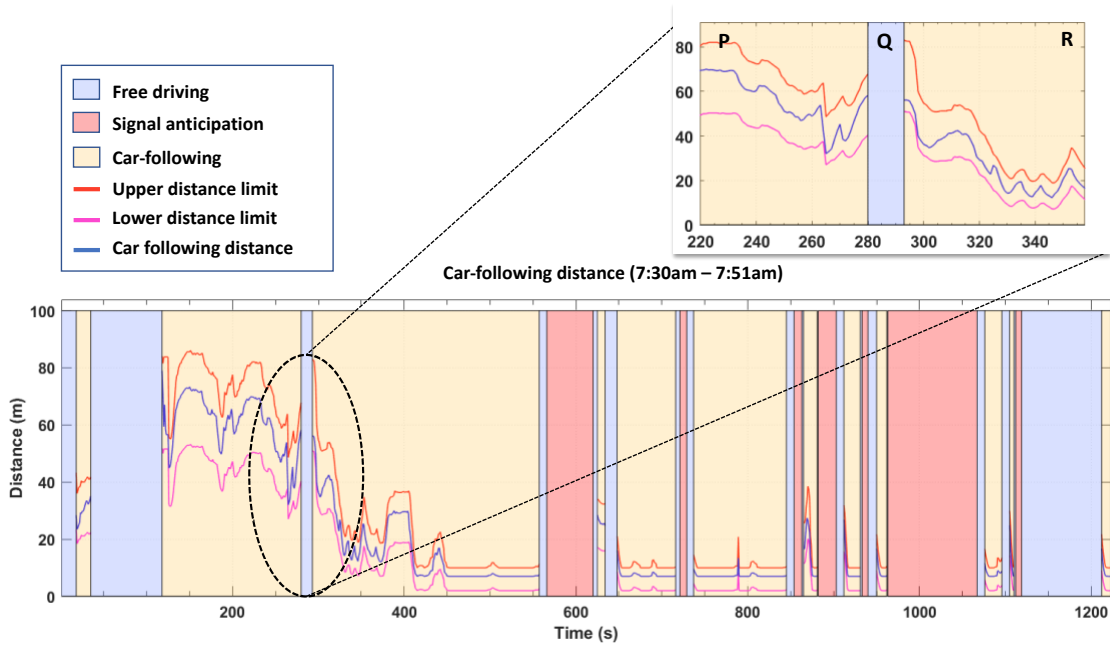


Fig. 5. 10 Car-following scenarios by MPC-based eco-driving strategy on an highway-urban trip

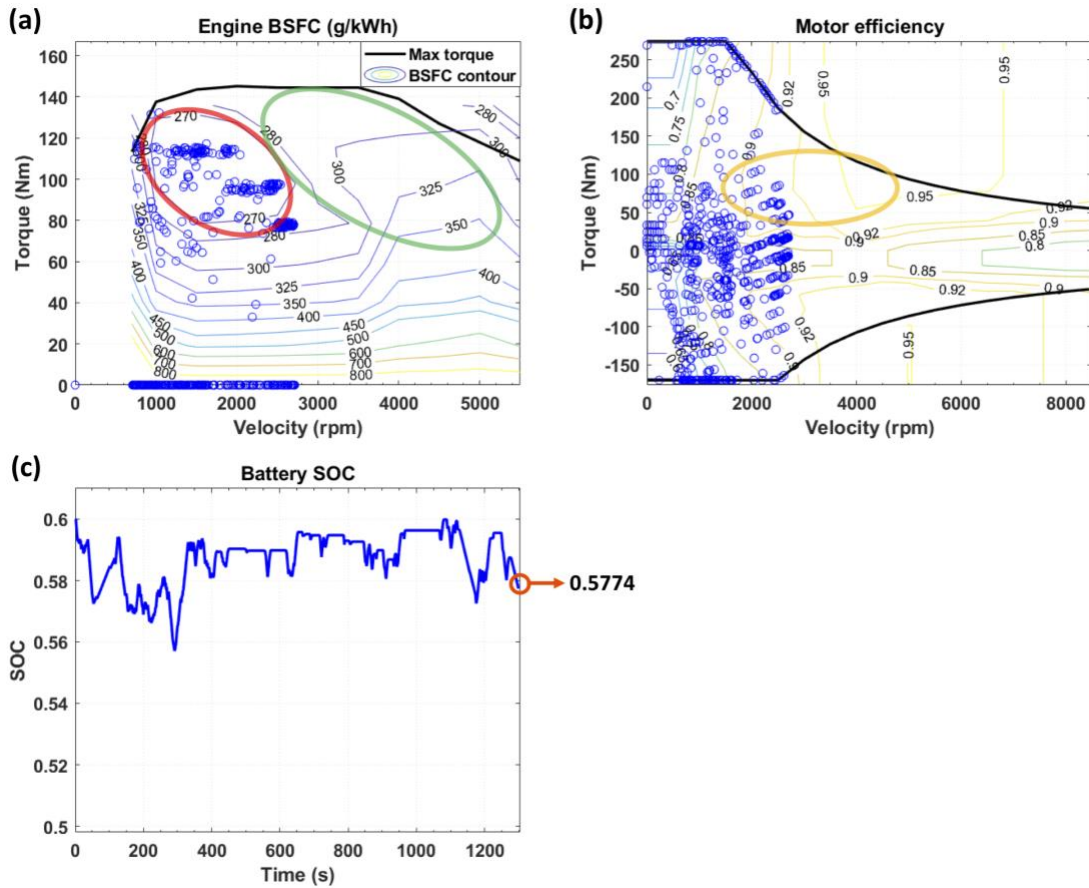


Fig. 5. 11 The MPC-based eco-driving strategy results including (a) Brake-specific fuel consumption (BSFC), (b) Efficiency of the electric motor (EM) and (c) SOC of the battery pack on an highway-urban trip

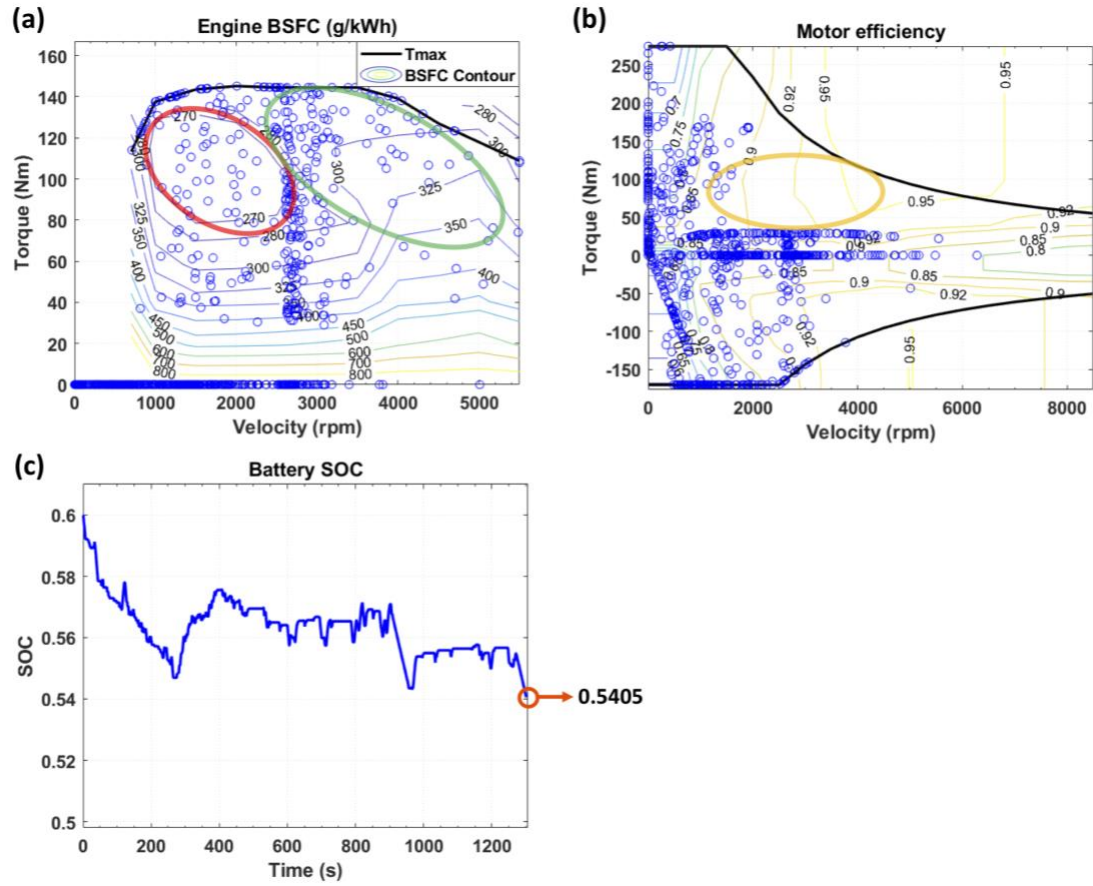


Fig. 5. 12 The EACS rule-based strategy results including (a) Brake-specific fuel consumption (BSFC), (b) Efficiency of the electric motor (EM) and (c) SOC of the battery pack on an highway-urban trip

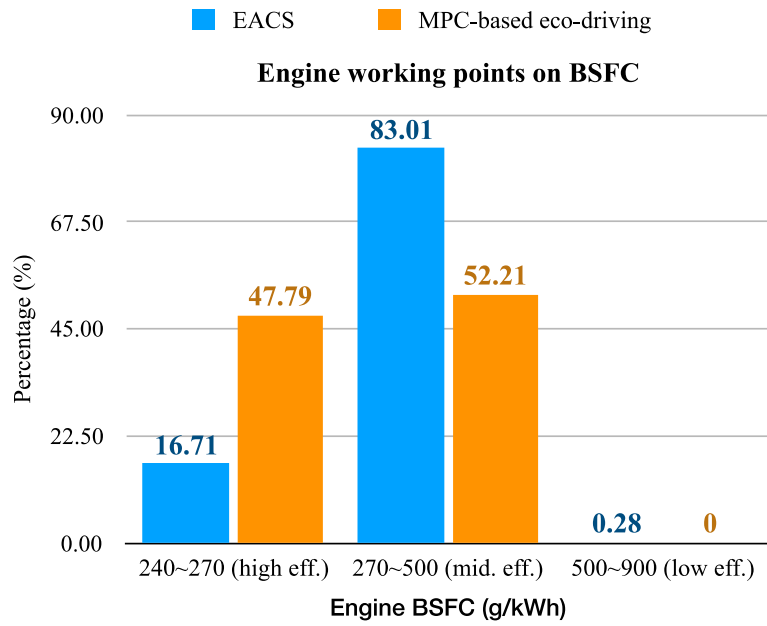


Fig. 5. 13 The distribution of engine working points by the MPC-based eco-driving strategy and the EACS rule-based strategy on an highway-urban trip

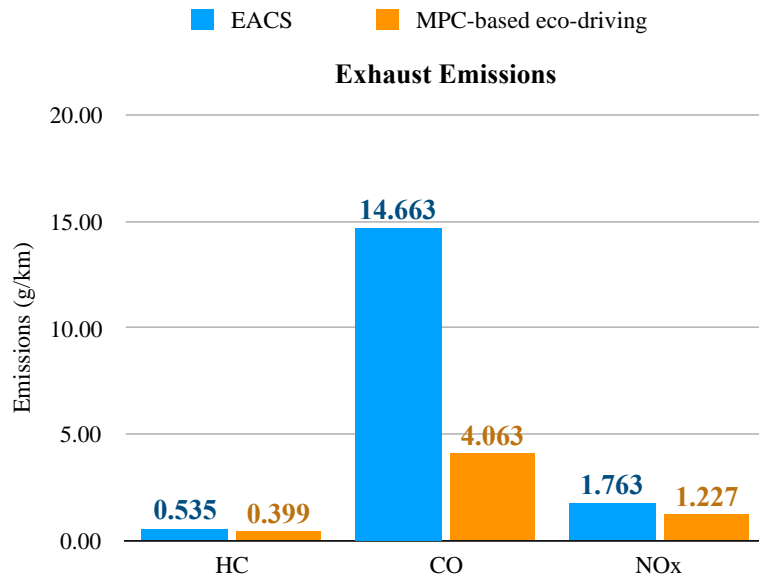


Fig. 5. 14 The exhaust emissions of HC, CO, NO_x produced by the MPC-based eco-driving strategy and the EACS rule-based strategy on an highway-urban trip

5.2.3 Energy consumption and emission reduction

The energy performances of the MPC-based strategy and the EACS rule-based strategy can be referred to in Fig. 5. 11 and Fig. 5. 12. In terms of engine efficiency, as shown in Fig. 5. 11 (a) and Fig. 5. 12 (a), the dashed line represents the engine optimal engine working line. Compared with the EACS rule-based strategy, the engine operation points produced by MPC-based strategy tends to aggregate in the high-efficiency region, illustrated as the red circled region on the left. While for the operations of the EACS rule-based strategy, due to the fact that a rigid set of rules rather than an accurate model-based optimizer is used, the engine working points tend to be more evenly distributed over the entire operation regions without a propensity for high-efficiency region. For this reason, the engine operation of the EACS rule-based strategy over the entire simulation duration results in a suboptimal efficiency. As a complement of Fig. 5. 11 (a) and Fig. 5. 12 (a), Fig. 5. 13 shows the distribution of engine working points in regions with different efficiency, where column 240~270 (g/kWh), column 270~500 (g/kWh) and column 500~900 (g/kWh) denote the high, middle, low BSFC map efficiency regions, respectively. It can be seen that for the MPC-based strategy, the distribution of working points in the high-efficiency region (240~270 (g/kWh)) is 47.49%, which is significantly higher than those from EACS strategy (16.71%). Besides, in the middle (270~500 (g/kWh)) and low (500~900 (g/kWh)) efficiency regions, the MPC-based strategy has working points that account for 52.21% and 0%, which are both fewer than those of the EACS strategy, as 83.01% and 0.28%, respectively. It means that the engine of the proposed MPC-based strategy works much efficiently than the EACS strategy over the same trip, resulting in a higher aggregation of high-efficiency working points in the figure.

In terms of the electric motor efficiency, as seen in Fig. 5. 11 (b) and Fig. 5. 12 (b) for the MPC-based strategy and the EACS rule-based strategy, respectively. It is clearly observed that the motors controlled by both methods take good use of regenerative braking kinetics to charge the battery pack, as indicated by the region corresponding to the negative motor torque. However, the motor working of the MPC-based strategy performs better than

the EACS rule-based strategy in the yellow circled region corresponding to the high-efficiency region, which demonstrates that the motor under the control of the MPC-based strategy is working more efficiently to assist the engine over the entire trip, thus saves more electrical energy.

In comparison to the SOC of the EACS rule-based strategy shown in Fig. 5. 12 (c), the SOC of the MPC-based strategy based on the current set of parameters (Fig. 5. 11 (c)) shows that a more energy sustaining policy is adopted to propel the vehicle. Therefore, a healthy battery SOC is balanced. Despite that, the terminal SOC of the MPC-based strategy shows that the battery still gets charged properly by good use of regenerative braking kinetic energy along with the redundant energy from the engine over the trip.

The numeric results from the proposed MPC-based strategy and the EACS rule-based strategy are presented in Table. 5. 5. It is obvious that the overall fuel consumption from the proposed strategy is reduced by 26.80% (SOC corrected) with respect to the one of the EACS rule-based strategy, which is a great improvement. Similar to the terminal SOC as 54.05% of the EACS rule-based strategy, the 57.74% terminal SOC of the MPC-based strategy shows that the proposed strategy is more likely to sustain the electrical energy to a healthy level when powering the vehicle, at the same time, the SOC level is much higher than the minimum allowed SOC level, 0.5, where a buffering room is left for battery use over the trip.

The vehicle emissions from the MPC-based strategy are also reduced by 27.69%, 73.91% and 47.59% for exhaust emissions hc , co and no_x , respectively, with respect to the results from the EACS rule-based strategy. The exceptional high saving in the 72.30% co consumption produced by the MPC-based strategy comes from the fact that in comparison to the engine working points from the EACS rule-based strategy (Fig. 5. 12 (a)) much less engine operation points under the control of MPC-based strategy Fig. 5. 11 (a)) tend to gather in the green circled region which corresponds to the high co cost region. The exhaust emission chart can be found in Fig. 5. 14.

The results over a day-to-day work-home commute trip demonstrate that the proposed MPC-based eco-driving strategy is capable of keeping the vehicle driving safely in highway and urban roads, while greatly improving the energy economy as well as reducing the vehicle emissions when the IDM + rule-based EACS strategy is used as the benchmark.

Table. 5. 5 Results from the proposed MPC-based eco-driving strategy and the EACS rule-based strategy (SOC corrected) on a highway-urban trip

| Strategies | EACS | MPC-based | Improvement |
|-----------------------------|-------------|------------------|--------------------|
| Fuel consumption (g) | 796.94 | 583.35 | -26.80% |
| Terminal SOC (%) | 54.05 | 57.74 | --- |
| HC | 6.61 | 4.78 | -27.69% |
| CO | 195.13 | 50.90 | -73.91% |
| NOx | 13.68 | 7.17 | -47.59% |

5.3 Simulation results on a suburban-urban trip

5.3.1 Trip Setup

In order to verify the result of the proposed strategy, another 10 km-trip is selected with road conditions consisting of mainly suburban and urban road types, which are different from the highway-urban trip. The trip details are presented in the following figure and table.

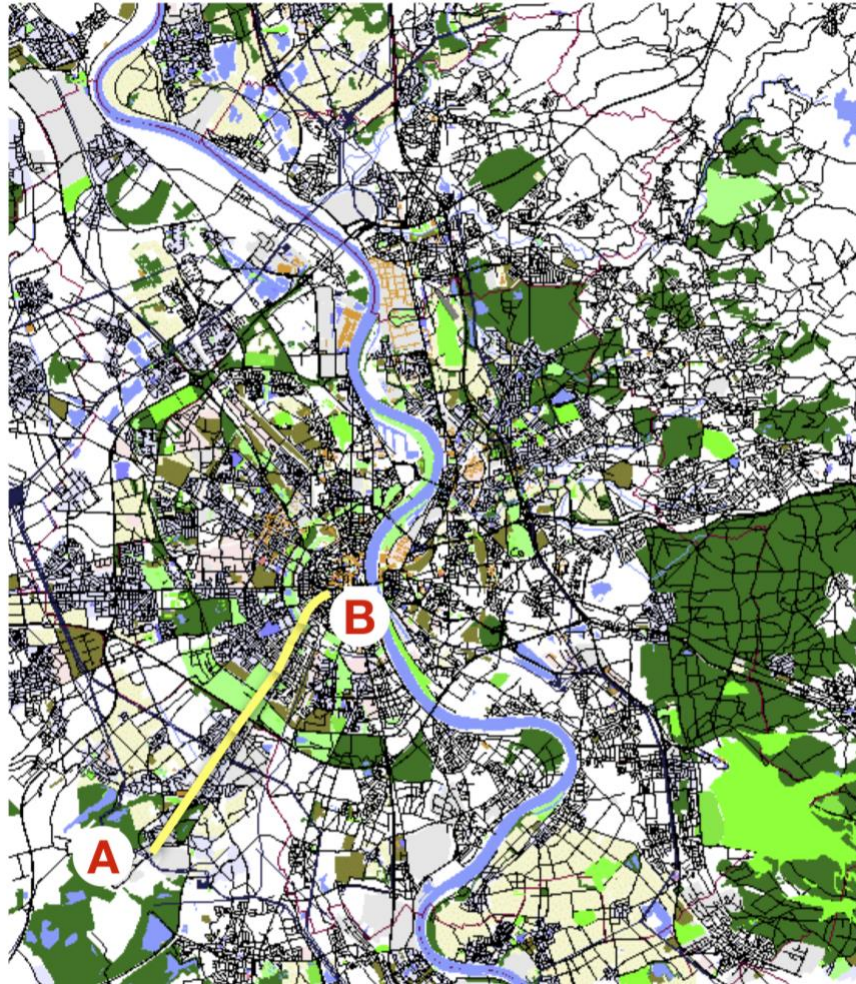


Fig. 5. 15 The simulated suburban-urban trip from point A to point B [77]

Table. 5. 6 Specifications of the suburban-urban trip

| | Highway-Urban Trip |
|--------------------------|---------------------------|
| Total Length (km) | 10.109 km |
| No. of Roads | 97 |
| Suburban (km) | 2.347 km |
| Urban (km) | 7.762 km |

The parameters remain the same as the previous trip, which can be seen in Table. 5. 3.

The speed profiles produced by the proposed eco-driving strategy and the IDM + EACS are presented in Fig. 5. 15 and Fig. 5. 16, respectively.

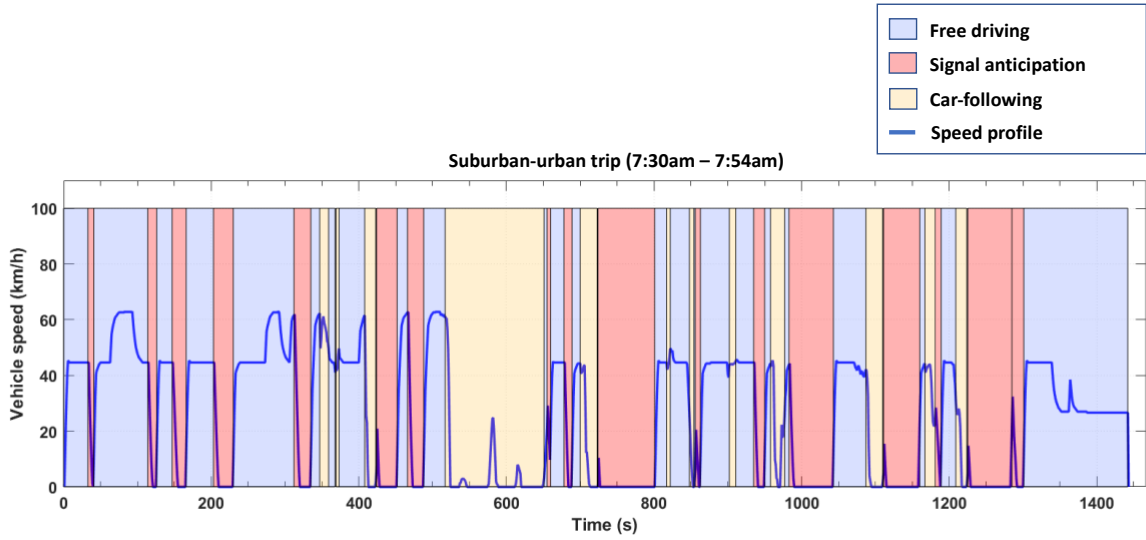


Fig. 5. 16 Speed profile by MPC-based eco-driving strategy on a suburban-urban trip

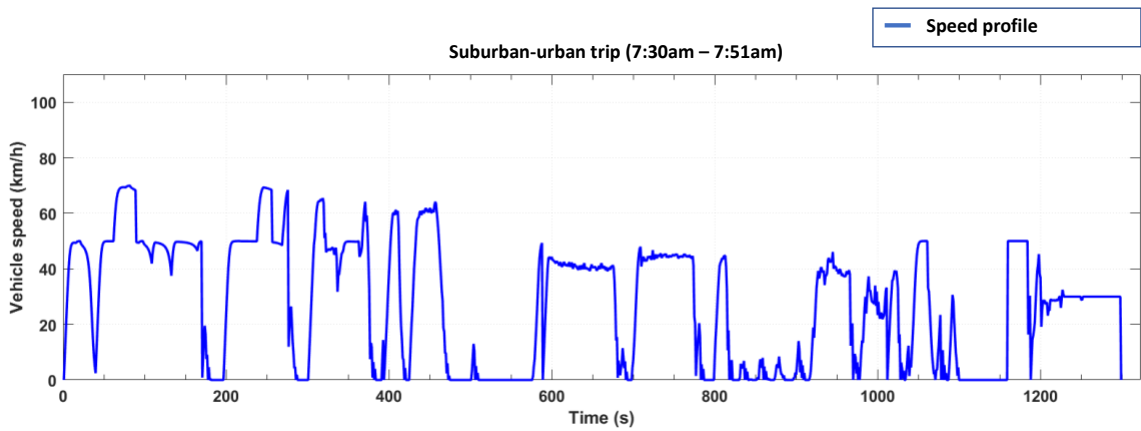


Fig. 5. 17 Speed profile by the rule-based EACS strategy on a suburban-urban trip

It is obvious in Fig. 5. 16 and Fig. 5. 18 that the trip is mixed with both the suburban road conditions (which are labelled as road segment #1, #2, #3 and #4 in Fig. 5. 18) and urban road conditions. The coloured regions in Fig. 5. 16 represent different driving scenarios switched by the on-board driving scenario classifier (DSC) in the control strategy. On the other hand, the speed profile produced by IDM results in a collision-free driving cycle over the trip.

5.3.2 Driving Safety

5.3.2.1 *Free driving*

With the cost of free driving applied in this strip, the speed profile in Fig. 5. 18 shows that the control system is able to prevent the instantaneous vehicle speed from violating the speed limit set by the roads where the vehicle is running on.

In addition, as displayed in the zoomed-in region in Fig. 5. 18, *J*, *K*, and *L* are three connecting roads on the trip with speed limit as 70 km/h, 50 km/h and 70 km/h, respectively. It can be seen that as the vehicle approaches the speed limit on the road *J*, it turns to the road *K* and gradually adapts the speed to the speed limit of 50 km/h. When the vehicle turns to the next road *L*, it accelerates to the speed limit of 70 km/h until the speed was stopped by a TSCI. The vehicle continues to drive when the signal turns to green. The above shows the effectiveness of the proposed control strategy in complying with the speed limits during the free driving mode.

5.3.2.2 *Signal anticipation*

There exist more TSCIs over this trip when compared to the highway-urban trip, as shown in Fig. 5. 19. The control strategy that aims to determine whether the pass/brake command

based on the current signal phase and phase remaining time is applied. It can be seen in the zoomed-region in Fig. 5. 19 that, after the control strategy receives the traffic signal-related data at entering the anticipating region, the brake command is executed since there is not sufficient time for the vehicle to pass the intersection even if the signal is green at the moment. The vehicle speed brakes to a complete stop in green phase #1 and remains static in yellow signal phase #2 and red signal phase #3 until the signal turns to green again with sufficient passing time for the vehicle. Then the vehicle starts up to pass the TSCI. The results from the signal anticipation principles show that safe vehicular actions can be expected at a TSCI with the help of data received via V2I communication.

5.3.2.3 *Car-following*

In the car-following scenario, the main goal of the vehicle is to keep a safe distance with the preceding vehicle during driving. The distance varies with instantaneous vehicle speed because a corresponding safe braking distance has to be set at different vehicle speeds. In Fig. 5. 20, the yellow shaded regions are the car-following cases recorded throughout this trip. Due to the mixture of driving conditions, the car-following actions could be interrupted by different cases. Over the trip, it's clearly shown that the inter-vehicle distances are kept in the upper and lower bounds of the allowed distance.

It can be observed that in the zoomed-in region in Fig. 5. 20, the vehicle first completes a safe car-following distance to a preceding vehicle, as denoted as case *P*, until a TSCI that stops the vehicle from following, in case *Q*. As the signal permits passing, the vehicle enters the free driving mode and catches a preceding vehicle and switches to the next car-following scenario, as shown in case *R* and *S*, respectively.

Therefore, the car-following mode controlled by the strategy enables the vehicle to have a collision-free and accident-free driving trip.

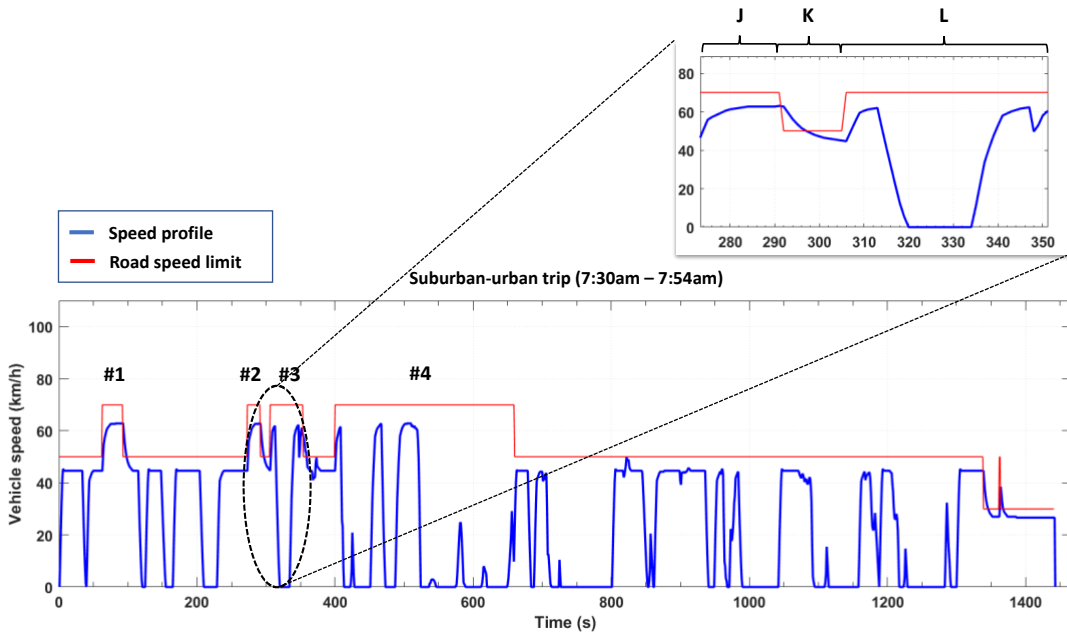


Fig. 5. 18 Speed profile by MPC-based eco-driving strategy with road speed limit throughout a suburban-urban trip

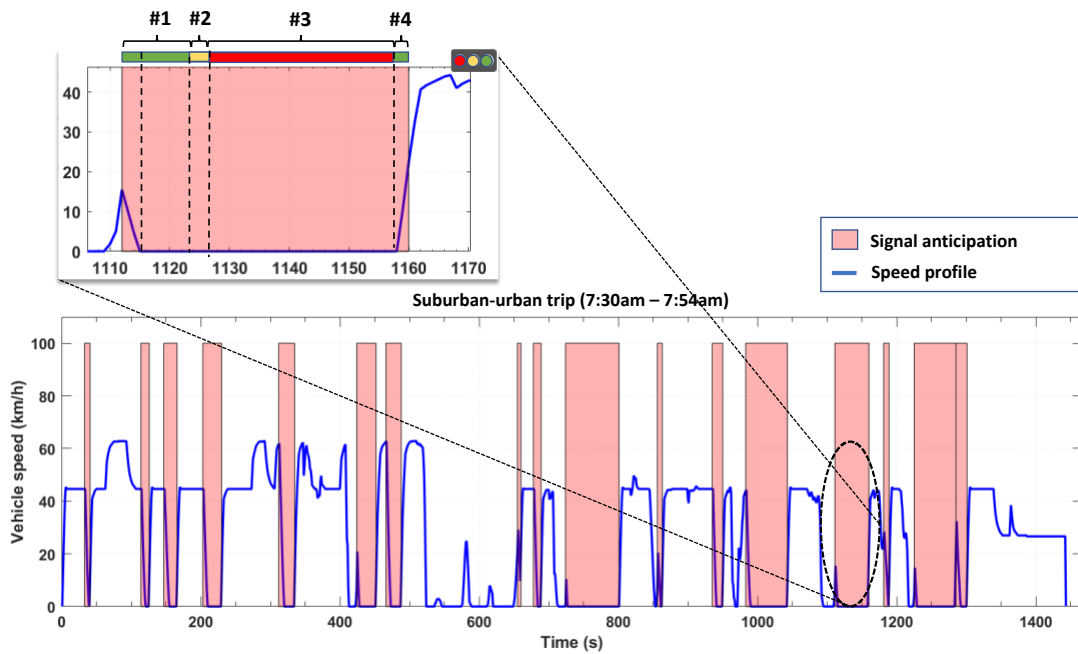


Fig. 5. 19 Signal anticipation by MPC-based eco-driving strategy on a suburban-urban trip

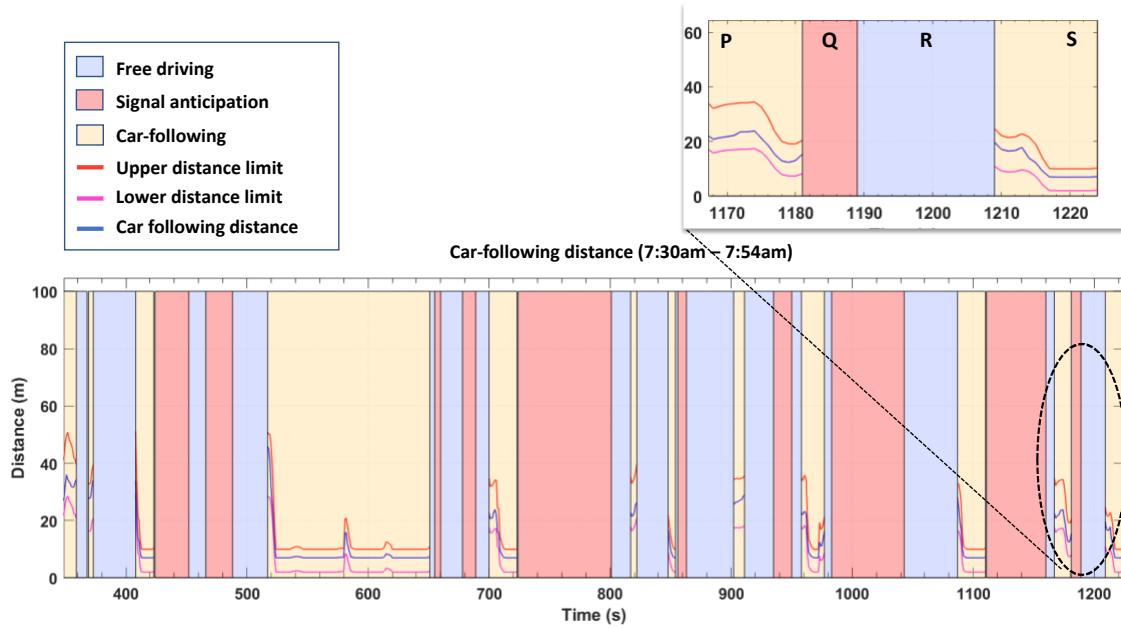


Fig. 5. 20 Car-following scenarios by MPC-based eco-driving strategy on a suburban-urban trip

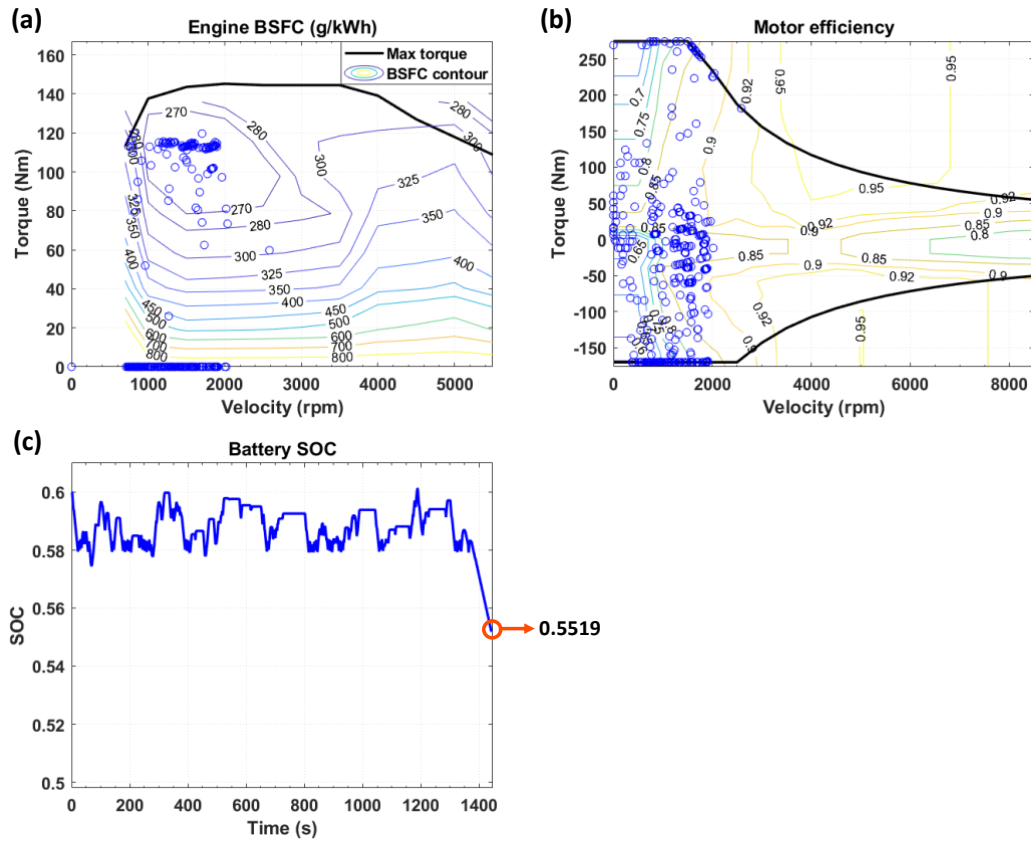


Fig. 5. 21 The MPC-based eco-driving strategy results including (a) Brake-specific fuel consumption (BSFC), (b) Efficiency of the electric motor (EM) and (c) SOC of the battery pack on a suburban-urban trip

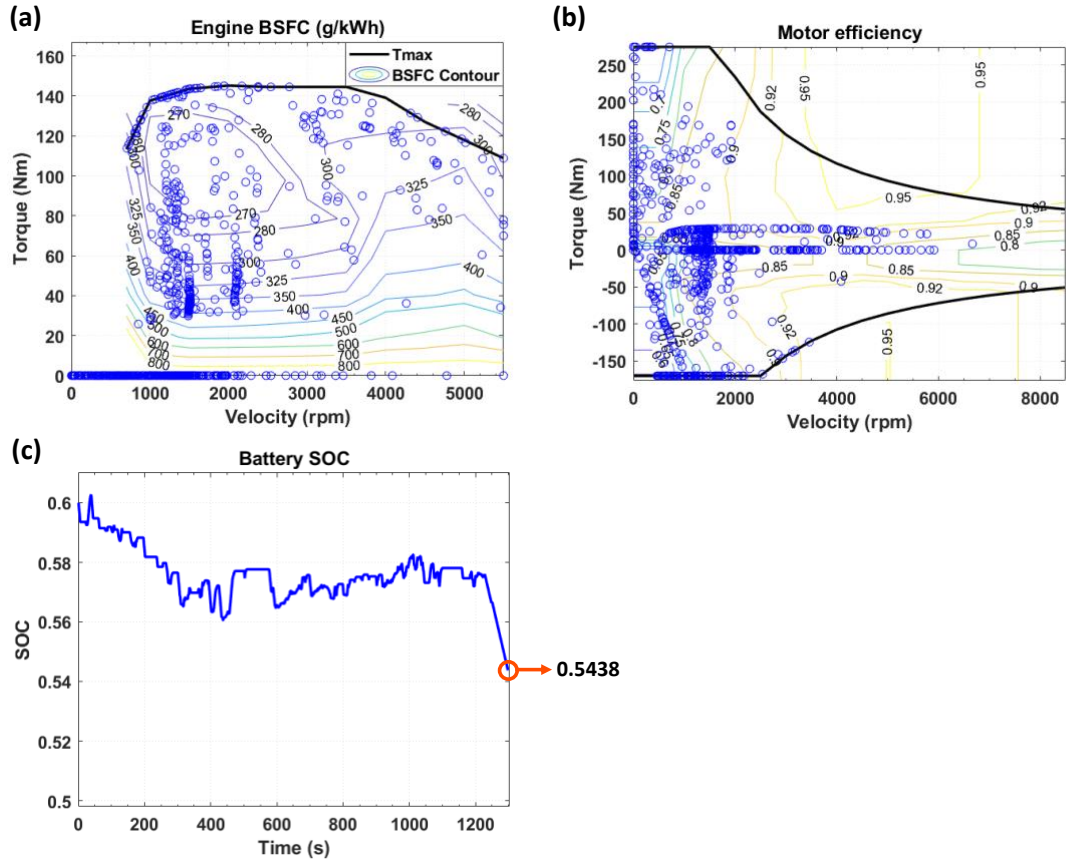


Fig. 5. 22 The EACS rule-based strategy results including (a) Brake-specific fuel consumption (BSFC), (b) Efficiency of the electric motor (EM) and (c) SOC of the battery pack on a suburban-urban trip

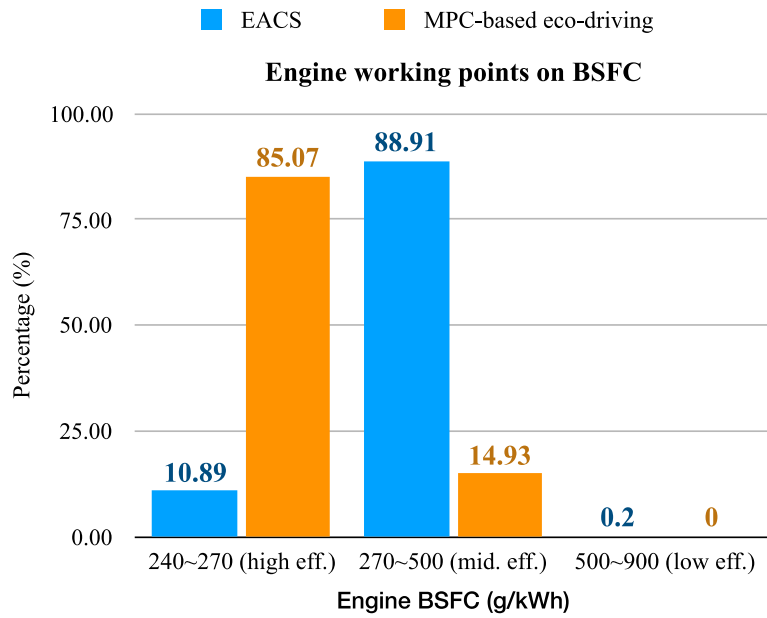


Fig. 5. 23 The distribution of engine working points by the MPC-based eco-driving strategy and the EACS rule-based strategy on a suburban-urban trip

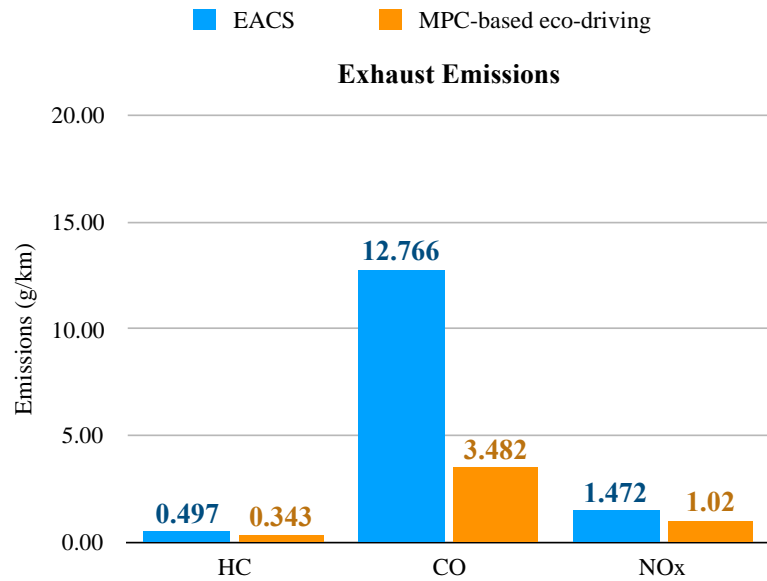


Fig. 5. 24 The exhaust emissions of HC, CO, and NOx produced by the MPC-based eco-driving strategy and the EACS rule-based strategy on a suburban-urban trip

5.3.3 Energy consumption and emission reduction

The energy performances of the MPC-based strategy and the EACS rule-based strategy can be seen in Fig. 5. 21 and Fig. 5. 22. It can be clearly seen that, with the proposed strategy applied, the engine can work in high efficiency over the suburban-urban trip, as depicted by the aggregation of engine working points found in the high-efficiency region 270 (g/kWh). Whereas for the results by the rule-based EACS strategy, the engine is working in an average state with operation points evenly distributed over the BSFC map. This can be explained by the nature of both strategies as the rule-based are designed by heuristic rules from experience or human expertise that are unable to be adapted on a case-by-case trip, while MPC-based control strategy aims to derive the optimal control results based on the information received in real-time, thus is more adaptive and yields better performance.

As a complement of Fig. 5. 21 (a) and Fig. 5. 22 (a), Fig. 5. 23 shows the distribution of engine working points in regions with different efficiency, where column 240~270 (g/kWh), column 270~500 (g/kWh) and column 500~900 (g/kWh) correspond to the high, middle, low BSFC map efficiency regions, respectively. It is shown in the figure that over the suburban-urban trip, the engine efficiency from the proposed control strategy is significantly higher than that from the EACS as working points in high-efficiency region (240~270 (g/kWh)) accounts for 85.07% of the entire working points, where they are 10.89% in EACS strategy.

Table. 5. 7 displays the numeric results. In comparison to the fuel consumption from the EACS, the fuel consumption from the proposed approach is greatly reduced by 38.15%. The SOC from both strategies are close in number, showing an energy-sustaining ability in the proposed strategy and the rule-based strategy.

The vehicle emissions from the MPC-based strategy are also decreased by 31.08%, 72.72% and 30.73% for exhaust emissions hc , co and no_x , respectively, when compared

with the results from the rule-based strategy. The visualization of emission reduction is shown in Fig. 5. 24.

In sum, the performance over a day-to-day suburban-urban trip show that, when compared to the widely applied rule-based strategy along with IDM for realistic speed profile generation, the vehicle controlled by the proposed eco-driving approach is able to achieve much better fuel economy and less engine-off emissions, while the safe driving is enabled over the entire trip.

Table. 5. 7 Results from the proposed MPC-based eco-driving strategy and the EACS rule-based strategy (SOC corrected) on a suburban trip

| Strategies | EACS | MPC-based | Improvement |
|-----------------------------|-------------|------------------|--------------------|
| Fuel consumption (g) | 671.21 | 415.14 | -38.15% |
| Terminal SOC (%) | 54.38 | 55.19 | --- |
| HC | 5.02 | 3.46 | -31.08% |
| CO | 128.94 | 35.17 | -72.72% |
| NOx | 14.87 | 10.30 | -30.73% |

5.4 Summary

The chapter examines the performance of the proposed strategy. First, a realistic urban map is set up to simulate a 24hr traffic condition as the background for the test. In order to evaluate the results of the proposed strategy, EACS, as a widely used rule-based strategy for HEV, and IDM, which is an intelligent driver model to generate realistic collision-free speed profile, are used as the benchmark. Next, a simulation over a selected highway-urban trip is carried out on both strategies. The results show that the proposed MPC-based strategy is able to ensure a safe driving distance to the preceding vehicle, legal speeds kept

on the road and anticipating actions on a TSCI. In addition, when compared with the benchmark strategy, the fuel consumption from the proposed strategy is greatly reduced by 26.80%, and much fewer exhaust emissions are produced, by 27.69%, 73.91% and 47.59% for *hc*, *co* and *no_x*, respectively, which demonstrates a great improvement. Moreover, a simulation on a suburban-urban trip is carried out to verify the approach. When compared to the EACS, The results from the MPC-based eco-driving achieve an even bigger improvement in fuel economy, by 38%, and much fewer emissions are generated, by 31.08%, 72.72% and 30.73% for *hc*, *co* and *no_x*, respectively, which show the robustness and adaptability of the proposed strategy. The proposed eco-driving strategy in this study is expected to be implemented to a vehicle onboard control device of a real-world CAHEV in highway and urban driving conditions when the conditions meet to provide ubiquitous and seamless V2V and V2I communications in the future intelligent transportation system (ITS).

Chapter 6. Conclusion and Future Works

6.1 Conclusion

In this study, a bi-level MPC-based strategy for connected and automated hybrid electric vehicles (CAHEVs) was proposed. The main objectives were to design an eco-driving strategy for CAHEVs that is able to improve fuel economy, minimize engine-out emissions and realize safe driving under trips with mixed driving scenarios.

In Chapter 2, the foundations of hybrid electric vehicles (HEVs) were introduced, followed by the description and classification of eco-driving scenarios. Then, the literature on energy management strategies (EMSs) for HEVs was discussed, emphasizing their principles, advantages, and limitations. Moreover, the control strategies for connected and automated hybrid electric vehicles (CAHEVs) were listed and discussed. Finally, the research gap was pointed out, which paved the way for the introduction to the proposed strategy.

In Chapter 3, a single-shaft, parallel hybrid electric powertrain was developed for the studied vehicle. As the real-time data sources for decision-making in intelligent transportation system (ITS), Vehicle-to-Vehicle (V2V) and Vehicle-to-Infrastructure (V2I) communications were then introduced.

In Chapter 4, the problem was described as an eco-driving problem and was then formulated into a multi-objective optimization problem in the context of the proposed MPC-based strategy. The objectives are (1) driving safety that aims to comply the vehicle speed with the road limit, ensure a collision-free following distance and anticipate the driving behaviour at an intersection over the entire trip, (2) fuel-saving that minimizes the fuel consumption over the entire trip and (3) exhaust emission reduction that minimizes the overall engine-out pollutants throughout the trip. The goal of driving safety is achieved through the use of a Driving Scenario Classifier (DSC) in this intelligent system which classifies the real-time driving scenario into three categories, namely, free driving scenario,

signal anticipation scenario and car-following scenario, such that a corresponding cost function can be applied in real-time. The optimal control actions are executed on multiple levels. At the upper level, the real-time vehicle acceleration is determined, while at the lower level, the optimal torque split ration between ICE and EM is derived. A widely used rule-based electric-assist control strategy (EACS) for powertrain management is adopted as the benchmark, and the intelligent driver model (IDM) is used for generating a collision-free realistic speed profile.

In Chapter 5, the simulation results showed that in a realistic highway-urban trip, the safe driving goal was achieved throughout the entire driving cycle in the selected urban traffic environment. Moreover, in comparison to the EACS benchmark strategy, the proposed MPC-based strategy could also reduce the fuel consumption by 26.80% while keeping the battery in a healthy range, and reducing the exhaust emissions (HC, CO, NO_x) by 27.69%, 73.91% and 47.59%, respectively. Verification was carried out on a suburban-urban trip. The results from the proposed eco-driving strategy demonstrated even better performance, as a 38.15% reduction in fuel, 31.08%, 72.72% and 30.73% reduction in the exhaust emissions (HC, CO, NO_x), respectively, and the capability to sustain a balanced battery SOC level throughout the trip, which demonstrated the effectiveness and robustness of the strategy over a random trip with complex types of driving conditions.

6.2 Future Works

As the strategy is mainly based on the vehicle longitudinal optimization, in the future, it will also include the dynamic lane-changing strategy to make it more comprehensive. In addition, the strategy will be improved by introducing the eco-routing algorithm, which selects the most fuel-efficient route by accurate estimation of the fuel cost on each road in the dynamic traffic environment. The application of the eco-routing approach in an urban traffic environment is highly correlated to the prediction accuracy of future driving conditions such as the traffic density and trends. Moreover, for the sake of realistic

application in the real world, the V2V and V2I communication delay will also be considered in the driving scenarios. Also, the travelling time of the host vehicle can be taken into consideration in the multi-objective optimization for a more practical driving experience, and the vehicle driving comfort can be considered to regulate the unnecessary fluctuation in the speed profile to better serve for human passengers. Besides, the work can be extended to the optimal control strategy for a CAHEV fleet in the urban driving conditions, in which case, more data such as the speed and intention of the neighboring vehicles are required for more efficient and safer coordination between vehicles in the same fleet. Finally, to make the proposed strategy applicable to the local traffic network in simulation, 24-hour traffic demands from the local city will be collected and modelled to build up a realistic urban traffic network for simulation. On the basis of that, to introduce more realistic conditions into this optimization problem, the locations of gas stations and electric charging stations can be considered in the urban map.

Reference

- [1] L. Li, Y. Zhang, C. Yang, X. Jiao, L. Zhang, and J. Song, "Hybrid genetic algorithm-based optimization of powertrain and control parameters of plug-in hybrid electric bus," *Journal of the Franklin Institute*, vol. 352, no. 3, pp. 776–801, 2015, doi: 10.1016/j.jfranklin.2014.10.016.
- [2] W. Enang and C. Bannister, "Modelling and control of hybrid electric vehicles (A comprehensive review)," *Renewable and Sustainable Energy Reviews*, vol. 74, pp. 1210–1239, 2017, doi: 10.1016/j.rser.2017.01.075.
- [3] C. Guardiola, B. Plá, S. Onori, and G. Rizzoni, "Insight into the HEV/PHEV optimal control solution based on a new tuning method," *Control Engineering Practice*, vol. 29, pp. 247–256, 2014, doi: 10.1016/j.conengprac.2014.01.022.
- [4] S. Zhang, T. Niu, Y. Wu, K. M. Zhang, T. J. Wallington, and Q. Xie, "Fine-grained vehicle emission management using intelligent transportation system data," *Environmental pollution (Barking, Essex : 1987)*, vol. 241, pp. 1027–1037, 2018, doi: 10.1016/j.envpol.2018.06.016.
- [5] U.S. Energy Information Administration (EIA), "ANNUAL ENERGY OUTLOOK 2020," 2020. [Online]. Available: <https://www.eia.gov/outlooks/aeo/pdf/AEO2020%20Full%20Report.pdf>
- [6] L. Li, X. Wang, and J. Song, "Fuel consumption optimization for smart hybrid electric vehicle during a car-following process," *Mechanical Systems and Signal Processing*, vol. 87, pp. 17–29, 2017, doi: 10.1016/j.ymsp.2016.03.002.
- [7] D. A. Crolla and D. Cao, "The impact of hybrid and electric powertrains on vehicle dynamics, control systems and energy regeneration," *Vehicle System Dynamics*, vol. 50, sup1, pp. 95–109, 2012, doi: 10.1080/00423114.2012.676651.
- [8] E. Silvaş, T. Hofman, and M. Steinbuch, "Review of Optimal Design Strategies for Hybrid Electric Vehicles," *IFAC Proceedings Volumes*, vol. 45, no. 30, pp. 57–64, 2012, doi: 10.3182/20121023-3-FR-4025.00054.
- [9] M. A. Hannan, F. A. Azidin, and A. Mohamed, "Hybrid electric vehicles and their challenges: A review," *Renewable and Sustainable Energy Reviews*, vol. 29, pp. 135–150, 2014, doi: 10.1016/j.rser.2013.08.097.
- [10] M. F. M. Sabri, K. A. Danapalasingam, and M. F. Rahmat, "A review on hybrid electric vehicles architecture and energy management strategies," *Renewable and Sustainable Energy Reviews*, vol. 53, pp. 1433–1442, 2016, doi: 10.1016/j.rser.2015.09.036.
- [11] Y. Huang, H. Wang, A. Khajepour, H. He, and J. Ji, "Model predictive control power management strategies for HEVs: A review," *Journal of Power Sources*, vol. 341, pp. 91–106, 2017, doi: 10.1016/j.jpowsour.2016.11.106.
- [12] T. Liu, Y. Zou, D. Liu, and F. Sun, "Reinforcement Learning of Adaptive Energy Management With Transition Probability for a Hybrid Electric Tracked Vehicle," *IEEE Trans. Ind. Electron.*, vol. 62, no. 12, pp. 7837–7846, 2015, doi: 10.1109/TIE.2015.2475419.

- [13] Y. Zou, T. Liu, D. Liu, and F. Sun, "Reinforcement learning-based real-time energy management for a hybrid tracked vehicle," *Applied Energy*, vol. 171, pp. 372–382, 2016, doi: 10.1016/j.apenergy.2016.03.082.
- [14] S.-Y. Chen, Y.-H. Hung, C.-H. Wu, and S.-T. Huang, "Optimal energy management of a hybrid electric powertrain system using improved particle swarm optimization," *Applied Energy*, vol. 160, pp. 132–145, 2015, doi: 10.1016/j.apenergy.2015.09.047.
- [15] Y. Hu, W. Li, K. Xu, T. Zahid, F. Qin, and C. Li, "Energy Management Strategy for a Hybrid Electric Vehicle Based on Deep Reinforcement Learning," *Applied Sciences*, vol. 8, no. 2, p. 187, 2018, doi: 10.3390/app8020187.
- [16] V. Ngo, T. Hofman, M. Steinbuch, and A. Serrarens, "Predictive gear shift control for a parallel Hybrid Electric Vehicle," in 2011 IEEE vehicle power and propulsion conference (VPPC 2011): Chicago, Illinois, USA 6-9 September 2011, Chicago, IL, USA, 2011, pp. 1–6.
- [17] D. Rotenberg, A. Vahidi, and I. Kolmanovsky, "Ultracapacitor Assisted Powertrains: Modeling, Control, Sizing, and the Impact on Fuel Economy," *IEEE Trans. Contr. Syst. Technol.*, vol. 19, no. 3, pp. 576–589, 2011, doi: 10.1109/TCST.2010.2048431.
- [18] H. Borhan, A. Vahidi, A. M. Phillips, M. L. Kuang, I. V. Kolmanovsky, and S. Di Cairano, "MPC-Based Energy Management of a Power-Split Hybrid Electric Vehicle," *IEEE Trans. Contr. Syst. Technol.*, vol. 20, no. 3, pp. 593–603, 2012, doi: 10.1109/TCST.2011.2134852.
- [19] L. Johannesson, M. Asbogard, and B. Egardt, "Assessing the Potential of Predictive Control for Hybrid Vehicle Powertrains Using Stochastic Dynamic Programming," *IEEE Trans. Intell. Transport. Syst.*, vol. 8, no. 1, pp. 71–83, 2007, doi: 10.1109/TITS.2006.884887.
- [20] J. Vales-Alonso, F. Vicente-Carrasco, and J. Alcaraz, "Optimal configuration of roadside beacons in V2I communications," *Computer Networks*, vol. 55, no. 14, pp. 3142–3153, 2011, doi: 10.1016/j.comnet.2011.05.006.
- [21] E. Ndashimye, S. Ray, N. Sarkar, and J. Gutiérrez, "Vehicle-to-infrastructure communication over multi-tier heterogeneous networks: A survey," *Computer Networks*, vol. 112, pp. 144–166, 2017, doi: 10.1016/j.comnet.2016.11.008.
- [22] D. Jia and D. Ngoduy, "Enhanced cooperative car-following traffic model with the combination of V2V and V2I communication," *Transportation Research Part B: Methodological*, vol. 90, pp. 172–191, 2016, doi: 10.1016/j.trb.2016.03.008.
- [23] Y. Wang, D. Zhang, Y. Liu, B. Dai, and L. H. Lee, "Enhancing transportation systems via deep learning: A survey," *Transportation Research Part C: Emerging Technologies*, vol. 99, pp. 144–163, 2019, doi: 10.1016/j.trc.2018.12.004.
- [24] K. Jadaan, S. Zeater, and Y. Abukhalil, "Connected Vehicles: An Innovative Transport Technology," *Procedia Engineering*, vol. 187, pp. 641–648, 2017, doi: 10.1016/j.proeng.2017.04.425.
- [25] A. Sciarretta and A. Vahidi, "Energy Saving Potentials of CAVs," in *Lecture notes in intelligent transportation and infrastructure*, 2523-3440, Energy-efficient driving of road vehicles: Toward cooperative, connected, and automated mobility / Antonio Sciarretta, Ardan Vahidi, A. Sciarretta and A. Vahidi, Eds., Cham: Springer, 2020, pp. 1–31. [Online]. Available: https://doi.org/10.1007/978-3-030-24127-8_1

- [26] J. Wu, X. Wang, L. Li, C. a. Qin, and Y. Du, "Hierarchical control strategy with battery aging consideration for hybrid electric vehicle regenerative braking control," *Energy*, vol. 145, pp. 301–312, 2018, doi: 10.1016/j.energy.2017.12.138.
- [27] L. Guo, B. Gao, Y. Gao, and H. Chen, "Optimal Energy Management for HEVs in Eco-Driving Applications Using Bi-Level MPC," *IEEE Trans. Intell. Transport. Syst.*, vol. 18, no. 8, pp. 2153–2162, 2017, doi: 10.1109/TITS.2016.2634019.
- [28] W.-Y. Chou, Y.-C. Lin, Y.-H. Lin, and S.-Y. Chen, "Intelligent eco-driving suggestion system based on vehicle loading model," in *ITS 2012: 2012 12th International Conference on ITS Telecommunications : 5-8 November 2012 in Taipei, Taiwan, Taipei, Taiwan, 2012*, pp. 558–562.
- [29] A. Rakotonirainy, G. S. Larue, S. Demmel, and H. Malik, "Fuel consumption and gas emissions of an automatic transmission vehicle following simple eco-driving instructions on urban roads," *IET Intelligent Transport Systems*, vol. 8, no. 7, pp. 590–597, 2014, doi: 10.1049/iet-its.2013.0076.
- [30] I Wengraf, "Easy on the Gas: The effectiveness of eco-driving," Royal Automobile Club Foundation, Tech. Rep., 2012.
- [31] T.-W. Sung, L.-C. Shiu, F.-T. Lin, and C.-S. Yang, "A Speed Control Scheme of Eco-Driving at Road Intersections," in *2015 Third International Conference on Robot, Vision and Signal Processing - RVSP 2015: 18-20 November 2015, Kaohsiung, Taiwan : proceedings, Kaohsiung, Taiwan, 2015*, pp. 51–54.
- [32] X. Xiang, K. Zhou, W.-B. Zhang, W. Qin, and Q. Mao, "A Closed-Loop Speed Advisory Model With Driver's Behavior Adaptability for Eco-Driving," *IEEE Trans. Intell. Transport. Syst.*, vol. 16, no. 6, pp. 3313–3324, 2015, doi: 10.1109/TITS.2015.2443980.
- [33] L. Li, X. Wang, R. Xiong, K. He, and X. Li, "AMT downshifting strategy design of HEV during regenerative braking process for energy conservation," *Applied Energy*, vol. 183, pp. 914–925, 2016, doi: 10.1016/j.apenergy.2016.09.031.
- [34] G. Wu, X. Zhang, and Z. Dong, "Powertrain architectures of electrified vehicles: Review, classification and comparison," *Journal of the Franklin Institute*, vol. 352, no. 2, pp. 425–448, 2015, doi: 10.1016/j.jfranklin.2014.04.018.
- [35] K. Çağatay Bayindir, M. A. Gözüküçük, and A. Teke, "A comprehensive overview of hybrid electric vehicle: Powertrain configurations, powertrain control techniques and electronic control units," *Energy Conversion and Management*, vol. 52, no. 2, pp. 1305–1313, 2011, doi: 10.1016/j.enconman.2010.09.028.
- [36] S. J. Moura, D. S. Callaway, H. K. Fathy, and J. L. Stein, "Tradeoffs between battery energy capacity and stochastic optimal power management in plug-in hybrid electric vehicles," *Journal of Power Sources*, vol. 195, no. 9, pp. 2979–2988, 2010, doi: 10.1016/j.jpowsour.2009.11.026.
- [37] S. F. Tie and C. W. Tan, "A review of energy sources and energy management system in electric vehicles," *Renewable and Sustainable Energy Reviews*, vol. 20, pp. 82–102, 2013, doi: 10.1016/j.rser.2012.11.077.
- [38] B. Jacobson, "On Vehicle Driving Cycle Simulation," in *SAE Technical Paper Series*, 1995.
- [39] H. Richter, V. Korte, and L. C. van Beckhoven, "Actual Driving Conditions in Europe and the Proposed EEC Extra Urban Driving Cycle," in *SAE Technical Paper Series*, 1989.

- [40] L. Berzi, M. Delogu, and M. Pierini, "Development of driving cycles for electric vehicles in the context of the city of Florence," *Transportation Research Part D: Transport and Environment*, vol. 47, pp. 299–322, 2016, doi: 10.1016/j.trd.2016.05.010.
- [41] B. Liu, Q. Shi, L. He, and D. Qiu, "A study on the construction of Hefei urban driving cycle for passenger vehicle," *IFAC-PapersOnLine*, vol. 51, no. 31, pp. 854–858, 2018, doi: 10.1016/j.ifacol.2018.10.100.
- [42] C. Kim, E. NamGoong, S. Lee, T. Kim, and H. Kim, "Fuel Economy Optimization for Parallel Hybrid Vehicles with CVT," in *SAE Technical Paper Series*, 1999.
- [43] J. Yang and G. G. Zhu, "Predictive Boundary Management Control of a Hybrid Powertrain," in *Proceedings of the ASME 7th annual dynamic systems and control conference 2014: October 22-24, 2014, San Antonio, Texas, USA, San Antonio, Texas, USA, 2014*.
- [44] N. Jalil, N. A. Kheir, and M. Salman, "A rule-based energy management strategy for a series hybrid vehicle," in *Proceedings of the 1997 American control conference, Albuquerque, NM, USA, 1997*, 689-693 vol.1.
- [45] V. H. Johnson, K. B. Wipke, and D. J. Rausen, "HEV Control Strategy for Real-Time Optimization of Fuel Economy and Emissions," *SAE Technical Paper 2000-01-1543*, Apr. 2000. [Online]. Available: <https://www.sae.org/gsdownload/?prodCd=2000-01-1543>
- [46] F. R. Salmasi, "Control Strategies for Hybrid Electric Vehicles: Evolution, Classification, Comparison, and Future Trends," *IEEE Trans. Veh. Technol.*, vol. 56, no. 5, pp. 2393–2404, 2007, doi: 10.1109/TVT.2007.899933.
- [47] H.-D. Lee and S.-K. Sul, "Fuzzy-logic-based torque control strategy for parallel-type hybrid electric vehicle," *IEEE Trans. Ind. Electron.*, vol. 45, no. 4, pp. 625–632, 1998, doi: 10.1109/41.704891.
- [48] A. Rajagopalan, G. Washington, G. Rizzoni, and Y. Guezennec, "Development of Fuzzy Logic and Neural Network Control and Advanced Emissions Modeling for Parallel Hybrid Vehicles," 2003.
- [49] S. Ichikawa et al., "Novel energy management system for hybrid electric vehicles utilizing car navigation over a commuting route," in *2004 IEEE intelligent vehicles symposium, Parma, Italy, 2004*, pp. 161–166.
- [50] C.-C. Lin, H. Peng, J. W. Grizzle, and J.-M. Kang, "Power management strategy for a parallel hybrid electric truck," *IEEE Trans. Contr. Syst. Technol.*, vol. 11, no. 6, pp. 839–849, 2003, doi: 10.1109/TCST.2003.815606.
- [51] C.-C. Lin, H. Peng, and J. W. Grizzle, "A stochastic control strategy for hybrid electric vehicles," in *2004 American control conference, Boston, MA, USA, 2004*, 4710-4715 vol.5.
- [52] B. Huang, Z. Wang, and Y. Xu, "Multi-Objective Genetic Algorithm for Hybrid Electric Vehicle Parameter Optimization," in *IEEE/RSJ International Conference on Intelligent Robots and Systems, 2006: Oct. 2006, [Beijing, China], Beijing, China, 2006*, pp. 5177–5182.
- [53] M. Huang and H. Yu, "Optimal Multilevel Hierarchical Control Strategy for Parallel Hybrid Electric Vehicle," in *IEEE Vehicle Power and Propulsion Conference, 2006: VPPC '06 ; 6-8 Sept. 2006, [Windsor, United Kingdom], Windsor, UK, 2006*, pp. 1–4.

- [54] Z. Chen, C. C. Mi, B. Xia, and C. You, "Energy management of power-split plug-in hybrid electric vehicles based on simulated annealing and Pontryagin's minimum principle," *Journal of Power Sources*, vol. 272, pp. 160–168, 2014, doi: 10.1016/j.jpowsour.2014.08.057.
- [55] Namwook Kim, Daeheung Lee, Suk-Won Cha, Huei Peng, (PDF) Optimal Control of a Plug-In Hybrid Electric Vehicle (PHEV) Based on Driving Patterns. [Online]. Available: https://www.researchgate.net/publication/267718169_Optimal_Control_of_a_Plug-In_Hybrid_Electric_Vehicle_PHEV_Based_on_Driving_Patterns (accessed: Feb. 23 2020).
- [56] G. Paganelli, T. M. Guerra, S. Delprat, J.-J. Santin, M. Delhom, and E. Combes, "Simulation and assessment of power control strategies for a parallel hybrid car," *Proceedings of the Institution of Mechanical Engineers, Part D: Journal of Automobile Engineering*, vol. 214, no. 7, pp. 705–717, 2000, doi: 10.1243/0954407001527583.
- [57] A. Sciarretta, M. Back, and L. Guzzella, "Optimal Control of Parallel Hybrid Electric Vehicles," *IEEE Trans. Contr. Syst. Technol.*, vol. 12, no. 3, pp. 352–363, 2004, doi: 10.1109/TCST.2004.824312.
- [58] K. R. Bouwman, T. H. Pham, S. Wilkins, and T. Hofman, "Predictive Energy Management Strategy Including Traffic Flow Data for Hybrid Electric Vehicles," *IFAC-PapersOnLine*, vol. 50, no. 1, pp. 10046–10051, 2017, doi: 10.1016/j.ifacol.2017.08.1775.
- [59] C. Sun, S. J. Moura, X. Hu, J. K. Hedrick, and F. Sun, "Dynamic Traffic Feedback Data Enabled Energy Management in Plug-in Hybrid Electric Vehicles," *IEEE Trans. Contr. Syst. Technol.*, vol. 23, no. 3, pp. 1075–1086, 2015, doi: 10.1109/TCST.2014.2361294.
- [60] Z. Xiuzheng, Z. Liguu, and Y. Kholodov, "Model predictive control of eco-driving for transit using V2I communication," in *Control Conference (CCC), 2015 34th Chinese*, Hangzhou, China, Jul. 2015 - Jul. 2015, pp. 2511–2516.
- [61] H. Bouvier, G. Colin, and Y. Chamaillard, "Determination and comparison of optimal eco-driving cycles for hybrid electric vehicles," in *Control Conference (ECC), 2015 European*, Linz, Austria, Jul. 2015 - Jul. 2015, pp. 142–147.
- [62] V. T. Minh and A. A. Rashid, "Modeling and model predictive control for hybrid electric vehicles," *Int.J Automot. Technol.*, vol. 13, no. 3, pp. 477–485, 2012, doi: 10.1007/s12239-012-0045-0.
- [63] K. Yu, J. Yang, and D. Yamaguchi, "Model predictive control for hybrid vehicle ecological driving using traffic signal and road slope information," *Control Theory Technol.*, vol. 13, no. 1, pp. 17–28, 2015, doi: 10.1007/s11768-015-4058-x.
- [64] S.-Y. Shieh, T. Ersal, and H. Peng, "Pulse-and-Glide Operation for Parallel Hybrid Electric Vehicles with Step-Gear Transmission in Automated Car-Following Scenario with Ride Comfort Consideration," in *2019 American Control Conference (ACC)*, Philadelphia, PA, USA, 2019, pp. 959–964.
- [65] S. Zhao, Y. Wu, Y. Zhai, C. Chen, J. Wu, and B. Sun, "An integrated control strategy for eco-driving of intelligent hybrid vehicles," in *2019 IEEE International Conference on Smart Manufacturing, Industrial & Logistics Engineering (SMILE)*, Hangzhou, China, Apr. 2019 - Apr. 2019, pp. 14–18.
- [66] B. Zhang, H. Lim, S. Xu, and W. Su, "Distance-oriented hierarchical control and ecological driving strategy for HEVs," *IET Electrical Systems in Transportation*, vol. 9, no. 1, pp. 44–52, 2019, doi: 10.1049/iet-est.2018.5044.

- [67] A. Sciarretta and A. Vahidi, Eds., *Energy-efficient driving of road vehicles: Toward cooperative, connected, and automated mobility* / Antonio Sciarretta, Ardalan Vahidi. Cham: Springer, 2020.
- [68] X. Hu, X. Zhang, X. Tang, and X. Lin, “Model predictive control of hybrid electric vehicles for fuel economy, emission reductions, and inter-vehicle safety in car-following scenarios,” *Energy*, vol. 196, p. 117101, 2020, doi: 10.1016/j.energy.2020.117101.
- [69] L. Liu, F. Kong, X. Liu, Y. Peng, and Q. Wang, “A review on electric vehicles interacting with renewable energy in smart grid,” *Renewable and Sustainable Energy Reviews*, vol. 51, pp. 648–661, 2015, doi: 10.1016/j.rser.2015.06.036.
- [70] C. Yi, B. Epureanu, S. K. Hong, T. Ge, and X. G. Yang, “Modeling, control, and performance of a novel architecture of hybrid electric powertrain system,” *Applied Energy*, vol. 178, pp. 454–467, 2016, doi: 10.1016/j.apenergy.2016.06.068.
- [71] B. Liu, L. Li, X. Wang, and S. Cheng, “Hybrid Electric Vehicle Downshifting Strategy Based on Stochastic Dynamic Programming During Regenerative Braking Process,” *IEEE Trans. Veh. Technol.*, vol. 67, no. 6, pp. 4716–4727, 2018, doi: 10.1109/TVT.2018.2815518.
- [72] J. Y. Wong, *Theory of ground vehicles*, 4th ed. Hoboken, N.J.: Wiley; Chichester : John Wiley [distributor], 2008.
- [73] J. Lee and D. J. Nelson, “Rotating Inertia Impact on Propulsion and Regenerative Braking for Electric Motor Driven Vehicles,” in 2005 IEEE Vehicle Power and Propulsion Conference, Chicago, IL, USA, Sep. 2005, pp. 308–314.
- [74] M. Ehsani, Y. Gao, S. Longo, and K. Ebrahimi, *Modern electric, hybrid electric, and fuel cell vehicles*, 3rd ed. Boca Raton: CRC Press/Taylor & Francis Group, 2019.
- [75] M. Treiber and A. Kesting, *Traffic flow dynamics: Data, models and simulation*. Heidelberg, New York: Springer, 2013. [Online]. Available: <https://www.eia.gov/outlooks/aeo/>
- [76] C. Osornio-Correa, R. C. Villarreal-Calva, J. Estavillo-Galsworthy, A. Molina-Cristóbal, and S. D. Santillán-Gutiérrez, “Optimization of Power Train and Control Strategy of a Hybrid Electric Vehicle for Maximum Energy Economy,” *Ingeniería, Investigación y Tecnología*, vol. 14, no. 1, pp. 65–80, 2013, doi: 10.1016/S1405-7743(13)72226-1.
- [77] H. Noori, “Modeling the impact of VANET-enabled traffic lights control on the response time of emergency vehicles in realistic large-scale urban area,” in *IEEE International Conference on Communications workshops (ICC)*, 2013: 9-13 June 2013, Budapest, Hungary, Budapest, Hungary, 2013, pp. 526–531.
- [78] K. B. Wipke, M. R. Cuddy, and S. D. Burch, “ADVISOR 2.1: a user-friendly advanced powertrain simulation using a combined backward/forward approach,” *IEEE Trans. Veh. Technol.*, vol. 48, no. 6, pp. 1751–1761, 1999, doi: 10.1109/25.806767.
- [79] P. A. Lopez et al., “Microscopic Traffic Simulation using SUMO,” in *2018 21st International Conference on Intelligent Transportation Systems (ITSC)*, Maui, HI, Nov. 2018 - Nov. 2018, pp. 2575–2582.
- [80] S. Uppoor and M. Fiore, “Characterizing Pervasive Vehicular Access to the Cellular RAN Infrastructure: An Urban Case Study,” *IEEE Trans. Veh. Technol.*, vol. 64, no. 6, pp. 2603–2614, 2015, doi: 10.1109/TVT.2014.2343651.

[81]J. Erdmann, “1 Lane-Changing Model in SUMO,” 2014. [Online]. Available: <https://pdfs.semanticscholar.org/5f36/bc7be59fd4546a5f3b5de4cd91f43bf11825.pdf>

[82]J. Song, Y. Wu, Z. Xu, and X. Lin, “Research on car-following model based on SUMO,” in Proceedings of 2014 IEEE 7th International Conference on Advanced Infocomm Technology (IEEE/ICAIT2014): November 14-16, 2014, Fuzhou, China, Fuzhou, China, IEEE/ICAIT2014, pp. 47–55.